TECHNISCHE UNIVERSITÄT MÜNCHEN
Lehrstuhl für Ernährungsphysiologie

Characterization of the PTR peptide transporter family of *Escherichia coli*

Daniel Harder

Vollständiger Abdruck der von der Fakultät Wissenschaftszentrum Weihenstephan für Ernährung, Landnutzung und Umwelt der Technischen Universität München zur Erlangung des akademischen Grades eines

Doktors der Naturwissenschaften

genehmigten Dissertation.

Vorsitzender: Univ.-Prof. Dr. M. Klingenspor

Prüfer der Dissertation:

1. Univ.-Prof. Dr. H. Daniel
2. Univ.-Prof. Dr. S. Scherer

Die Dissertation wurde am 18.12.2008 bei der Technischen Universität München eingereicht und durch die Fakultät Wissenschaftszentrum Weihenstephan für Ernährung, Landnutzung und Umwelt am 20.04.2009 angenommen.

Even the longest journey begins with a single step.
(Lao-tzu)

TABLE OF CONTENTS

1. SUMMARY 1
ZUSAMMENFASSUNG 2

2. INTRODUCTION 3
2.1. Peptide transport 3
2.1.1. The PTR family 3
2.1.2. Mammalian PEPT1 and PEPT2 6
2.1.3. Peptide transport in *E. coli* 8
2.2. Protein structure of PTR transporters 8

3. AIM OF THE THESIS 11

4. RESULTS 13

4.1. Sequence analysis 13
4.1.1. Homology search in *E. coli* 13
4.1.2. Transmembrane domain structure prediction of the PTR family members 16
4.1.3. Genetic localization of the PTR members of *E. coli* 17

4.2. Overexpression in *E. coli* 19

4.3. Purification of proteins by Ni^{2+} affinity chromatography 21

4.4. Functional characterization 24
4.4.1. *In vivo* uptake experiments 24
4.4.1.1. DtpA - transport characteristics and substrate specificity 25
4.4.1.2. DtpB - transport characteristics and substrate specificity 32
4.4.1.3. DtpC - transport characteristics and substrate specificity 36
4.4.1.4. DtpD - transport characteristics and substrate specificity 42
4.4.2. *In vitro* uptake studies 47
4.4.2.1. Transport in membrane vesicles 48
4.4.2.2. Uptake into proteoliposomes 49
4.4.2.3. Electrical measurements employing proteoliposomes 50
4.4.3. Analysis of KO-strains 51
4.4.4. Growth curves 53
4.4.4.1. Growth curves - alafosfalin 53
4.4.4.2. Growth curves - chloramphenicol 54

4.5. Expression of the transporters in *Xenopus* oocytes 55

4.6. Structural characterization 58
4.6.1. Crosslink experiments 58
4.6.2. Gel filtration 61
4.6.3. Dynamic light scattering 62
4.6.4. Circular dichroism spectrometry 63
4.6.5. MALDI-TOF mass spectrometry 63
4.6.6. Protein crystallization 65
4.6.6.1. 2D crystallization 65
4.6.6.2. 3D crystallization 67

5. DISCUSSION 69
5.1. Sequence analysis 69
5.2. Overexpression 70
5.3. Purification 71
5.4. Functional characterization: substrate specificity 71
5.5. Functional characterization: transport mode 76
5.6. Studies with deletion mutant *E. coli* lines 77
5.7. Growth curves 78
5.8. Protein structural information 79

6. OUTLOOK 83

7. MATERIALS AND METHODS 85
7.1. Protein sequence analysis 85
7.2. Statistical data analysis and calculation 85
7.3. Cloning 85
7.4. Overexpression in *E. coli* 87
7.5. Growth experiments 87
7.6. Western blot analysis 88
7.7. Transport assays with β-Ala-Lys(AMCA) 88
7.8. Transport assays with radiolabeled tracer substrates 89
7.9. Transport assays with KO-strains 90
7.10. Purification by Ni^{2+} affinity chromatography 91
7.11. Reconstitution into proteoliposomes 92
7.12. Uptake in cytochrome *c* oxidase energized proteoliposomes 92
7.13. Electrical measurements with the $SURFE^2R^{one}$ setup 93
7.14. Expression in *Xenopus* oocytes 94
7.14.1. RNA production by *in vitro* transcription 95
7.14.2. Two-electrode voltage clamp 96
7.14.3. Lysis of oocytes for Western blot 96
7.14.4. Immunohistochemistry 96
7.14.5. Radiolabeled uptake in *Xenopus* oocytes 97
7.15. Chemical crosslink experiments 97
7.16. Gel filtration 98
7.17. Dynamic light scattering 99
7.18. Circular dichroism spectrometry 99
7.19. MALDI-TOF 100
7.19.1. Analysis of undigested protein 101
7.19.2. Analysis of trypsin digested protein 101
7.20. Protein crystallization 102
7.20.1. 2D-crystallization 102
7.20.2. 3D-crystallization 104
7.21. Transmission electron microscopy 105

8. REFERENCES 107

9. APPENDIX 115
9.1. Abbreviations 115
9.2. Proteinparameters 116
9.3. Acknowledgments 118
9.4. Curriculum Vitae 120
9.5. List of publications 121

1. SUMMARY

In the genome of *E. coli* four genes can be identified that carry the peptide transporter family (PTR) sequence motives. Proteins of the PTR family are integral plasma membrane proteins that can transport di- and tripeptides in a proton-symport mode into the cell. They are found in cell membranes of virtually all organisms from bacteria to man. There is a considerable scientific and commercial interest in these transport systems since the human PTR-family representatives, PEPT1 and PEPT2, are relevant drug transporting systems determining intestinal bioavailability of a variety of peptidomimetic drugs and affecting drug disposition. For *E. coli* there was just one member known and described as TppB (tripeptide permease). Here, all four genes were overexpressed in *E. coli* as tagged proteins and functionally characterized. Based on the results, a coherent naming as di- and tripeptide permeases is proposed, with the four members *dtpA* (*tppB, ydgR*), *dtpB* (*yhiP*), *dtpC* (*yjdL*) and *dtpD* (*ybgH*). DtpA was functionally characterized as a prototypical peptide transporter with a broad substrate spectrum for di- and tripeptides and a very high similarity to the mammalian PEPT1. For DtpB [^{14}C]glycyl-sarcosine was identified as a substrate and used for characterization of transport function and a similar substrate specificity as for DtpA was observed. Both transporters also were shown to be proton-dependent by experiments using the proton-ionophore CCCP, by electrical transport measurements and by tracer uptake studies in proteoliposomes with the reconstituted purified transporters and an artificial proton-gradient serving as a driving force. DtpC was characterized by using the amino acid [^{3}H]lysine and found to transport also arginine and histidine. It also displayed a high affinity for di- and tripeptides containing amino acids with positively charged side chains. For DtpD [^{14}C]6-aminohexanoic acid was identified as a reporter substrate and uptake experiments revealed a substrate pattern that was also restricted to charged short chain peptides. Whether DtpC and DtpD also utilize a proton-gradient for transport remains to be determined. Experiments with knockout mutants suggest that all *E. coli* PTR transporters except DtpB are active under standard culture conditions and growth experiments with toxic substrates were established as an alternative for demonstration of functional overexpression. For structural examination, the four proteins were overproduced in larger amounts and purified by a C-terminal His_6-tag using Ni^{2+} affinity chromatography. This was most successful with DtpA and DtpD yielding up to 8 mg/l culture of relatively pure protein that was demonstrated to be still active after purification by functional reconstitution in proteoliposomes. Studies to elucidate the oligomeric state by cross-linking, gel-filtration and dynamic light scattering suggested a monomeric form. Initial 2D crystallization trails yielded promising results with DtpA and DtpD, which have to be improved further for structural analysis. 3D crystallization trails did not reveal satisfying results.

1. ZUSAMMENFASSUNG

Das Genom von *E. coli* enthält vier Gene die das Peptidtransporter (PTR) Sequenzmotiv tragen. Mitglieder dieser Familie sind integrale Membranproteine, die als protonenabhängige Symporter für Di- und Tripeptide die Peptidaufnahme in die Zelle vermitteln. Sie kommen in den Zellmembranen von praktisch allen Lebewesen vor; von Bakterien bis zum Menschen. Es besteht ein großes wissenschaftliches wie kommerzielles Interesse an Peptidtransportproteinen da die Säugerproteine PEPT1 und PEPT2 die Bioverfügbarkeit und Pharmakodynamik von Peptidmimetika determinieren. In *E. coli* wurde bisher nur ein Vertreter der PTR-Familie als TppB (Tripeptid Permease) beschrieben. In der vorliegenden Arbeit wurden alle vier Gene in *E. coli* kloniert und als Fusionsproteine mit „Tag" überexprimiert sowie funktionell charakterisiert. Auf Grundlage der Ergebnisse wird für die Gruppe die Bezeichnung Di- und Tripeptid Permeasen vorgeschlagen, mit den vier Vertretern *dtpA* (*tppB, ydgR*), *dtpB* (*yhiP*), *dtpC* (*yjdL*) und *dtpD* (*ybgH*). DtpA wurde mit dem fluoreszierenden Dipeptid β-Ala-Lys(AMCA) funktionell charakterisiert, wobei sich ein breites Substratspektrum von Di- und Tripeptiden mit sehr hoher Ähnlichkeit zum menschlichen PEPT1 zeigte. Dies war auch der Fall für DtpB, welches mit Hilfe von [^{14}C]Glycyl-Sarcosin als Substrat charakterisiert wurde. Für beide Transporter wurde auch die Protonenabhängigkeit gezeigt, wofür Experimente mit dem Protonenionophor CCCP, elektrische Transportmessungen und Aufnahmexperimente in Proteoliposomen mit rekonstituiertem gereinigtem Protein und einem künstlichen Protonengradient als treibende Kraft, eingesetzt wurden. DtpC wurde mit der Aminosäure [^{3}H]Lysin als möglicher Aminosäuretransporter charakterisiert der vermutlich spezifisch kationische Aminosäuren zu transportieren vermag. Dennoch zeigt DtpC auch Affinität zu Di- und Tripeptiden, allerdings mit der Beschränkung auf Peptide die Aminosäuren mit kationischen Seitenketten enthalten. Für DtpD wurde [^{14}C]6-Aminohexansäure als Reportersubstrat verwendet und ein Substratspektrum identifiziert welches auch auf geladene Peptide beschränkt ist. Für diese beiden Transporter blieb bisher ungeklärt ob sie den Protonengradienten nutzen. Experimente mit Deletionsmutanten zeigten, dass die *E. coli* PTR-Transporter - außer DtpB - unter Standard-Kulturbedingungen aktiv sind und durch Wachstumsexperimente mit toxischen Peptidsubstraten wurde die Funktion der Transporter nach Überexpression ebenso belegt. Zur Strukturaufklärung wurden die vier Proteine in größeren Mengen produziert und mittels des C-terminalen His_6-tag durch Ni^{2+} Affinitätschromatographie gereinigt. Die besten Ergebnisse lieferte DtpA mit Ausbeuten von bis zu 8 mg/l Kultur von relativ reinem Protein, dessen erhaltene Funktionalität nach der Reinigung gezeigt werden konnte. Die Quartärstruktur wurde durch chemisches „Crosslinken", Gelfiltration und dynamische Lichtstreuung untersucht, wodurch sich Hinweise auf eine monomere Form ergaben. Erste 2D-Kristallisationsversuche mit DtpD und DtpA lieferten versprechende Befunde und werden weiter optimiert.

2. INTRODUCTION

2.1. Peptide transport

Peptides are amino acid polymers connected by peptide bonds. They are subdivided into the long-chain proteins and the short oligopeptides. The interest of the project underlying this thesis is in the transport processes for di- and tri-peptides. Peptide transport represents an important system in supply of amino acids for nutritional purposes; virtually all organisms from bacteria to man express peptide transport systems. They supply the cell with amino acids as energy source or as building blocks without the necessity of extracellular cleavage and uptake of the constituent amino acids requiring more cellular energy. Beyond this, peptide transport processes seem to be involved in signaling, gene regulation or metabolic adaptation (Detmers *et al.*, 2001).

2.1.1. The PTR family

The peptide transport (PTR) family was proposed 1995 by Steiner et al. (Steiner *et al.*, 1995) representing basically the earlier proposed proton-dependent oligopeptide transporter (POT) family (Paulsen and Skurray, 1994). Since it is not clear if all family members are proton-dependent and transport oligopeptides, the name PTR appears more appropriate. It is defined by two common sequence motives originally identified by (Paulsen and Skurray, 1994) as **G****D***G***TI*********G** and **F**F***IN*GSL** using an alignment of PEPT1 (rabbit), CHL1 (*Arabidopsis thaliana*), PTR2 (yeast), DtpT (*Lactococcus lactis*) and YhiP (*E. coli*) (Fig. 1, upper left panel). In the proposal of the PTR family (Steiner *et al.*, 1995) the alignment was done with the same sequences but AtPTP2-A and AtPTR2-B (both *Arabidopsis thaliana*) instead of YhiP, and a slightly different consensus line for the motives was obtained (**GG**AD**LGRY*TI*****IY*IG** and **FY**IN*GSL**). In a more recent paper (Daniel *et al.*, 2006) using more sequences an additional highly conserved domain was described as **EF*ERF*YYG** followed by **G***AD***GK**TI***S**Y**G** and **FS*FY*AIN*GSL** (Fig. 1). Fig. 1 shows also the localization of these sequences in the topology model between transmembrane domain (TM) 2 and TM 3 and at the beginning of TM 5. An easy comparison of the different motive versions shows Fig. 6 (p. 15) where also further conserved regions between eukaryotes and prokaryotes are marked.

Members of the PTR family are found in virtually all organisms, in animals, plants, yeast and bacteria with sometimes multiple paralogues. Some examples are shown in Fig. 2, where also the diversity of the sequences is indicated by the branch length. The number of amino acid residues varies from about 450-700 (the prokaryotic transporters have generally shorter

sequences) and a 12 α-helical transmembrane domain structure is assumed (varying with the prediction program, see 4.1.2, p. 16). There is not yet a crystal structure available for any PTR member that would prove this topology, but in some cases the topology model was verified by labeling assays, like for the bacterial DtpT (Hagting *et al.*, 1997b) or mammalian PEPT1 (Covitz *et al.*, 1998).

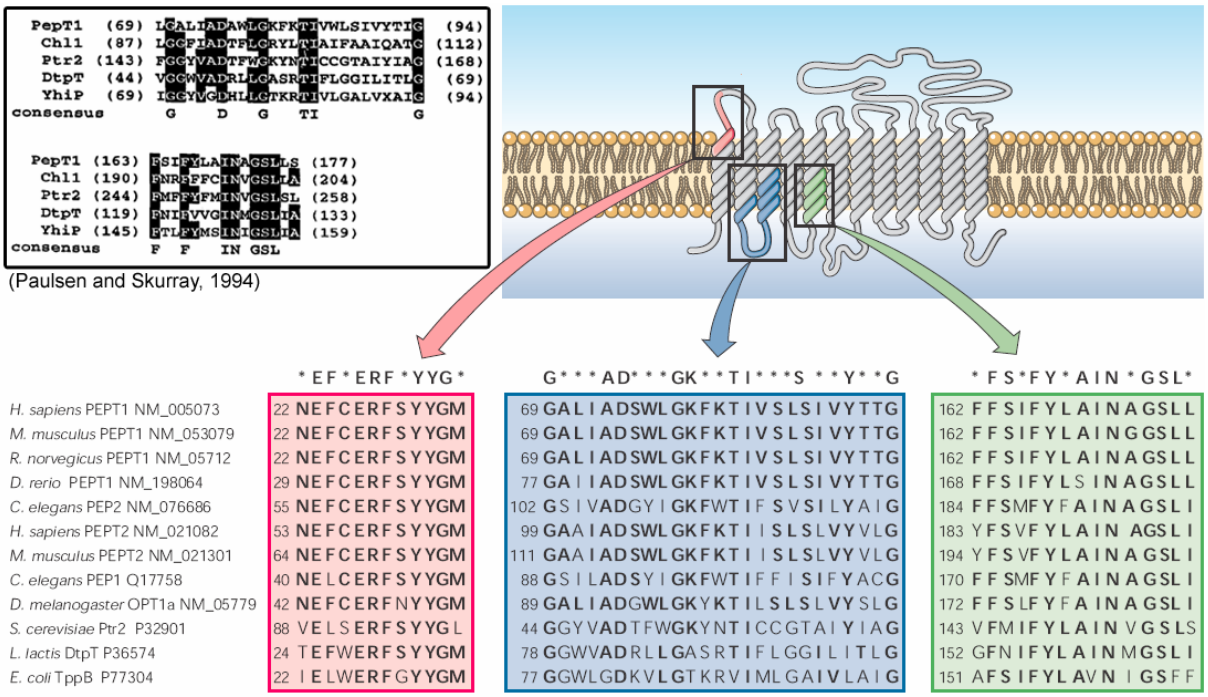

Fig. 1: Conserved sequence motives of the PTR family. Based on the predicted protein structure of PEPT1, the location of the three conserved domains is shown. Taken from (Daniel *et al.*, 2006): Alignment done with MultAlin with identical amino acids indicated in bold letters. NCBI GEO accession numbers of the proteins are shown. Upper left panel from (Paulsen and Skurray, 1994)

Substrates are in most cases peptides, but in some cases also other compounds have been shown to be transported or at least have been demonstrated to interfere with the transport process. The peptide histidine transporters (PHT1, PHT2) for example additionally take up histidine (Sakata *et al.*, 2001; Yamashita *et al.*, 1997) and in plants the transport of nitrate by AtNRT1.1 (CHL1) of *Arabidopsis thaliana* (Tsay *et al.*, 1993; Tsay *et al.*, 2007) was shown with the additional feature of a phosphorylation sensitivity. When the protein is phosphorylated at threonine 101 it exhibits high affinity (50 µM) for nitrate, otherwise it possess low affinity (~4 mM) (Liu and Tsay, 2003). In *A. thaliana* also AtPTR1 and AtPTR2 transport peptides with high efficiency and histidine with low efficiency (Chiang *et al.*, 2004; Dietrich *et al.*, 2004) and *Brassica napus* was reported to transport nitrate, histidine, arginine and lysine via the BnNTR1;2 transporter (Zhou *et al.*, 1998) and AgDCAT1 of alder (*Alnus glutinosa*) was shown to transport dicarboxylates with a K_t of 70 µM as shown for malate (Jeong *et al.*, 2004).

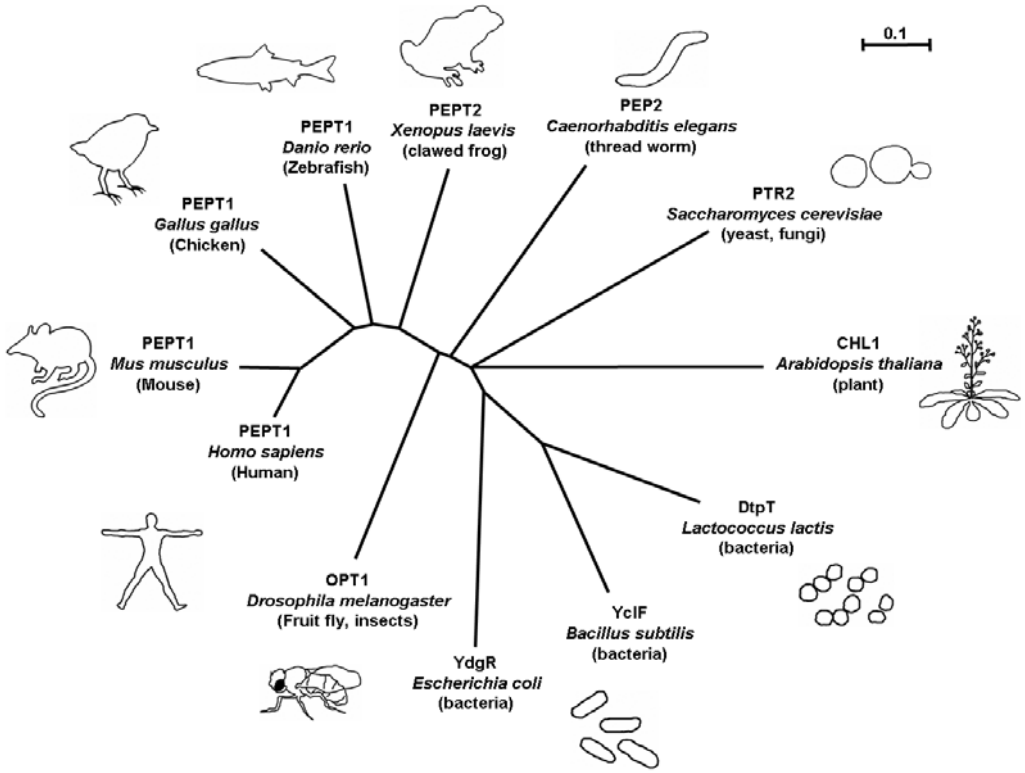

Fig. 2: Diversity of PTR transporters in different organisms. Done with Clustal W (Larkin *et al.*, 2007) and NJplot (Perriere and Gouy, 1996). Branch lengths are a measure of the amount of sequence divergence (scale bar indicates the number of amino acid substitutions per site).

An especially interesting feature that is described for the mammalian PEPT1 and PEPT2 is the ability of transporting antibiotics or other drugs that resemble di- or tripeptides in structure. These are in particular the β-lactam antibiotics (Bretschneider *et al.*, 1999; Ganapathy *et al.*, 1995), angiotensin converting enzyme (ACE) inhibitors and prodrugs like Val-acylovir or L-DOPA-Phe (Ganapathy *et al.*, 1998; Terada and Inui, 2004). In this respect the PTR family becomes an important research target for the design of pharmaceutically active substances and their delivery.

The general transport mechanism is based on a cotransport of the substrate with protons along the transmembrane electrochemical proton gradient. It can be formulated as follows:

$$\text{substrate (out)} + n\ H^+\text{ (out)} \rightarrow \text{substrate (in)} + n\ H^+\text{ (in)}$$

The stoichiometry was determined for PEPT2 with 2 H^+ per neutral and 3 H^+ per anionic dipeptides (Chen *et al.*, 1999), but for the low affinity type PEPT1 only 1 H^+ per neutral peptide (Amasheh *et al.*, 1997; Fei *et al.*, 1994) was proposed for flux coupling.

Since PTR proteins use the transmembrane proton gradient and not ATP or other chemical bound energy as driving force, these transporters are called secondary (or tertiary if another

step is in between) active transporters. In bacteria the proton gradient is secondary energy because it is generated by the plasma membrane respiratory chain using the primary chemical energy (Fig. 3, upper part). In case of polarized mammalian cells the chemical energy in form of ATP is transformed to a Na^+ gradient by the Na^+/K^+-ATPase in the basolateral membrane, which then is transformed into a proton gradient by the activity of the electroneutral Na^+/H^+-exchanger NHE3 (Fig. 3, lower part).

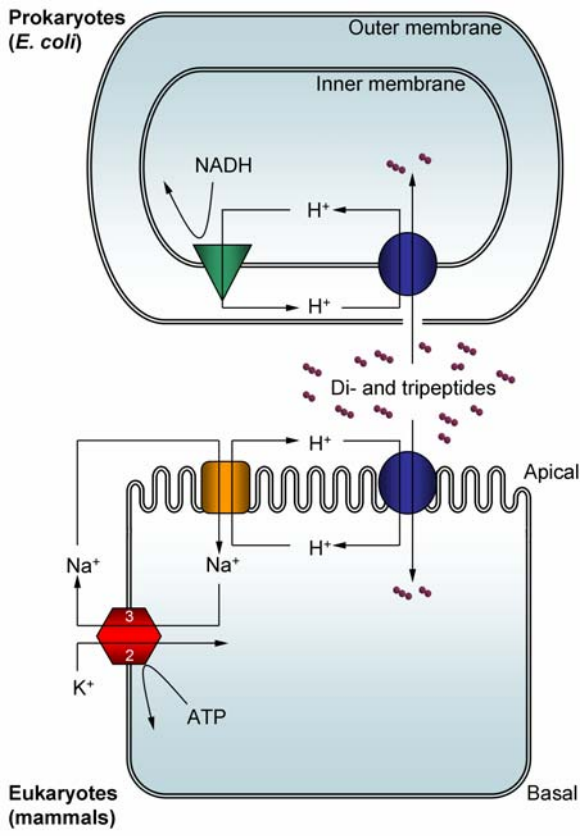

Fig. 3: Model for uptake of peptides by PTR transporters in bacterial or mammalian cells: In both cases the proton gradient is used as driving force to import di- and tripeptides in cotransport. The upper panel shows the situation in prokaryotes like *E. coli*, where the proton gradient is generated by the respiratory chain. The lower panel shows the situation in epithelial cells of higher eukaryotes. Here the proton gradient is regenerated by Na^+/H^+ exchange while the Na^+ gradient is generated by the Na^+/K^+-ATPase.

2.1.2. Mammalian PEPT1 and PEPT2

The PTR transporter family in mammals (SLC15 family) consists of PEPT1 (SLC15A1), PEPT2 (SLC15A2), PHT1 (SLC15A4) and PHT2 (SLC15A3). The latter two proteins seem to transport primarily histidine in addition to selected dipeptides but are yet not well characterized (Daniel *et al.*, 2006). PEPT1 and PEPT2 transport di- and tripeptides and have been studied extensively (Daniel and Rubio-Aliaga, 2003; Daniel and Kottra, 2004). PEPT1 is a low-affinity but high-capacity transporter mainly located in the intestine while PEPT2 is

the high-affinity low-capacity variant found in kidney, lung, brain and other cells. Their main functions are the uptake of peptides for nutrition from the gut or reabsorption of peptides in the kidney.

There is a considerable interest in mammalian transporters, not only because of their crucial role for human and animal nutrition, but also as they additionally mediate uptake of pharmaceutical substances (β-lactam antibiotics (Bretschneider *et al.*, 1999; Ganapathy *et al.*, 1995), angiotensin converting enzyme (ACE) inhibitors, the anti-cancer agent bestatin and prodrugs like Val-acylovir or L-DOPA-Phe (Ganapathy *et al.*, 1998; Terada and Inui, 2004)). Therefore much research is done to elucidate the crucial features that define a substance that is transported (Biegel *et al.*, 2006; Brandsch *et al.*, 2004; Daniel *et al.*, 1992; Terada *et al.*, 2000; Theis *et al.*, 2002). With this knowledge it is possible to modify drugs in a way that they are transported by PEPT1, which has the advantage that the drug can be applied orally and is absorbed in the gut with proper bioavailability.

Substrate patterns of PEPT1 and PEPT2 are very similar with PEPT2 being slightly more restrictive but having generally higher affinities (~5-15 fold). A fascinating feature is the promiscuity of transport, considering the large number of possible di- and tripeptides (400 and 8000) with their variability in size, charge and polarity. Inhibitory constants (K_i) for dipeptides vary from 0.8 µM for Trp-Trp (PEPT2) to >10 mM for D-Ala-D-Ala with most natural peptides being high-affinity substrates (0.1 mM < K_i < 1 mM) of which in case of PEPT2 hydrophobic peptides possess highest affinities (Biegel *et al.*, 2006). The affinity is dependent on the position of a charged side chain in a peptide backbone. Positively charged amino acids are preferred at the aminoterminus while negatively charged amino acids are preferred at the carboxyterminus. Transport is also stereoselective: while L-amino acids are favored in all positions, D-amino acids are better tolerated at the aminoterminus (Daniel *et al.*, 1992). For tripeptides there are fewer studies, but also here the presence and position of charged and D-amino acids affects the affinity. Neither PEPT1 nor PEPT2 requires a peptide bond in the substrate. The minimal substrate features are just a positively charged aminoterminus and a negatively charged carboxyterminus separated by the minimal distance of four methyl groups with a spatial distance of 500-630 pm (Doring *et al.*, 1998). In case of PEPT2 there is also a central carbonyl group (like in 5-aminolevulinic acid) obligatory for high affinity (Theis *et al.*, 2002). In experiments using omega-amino acids, also compounds with chain lengths exceeding those of tripeptides were substrates, what might be caused by the higher flexibility of these structures compared with peptides (Doring *et al.*, 1998).

The current topology model (based on hydrophobicity analysis and biochemical analysis) shows 12 transmembrane helices (TM) with amino- and carboxyterminus facing the cytosol (Fig. 1, p. 4). Between TM 9 and TM 10 lies a large extracellular loop. Still missing is a high resolution protein structure and a final understanding of the mechanism of the transport. This can be elucidated by protein crystallization, which was yet unsuccessful because of the difficulty to produce large amounts of the proteins.

2.1.3. Peptide transport in *E. coli*

Unlike to the situation in higher organisms, the transport of peptides in *E. coli* is obviously not only done by PTR transporters. Early studies reported three components, the oligopeptide permease Opp, the dipeptide permease Dpp and the tripeptide permease TppB (Higgins and Gibson, 1986; Payne and Smith, 1994; Payne and Marshall, 2001). Opp and Dpp belong to the ATP binding cassette (ABC) transporters and consist of a membrane spanning protein and a separate periplasmatic binding protein (Abouhamad *et al.*, 1991; Higgins, 2001; Hiles *et al.*, 1987). Opp transports larger peptides while the substrates of Dpp are di- and tripeptides. TppB (YdgR) as a PTR member is a different type of transporter and uses the proton-gradient as energy source by cotransport of peptides with protons into the cytoplasm. When the sequence of TppB was available it was identified as a member of the peptide transport (PTR) family (Smith *et al.*, 1999; Weitz *et al.*, 2007). Early functional studies with TppB were basically conducted in *Salmonella thyphimurium* (Gibson *et al.*, 1984; Jamieson and Higgins, 1984) and *E. coli* (Payne *et al.*, 2000a; Payne *et al.*, 2000b) using deletion mutants selected with the toxic phosphono-peptide alafosfalin. The up-regulation in cells exposed to anaerobic conditions or to leucine was also demonstrated (Jamieson and Higgins, 1984, , 1986). Concerning substrate patterns, TppB seemed to prefer tripeptides, in particular those of hydrophobic nature. The transport mode was poorly characterized and not documented in literature. In the genome of *E. coli* there are three more members of the PTR family: *yhiP*, *yjdL* and *ybgH* about which nothing was known. Based on the data reported here and in analogy to other PTR transporters in bacteria, the coherent naming of this family as di- and tripeptide permease *dtpA*, *dtpB*, *dtpC* and *dtpD* for *ydgR* (*tppB*), *yhiP*, *yjdL* and *ybgH* is proposed.

2.2. Protein structure of PTR transporters

One aim of this project was to obtain high quality structural information of a PTR family transporter. This would give new insights into the transport mechanism and substrate binding domain and subsequently enable the design of compounds that are good substrates. As the

mammalian PEPT1 is an efficient uptake system in the gut, this would be of very high value for the design of orally available drugs.

The method of choice for high resolution structural information is protein-crystallization and diffraction analysis of the crystals (McPherson, 2004). Two problems arise here with membrane proteins: (1) a high amount protein production is difficult to achieve because of the limited membrane space and (2) the proteins need detergents to become water soluble for purification, which can disrupt structure or hinder crystal formation. Therefore, there are not many crystal structures of membrane proteins available: the most similar candidates to the PTR transporters that are in the same superfamily, the major facilitator superfamily (MFS), are the proton coupled *E. coli* lactose permease LacY (Abramson *et al.*, 2003), and *E. coli* GlpT, the glycerol-3-phosphate/inorganic phosphate antiporter (Huang *et al.*, 2003).

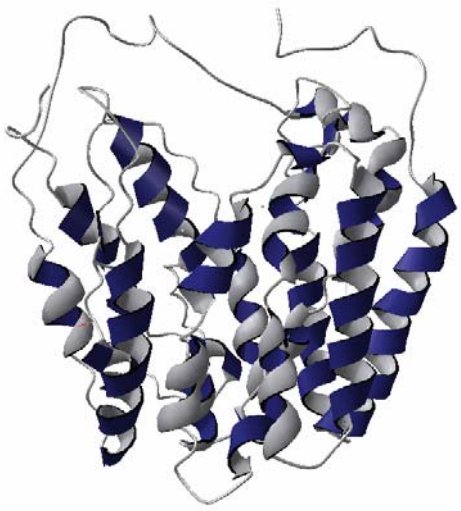

Fig. 4 Structural model of LacY with locations of the transmembrane α-helices: Based on x-ray diffraction data of Abramson et al. (Abramson *et al.*, 2003). Generated with Swiss-PdbViewer.

A solved crystal structure reveals the location of single atoms in the protein and enables the design of a 3-dimensional model showing the exact location of the transmembrane helices, which is shown for LacY in Fig. 4. Because both proteins show 12 transmembrane helices, like it is predicted for PEPT1, attempts were undertaken to model the structure of the PTR transporters on basis of LacY and GlpT structures (Meredith and Price, 2006). Also complete computer based modeling with refining on basis of mutation data was applied (Bolger *et al.*, 1998). The more reliable strategy is to use another PTR transporter as model; best chances provide prokaryotic candidates, because they are available in high amounts for crystallization (Granseth *et al.*, 2007; Wang *et al.*, 2003).

For the crystallization of membrane proteins, 2D electron crystallization is especially suitable because proteins are in their natural hydrophobic environment, where detergents are not necessary (Hite *et al.*, 2007; Tsai and Ziegler, 2005). It is also provides a better option to obtain different transport states for example with bound substrate. 2D crystals are essentially proteoliposomes with a very high protein to lipid ratio. The proteins arrange themselves in the membrane as crystalline grids, which are used for diffraction of an electron beam. Reverse Fourier-transformation of the diffraction data results in pictures with higher resolution, while 3D information can be obtained by tilting the sample in the beam. The advantage of 2D approaches is that it is not like 3D X-ray crystallization an “all or nothing” process, and even poorly ordered crystals may allow at least the TM arrangement to be extracted (Hite *et al.*, 2007). Although the maximal resolution of 3D X-ray crystallization is higher with around 1 Å (0.1 nm) and even subatomic insights (Lecomte *et al.*, 2004), in 2D electron crystallization a resolution of up to 1.9 Å (0.19 nm) can be achieved (Hite *et al.*, 2007).

3. AIM OF THE THESIS

This thesis is part of a project aiming towards obtaining high quality structural information on PTR transporter proteins. This is possible with 2D and 3D crystallization, for which high quantities of purified PTR transporter proteins have to be produced. As high amounts of the candidates that are most interesting, human PEPT1 and PEPT2, are very unlikely to obtain, the strategy was to use prokaryotic homologues proteins as models. *E. coli* was chosen and four homologues of human PEPT1 were identified in the bacteria. The focus of the project underlying this thesis was the overexpression of the *E. coli* homologues with high protein yields for crystallization trials. Additionally, the proteins were functionally characterized to elucidate their functional similarity to other members of the PTR family, and thereby prove the suitability of the *E. coli* transporters as models.

Obtaining a structure of such a PTR model protein would provide a much better understanding of the arrangement in the membrane, the definition of the substrate binding site and on the transport mechanism. It also could eventually enable a better and rational design of drugs to be transported by the intestinal PEPT1 for improved oral availability.

4. RESULTS

4.1. Sequence analysis

Protein sequences and calculated parameters of the four transporters (with His-tag) are available in the Appendix (9.2, p. 116).

4.1.1. Homology search in *E. coli*

Four members of the PTR transporter family can be identified by sequence homology search using BLAST (Altschul *et al.*, 1997) with a known PTR transporter. As the mammalian transporters are especially interesting, human PEPT1 and PEPT2 were used as templates for protein BLAST search. A multiple sequence alignment is shown in Fig. 6, where the amino acid sequences of DtpA, DtpB, DtpC, DtpD, PEPT1 and PEPT2 are compared. Strong homology (indicated by the black and grey highlighted areas) is found in the N-terminal region, whereas the middle part of the protein shows only weak homology and large gaps are found. PEPT1 and PEPT2 are considerably larger with 708 and 729 amino acids and possess ~200 amino acids more than the *E. coli* transporters with 500, 489, 485 and 493 amino acids for DtpA, DtpB, DtpC and DtpD. The missing regions in the *E. coli* transporters are mainly localized in hydrophilic regions especially in the large extracellular loop of PEPT1 and PEPT2 that is found between transmembrane domain (TM) 9 and TM 10.

Table 1: Sequence similarity between human and *E. coli* PTR transporters

	PEPT1	PEPT2	DtpA	DtpB	DtpC
PEPT1	100 / - / -				
PEPT2	**47** / 22 / 9	100 / - / -			
DtpA	22 / 28 / 13	21 / 28 / 14	100 / - / -		
DtpB	20 / 29 / 17	21 / 26 / 14	**52** / 24 / 10	100 / - / -	
DtpC	22 / 29 / 14	23 / 26 / 13	26 / 28 / 15	26 / 40 / 15	100 / - / -
DtpD	24 / 30 / 15	24 / 27 / 14	26 / 29 / 13	25 / 28 / 14	**56** / 18 / 8

% identical amino acids / % conserved amino acids / % semi-conserved amino acids
Based on Clustal W alignment

A quantitative analysis of sequence similarity between all six transporters is shown in Table 1. Here the identical, conserved and semi-conserved (week homology) amino acids in each protein are compared to the others, as derived from Clustal W alignments (Larkin *et al.*, 2007). Highest similarity is found in the pairs PEPT1/PEPT2, DtpA/DtpB and DtpC/DtpD.

As a more general comparison of the sequence similarity within the PTR family, selected members from different species were compiled using Clustal W (Larkin *et al.*, 2007). Instead of a multiple alignment (like Fig. 6) the sequence similarity is displayed as a dendrogram (Fig. 5). Here the length of the branches that separate two proteins is equivalent to the differences in the amino acid sequences. It is obvious that the eukaryotic candidates cluster together and the prokaryotic DtpT from *Lactococcus lactis* is slightly nearer to the eukaryotes than the *E. coli* proteins. OPT1 from *Drosophila melanogaster* is found closer to the mammalian PEPT1 and PEPT2 than PEP1 and PEP2 from *Caenorhabditis elegans*. A little more separated are the proteins from yeast and plants that are about the same distance away from PEPT1 and PEPT2.

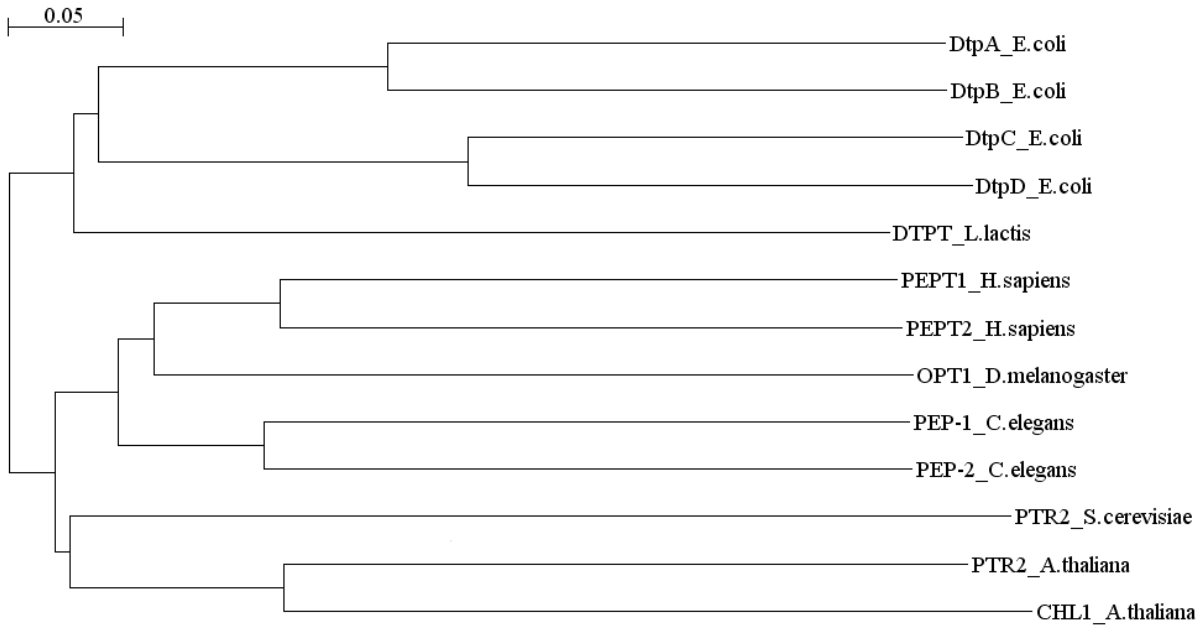

Fig. 5: Dendrogram of sequence similarity amongst PTR transporters. Analysis was done with Clustal W (Larkin *et al.*, 2007) and NJplot (Perriere and Gouy, 1996) Branch lengths are a measure of the amount of sequence divergence (scale bar indicates the number of amino acid substitutions per site).

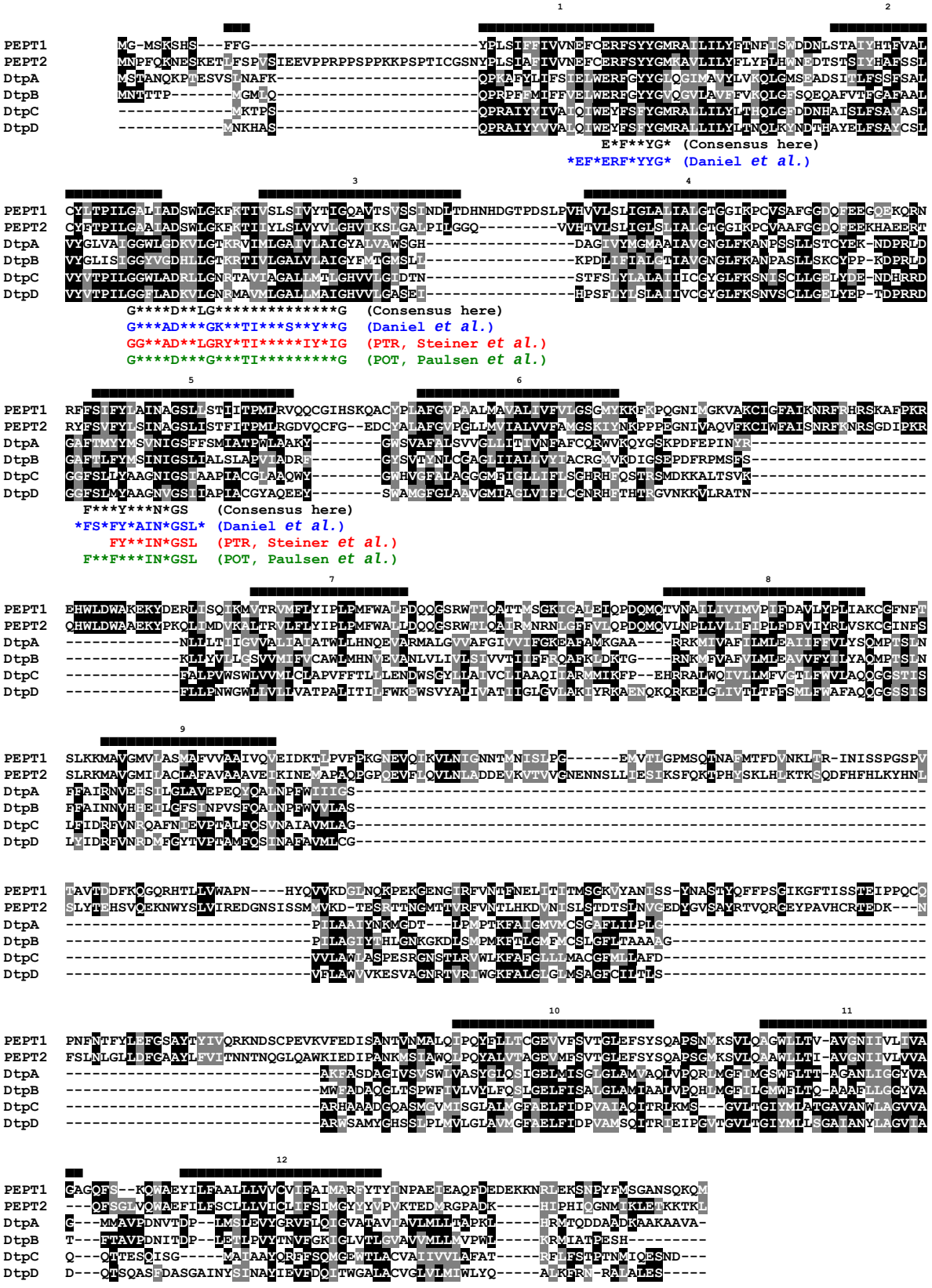

Fig. 6: Multiple sequence alignment of PTR transporters from human and *E. coli*. Done with Clustal W (Larkin *et al.*, 2007) and boxshade. Black shading if ≥30% of the sequences have identical amino acids and grey shading if ≥30% of the sequences have similar amino acids. The predicted transmembrane domains for PEPT1 are shown above and the sequence motives that are characteristic for the family from different sources are indicated below (Daniel *et al.*, 2006; Paulsen and Skurray, 1994; Steiner *et al.*, 1995).

4.1.2. Transmembrane domain structure prediction of the PTR family members

As a first attempt for structure predictions of membrane proteins the sequence is analyzed with transmembrane domain (TM) detection software. This is based on the calculation of hydrophobicity and alpha-helical character in clusters of appropriate length. Many different programs have been developed by the scientific community and are accessible on the internet. For DtpA several programs were tested using the preset default parameters. As Table 2 shows, the results are not definite but vary from 10 to 15 transmembrane domains. Some programs also give different possibilities or state high or low probability for TMs.

Table 2: Transmembrane domain prediction for DtpA

Program	TM prediction
TMHMM 2.0 (Krogh *et al.*, 2001)	14
MEMSAT 1.5 (Jones *et al.*, 1994)	13
MEMSAT 2 (McGuffin *et al.*, 2000)	14
SOSUI (Hirokawa *et al.*, 1998)	14
DAS (Cserzo *et al.*, 1997)	11-15
TM-Finder (Deber *et al.*, 2001)	10-12
TM-Pred (Hofmann and Stoffel, 1993)	12-13
PRED-TMR2 (Pasquier *et al.*, 1999)	12
HMMTOP 2.0 (Tusnady and Simon, 2001)	14
TMAP (Persson and Argos, 1997)	12

TMHMM (Krogh *et al.*, 2001) was reported as one of the most reliable programs for membrane domain prediction (Moller *et al.*, 2001); therefore, it was chosen for comparison of the TM predictions of some of the PTR family members. The result is shown in Fig. 7 where the longer eukaryotic proteins are predicted to possess 10-12 TMs and the shorter bacterial transporters to have 13 or 14 TMs. This is not ideal if the structure from the prokaryotes should be taken as model for the eukaryotes, but as already indicated by the variance between different programs TM prediction is just a prediction which needs experimental verification. For example in case of DtpT alkaline phosphatase fusion protein studies indicate 12 TMs (Hagting *et al.*, 1997b) although TMHMM predicts 13 TMs. Generally the PTR members are considered to form 12 TMs like predicted for PEPT1 (Daniel *et al.*, 2006), but TMHMM shows differing numbers even for the highly similar PEPT2.

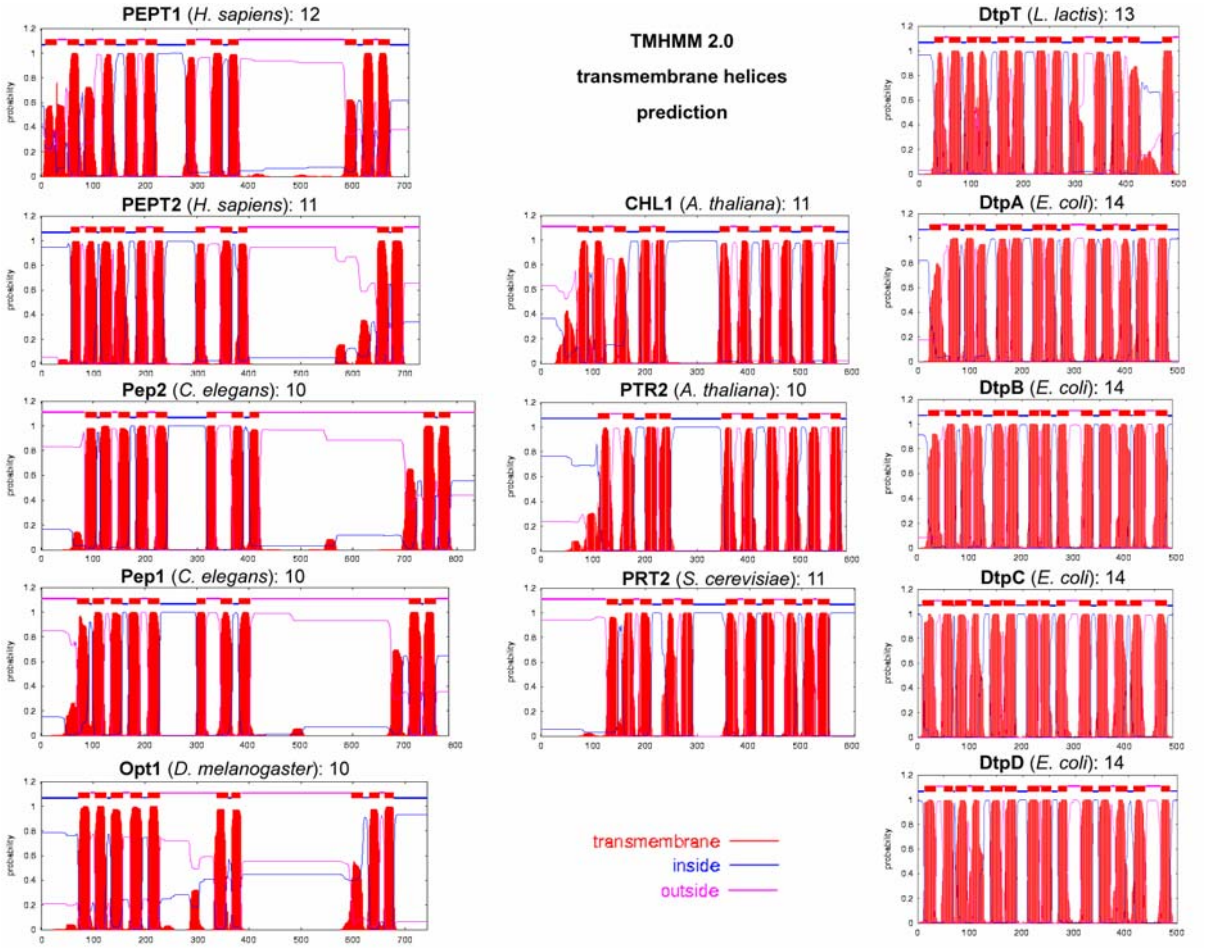

Fig. 7: Transmembrane domain prediction of PTR transporters. Done with TMHMM 2.0 (Krogh *et al.*, 2001). The x-axis represents the length of the protein and the y-axis the probability for a transmembrane helix. On top is always a small scheme of the topology of the protein with inside, outside and transmembrane parts marked.

4.1.3. Genetic localization of the PTR members of *E. coli*

Genetic localization of the transporter genes in the *E. coli* genome was examined to identify surrounding genes and predict regulatory processes that may provide hints for the physiological importance of the multiple transporters. The genetic area of each transporter is shown in Fig. 8 as exported from the EcoGene *E. coli* genome database (Rudd, 2000) (www.ecogene.org). Especially an affiliation with an operon was considered as informative, but also clusters of related genes. The first, *dtpD* (*ybgH*), reads in the opposite direction than the surrounding genes and hence is not part of an operon. Of the nearby genes only *phr* has a described function as photolyase in DNA repair. In contrast *dtpA* (*tppB*, *ydgR*) has only known neighbors. Directly behind and in the same direction comes *gst* coding for a glutathione S-transferase (conjugation of reduced glutathione to a wide number of exogenous and endogenous hydrophobic electrophiles; hydrogen peroxide resistence). Then follows in the other direction *pdxY* (pyridoxal kinase), *tyrS* (tyrosine t-RNA ligase) and *pdxH* (Pyridoxine/pyridoxamine phosphate oxidase; isoniazid resistance). Upstream of *dtpA* there

is in the same direction but with some distance *nht* (Endonuclease III, DNA glycosylase/apyrimidinic lyase; DNA repair), *rsxA* - *rsxE* (Reducer of SoxR (regulator of superoxide defense)). None of these genes shows obvious relation to peptide transport. Before *dtpB* (*yhiP*) lies in the same orientation *uspA* (Universal stress protein) and in the other orientation *uspB* (Universal stress protein; ethanol resistance in stationary phase) preceded by *pitA* (low-affinity inorganic phosphate transport protein). Downstream of *dtpB* but in the other direction follows *prlC* (Protein localization: Oligopeptidase A, zinc metalloprotease; involved in the degradation of cleaved signal peptides; suppressor allele of LamB signal sequence mutations; heat shock regulon; multifunctional protease) and a yet undescribed second gene of the *prlC* operon. These genes are at least to some extent related to peptides, particularly signal peptides.

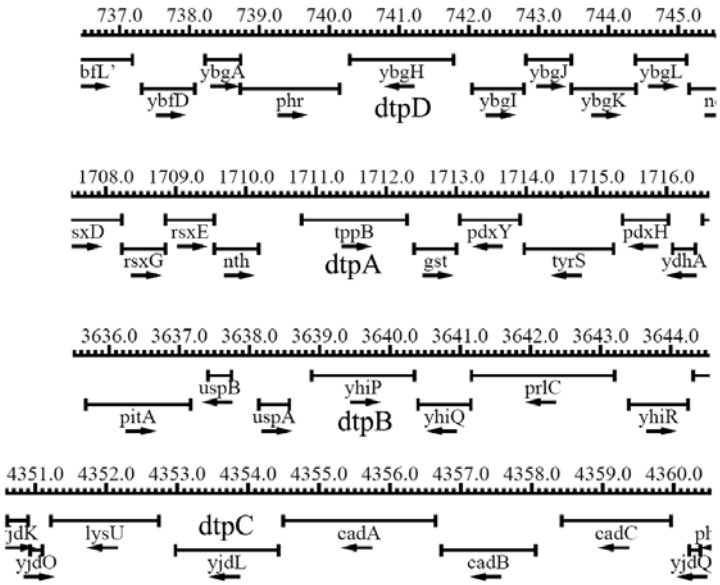

Fig. 8: Genetic localization of the PTR genes in the *E. coli* genome. Data from the EcoGene database (Rudd, 2000). The scale is in kb.

In case of *dtpC* several of the surrounding genes are related to lysine and lysine metabolism. It is also striking that they are all orientated in the same direction, starting with the *cad* operon *cadC* (Transcriptional activator for cadBA, low external pH-, low oxygen-, excess lysine-responsive), *cadB* (cadaverine operon; lysine-cadaverine antiporter) and *cadA* (cadaverine operon; lysine decarboxylase, acid-inducible) directly followed by *dtpC*. It has been speculated that *dtpC* (*yjdL*) might be part of the operon, but a strong transcriptional terminator is located after *cadA* (Meng and Bennett, 1992). Further downstream lies *lysU* (lysine tRNA ligase, heat inducible) followed by four small and divergent genes of unknown function.

4.2. Overexpression in *E. coli*

Basis of the functional characterization as well as for the structural characterization was the overexpression of the transporter genes in *E. coli*. This was done using the pET-21 over-expression system as described in the methods section (7.4, p. 87). The genes were cloned in the pET-21 vector which adds a carboxy-terminal hexahistidine tag (His-tag) as described in the methods section (7.3, p. 85). This tag was used for detection by Western blot and for Ni^{2+} affinity purification. Fig. 9 is the Western blot analysis of overexpression experiments with all four transporters. It shows in panel A for DtpA that with no induction by Isopropyl-β-D-thiogalactopyranosid (IPTG) there is no signal in the soluble protein fraction (lane 1, sol), the detergent solubilized membrane protein fraction (lane 2, ddm) and the insoluble fraction (lane 3, pellet). If protein production was induced by IPTG, there appears a band at about 40 kDa. It is absent in the soluble protein fraction (lane 4, sol), dominant in the detergent solubilized membrane protein fraction (lane 5, ddm) and weak the insoluble fraction (lane 6, pellet). As 40 kDa is smaller than the calculated 55 kDa based on the amino acid sequence of DtpA, it had to be tested if degradation had occurred. Therefore, a new construct was cloned for DtpA (pET-21b-T7-YdgR-His), where in addition to the C-terminal His-tag an N-terminal T7-tag is present.

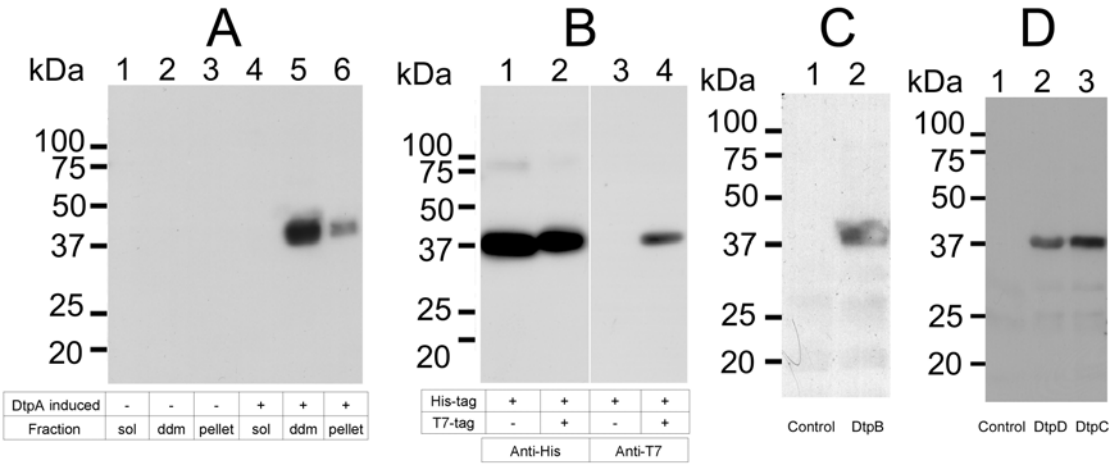

Fig. 9: Western blot analysis of DtpA, DtpB, DtpC and DtpD proteins overproduced. Separation done on 12.5% SDS-PAA gels **(A)** Soluble and membrane fractions of uninduced (lane 1-3) and IPTG-induced (lane 4-6) *E. coli* containing the *dtpA* expression plasmid; probed with the His-tag antibody. Each lane contains protein from an equivalent of 40 µl bacterial culture: soluble proteins (lane 1 and 4), DDM solubilized membrane proteins (lane 2 and 5) and non-solubilized proteins (lane 3 and 6). **(B)** Comparison of DtpA protein expressed with a C-terminal His-tag and DtpA exhibiting a C-terminal His-tag and an N-terminal T7-tag. Membrane proteins of IPTG-induced *E. coli* cells were probed with the His-tag antibody (lane 1 and 2) or an anti-T7 antibody (lane 3 and 4). Each lane contains protein from an equivalent of 100 µl bacterial culture. **(C)** Anti His-tag Western blot of *E. coli* membranes of control cells (lane 1) or membranes containing over-produced DtpB (lane 2). Each lane contains 50 µg total protein from an equivalent of ~600 µl bacterial culture. **(D)** Anti His-tag Western Blot of *E. coli* membranes of control cells (lane 1), membranes containing overproduced DtpD (lane 2) or DtpC (lane 3). Each lane contains 50 µg total protein from an equivalent of ~600 µl bacterial culture.

If both tags can be detected in the 40 kDa band, then it is probable that the protein is full length. Fig. 9 B shows in lane 1 the construct with the carboxy-terminal His-tag and in lane 2 with the additional T7-tag probed with the His-tag antibody. In both lanes the 40 kDa band is visible with the T7-tag construct being slightly bigger, probably due to the additional tag (11 amino terminal amino acids of the T7 gene 10, plus ten amino acids spacer). The same samples probed with the T7-tag antibody show a signal of similar molecular mass in case of the protein with the T7-tag (lane 4) but not with the normal construct (lane 3). Therefore it can be concluded that both termini are present and the abnormal running behavior or mass might be due to an excess of SDS bound because of the high hydrophobicity of membrane proteins. This is the same with DtpB as shown in Fig. 9 C. A band of 40 kDa (expected mass 54.6 kDa) appears in induced *E. coli* cells carrying the expression plasmid for *dtpB*, but not in induced control cells with the empty vector. Fig. 9 D shows the situation for DtpC and DtpD, which also appear as 40 kDa bands, which is smaller than expected (54.1 kDa and 55.2 kDa, respectively).

The **expression level** of the four proteins differed markedly. Fig. 10 shows a Coomassie gel and a Western blot of DDM-solubilized and pelleted fractions of overexpressing *E. coli* membranes. Especially in case of DtpA, but also with DtpB and DtpD, a strong band is already visible in the Coomassie gel at the expected height. For DtpA and DtpD a considerable amount of protein seems also to be in the pellet fraction. This was confirmed in the Western blot and may represent aggregated protein, inclusion bodies or inefficient cell extraction. As usually, the major signal was in the solubilized fraction (for DtpA see Fig. 9 A), the reason here is probably variance in extraction efficiency. In the Western blot, DtpA appears as most strongly produced followed by DtpB. DtpD appears in the Western blot much weaker than expected from the Coomassie gel, which was also confirmed later with purified DtpD and indicates a weaker recognition of the protein by the His-tag antibody. DtpC produced only a very faint band, but was usually slightly stronger (see Fig. 9 D). Together with the later observation from purified DtpC that it is recognized well by the His-tag antibody, it can be concluded that DtpC is produced only in small quantities. The amounts of produced protein in membranes were estimated by comparison on Western blot to the corresponding purified protein. For DtpA this resulted in about 15 mg/L culture, for DtpB and DtpD about 6 mg/L culture and for DtpC 0.8 mg /L culture. The amounts that were actually available after purification were about one third of this. For optimization of the production, several parameters were modified. The expression was best for induction of cells at an OD_{600} of 0.8 with an Isopropyl-β-D-thiogalactopyranosid (IPTG) concentration of 0.1 mM and 2-3 h growth after induction. Variation of the temperature from 37 °C to 30 °C or 25 °C did not improve the amount of protein in the DDM-solubilized fraction.

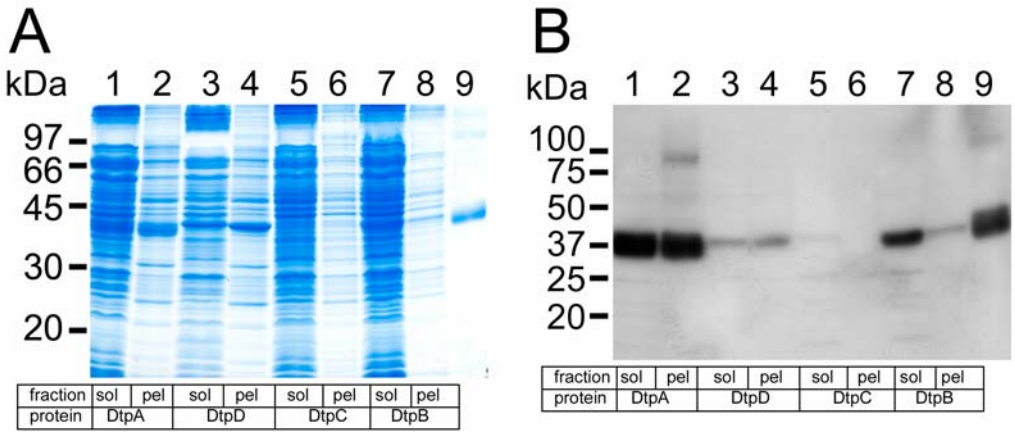

Fig. 10: Expression level of the four transporters. (A) Coomassie stained 12.5% SDS-PAA gel. Samples correspond to 200 µl culture of overexpressing *E. coli*. Uneven numbered lanes are DDM-solubilized membranes and even numbered lanes are pellets after solubilization. Lanes 1-2 is DtpA, lanes 3-4 is DtpD, lanes 5-6 is DtpC, lanes 7-8 is DtpB and lane 9 is 1.3 µg purified DtpA. **(B)** Anti His-tag Western blot of the same samples as (A) but only half the amount.

4.3. Purification of proteins by Ni^{2+} affinity chromatography

Solubilization with the different mild detergents CHAPS, Triton-x-100 and dodecyl-β-D-maltopyranoside (DDM) showed for DtpA highest stability in DDM. In Western blotting here the highest amount of protein was visible at the expected height and no degradation bands or aggregates were observed. The detergents decylmaltopyranoside (DM); nonylglucopyranoside (NG); octylthioglucopyranoside (OTG); undecylmaltopyranoside (UDM); decylphosphocholine (FOS-10); pentadecafluorooctanic acid (PDFOA) and cyclohexyl-heptyl-β-D-maltopyranoside (CYMAL-7) were screened by the cooperation partner in Basel, from which only Cymal-7 appeared similarly suitable. DDM was chosen as standard detergent for all four proteins.

The chromatogram of a DtpA purification using a Ni^{2+}-affinity column on a FPLC system is shown in Fig. 11. Protein was detected by UV absorption in the solution after column separation. The first broad absorption maximum is the flow-through of unbound proteins. After washing with buffer an imidazole gradient was applied leading at about 25% (~125 mM) to the elution of the bound protein in a sharp peak. Protein concentration of the peak fractions was tested and purity was controlled on Coomassie gels.

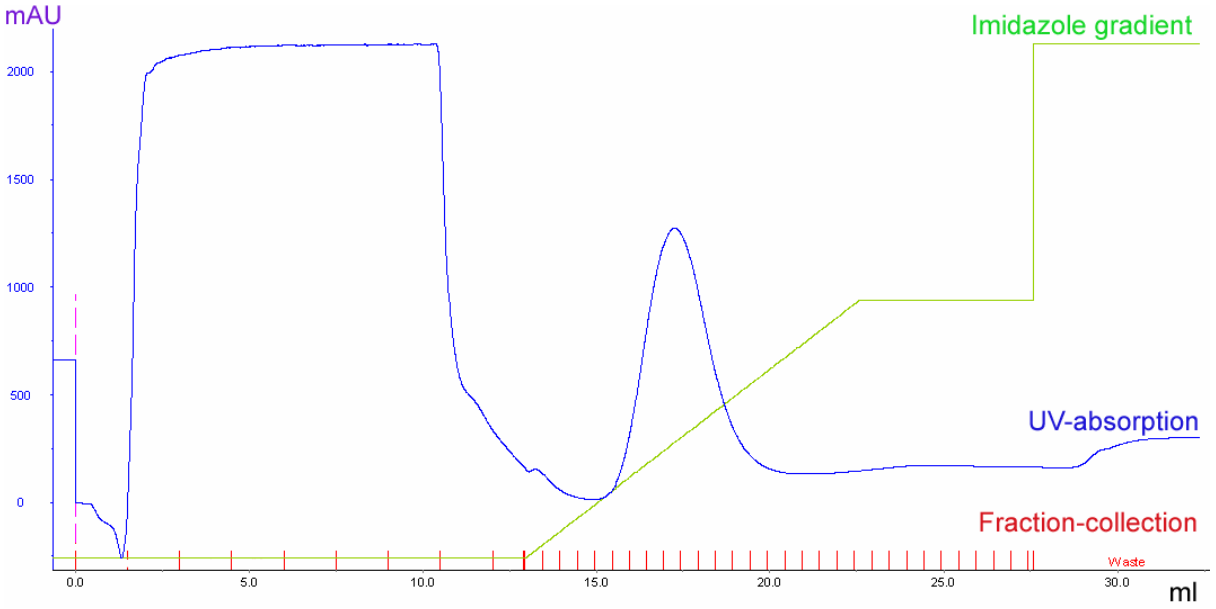

Fig. 11: Chromatogram of a Ni^{2+} based purification of DtpA. Inner membranes from *dtpA* overexpressing *E. coli* were solubilized with 1% DDM and loaded on a 1 ml Ni^{2+}-affinity column using an FPLC system. Elution was performed by a linear imidazole gradient from 30 mM to 280 mM. DtpA eluted at about 125 mM imidazole in a sharp peak.

Gels from purifications of all four transporters are shown in Fig. 12. In the elution fractions (always lane 6), there is an obvious variance found in purification efficiency. This correlates in part with the expression level, as DtpC, with lowest expression level was also less successfully purified. Here the contaminating bands were as strong as the DtpC band at ~40 kDa (verified by Western blot of the elution fraction; not shown); the two strongest contaminating bands at 45 kDa and 66 kDa also weakly appear in the DtpB elution. DtpD is most pure and shows a clear, dense band, which has a medium expression level. DtpA, which has the highest expression level is quite pure but has a broad, blurry band. DtpB is again less pure despite its intermediate expression level.

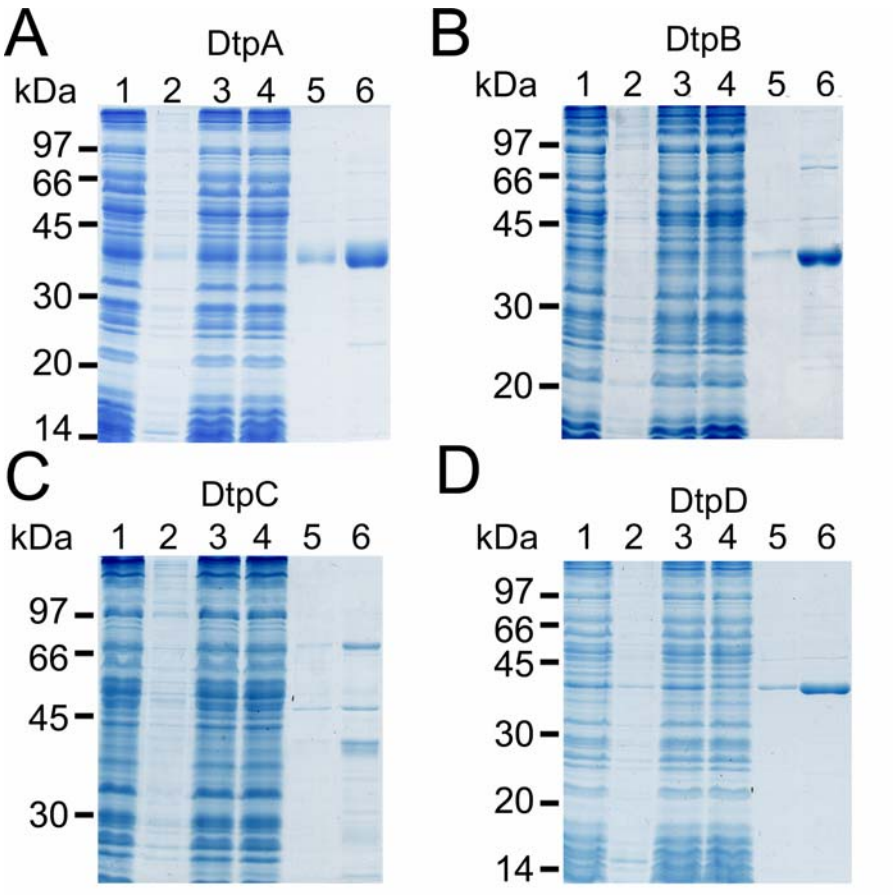

Fig. 12: Coomassie-gels from N^{2+}-affinity purifications of the proteins. In all four panels loading of 7 µl (except C6: 10 µl) of, in lane 1: DDM-solubilized membranes; lane 2: pellet after solubilization; lane 3: supernatant after solubilization; lane 4: flow-through; lane 5: wash; lane 6: elution peak fraction (at ~125 mM imidazole) **(A)** DtpA; **(B)** DtpB; **(C)** DtpC; **(D)** DtpD.

4.4. Functional characterization

Most experiments for functional characterization were performed by uptake of labeled substrates into living *E. coli* cells. Additionally in vitro characterizations were performed in liposomes by uptake of labeled substrates or via electrical measurement of transport functions. Further functional information was gained from uptake studies in KO mutant *E. coli* lines and in form of growth experiments in presence of toxic substrates.

4.4.1. *In vivo* uptake experiments

For the detection of uptake, labeled reporter substrates had to be identified for each transporter. Therefore, the PEPT1 substrate β-Ala-Lys-N_ε-7-amino-4-methyl-coumarin-3-acetic acid (β-Ala-Lys(AMCA)) was tested first. From the four transporters only DtpA showed sufficient uptake of the fluorescent reporter (Fig. 13 A) and therefore this substrate could be used for further characterization of DtpA. As second PEPT1 substrate [^{14}C]Gly-Sar was tested as well and was shown to be transported by DtpA and by DtpB (Fig. 13 B). Further potential substrates were screened, from which [^{3}H]lysine was identified as suitable for DtpC and [^{14}C]6-aminohexanoic acid for DtpD. Using the respective reporter substrates, for each transporter the time-dependence of uptake and the affinity of the corresponding substrate was determined, followed by analysis of their proton-, Na^+- and pH dependence. The substrate specificity was elucidated with competition experiments employing larger groups of test compounds.

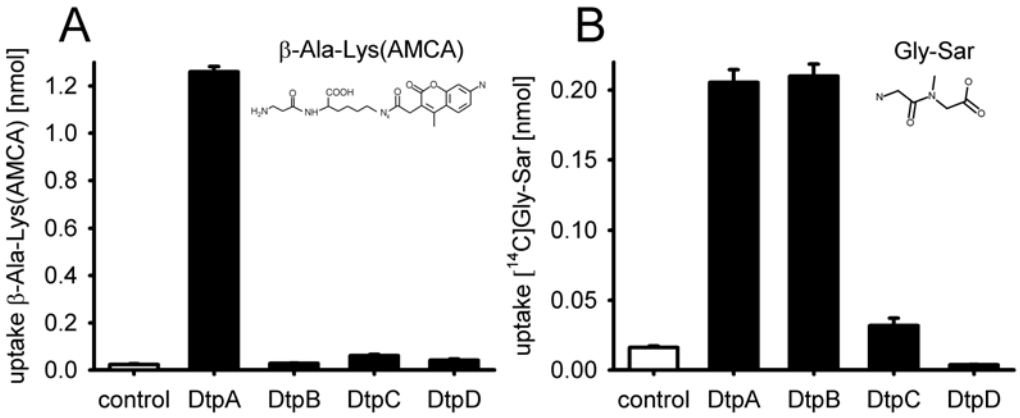

Fig. 13: Uptake of β-Ala-Lys(AMCA) and Gly-Sar into *E. coli* cells overexpressing individual transporters. (A) Incubation of *E. coli* cells overexpressing the transporters with 500 µM β-Ala-Lys(AMCA). n=2 **(B)** Incubation with 17.5 µM [^{14}C]Gly-Sar (0.1 µCi). n=2.

4.4.1.1. DtpA - transport characteristics and substrate specificity

Although for DtpA already two suitable reporter substrates were identified, further compounds that were tested for DtpC and DtpD were also applied to study DtpA for comparison. All compounds tested as effectors for uptake by DtpA are shown in Fig. 14 and uptake rates are expressed as percent of the background transport activity by control cells that carry only the empty vector. β-Ala-Lys(AMCA) appeared most suitable with the lowest background uptake, but also Gly-Sar, 5-aminolevulinic acid and 6-aminohexanoic acid (6-AHA) showed substantial transport rates. Only low uptake rates were observed for biphenylalanylproline (Bip-Pro), which was developed as a PEPT1 inhibitor; but later Bip-Pro was shown to be a high affinity substrate for PEPT1 with lowest transport rate (Knutter *et al.*, 2007). No significant uptake for D-Phe-Ala (a PEPT1 substrate (Theis *et al.*, 2001)) or lysine (substrate of DtpC) was observed.

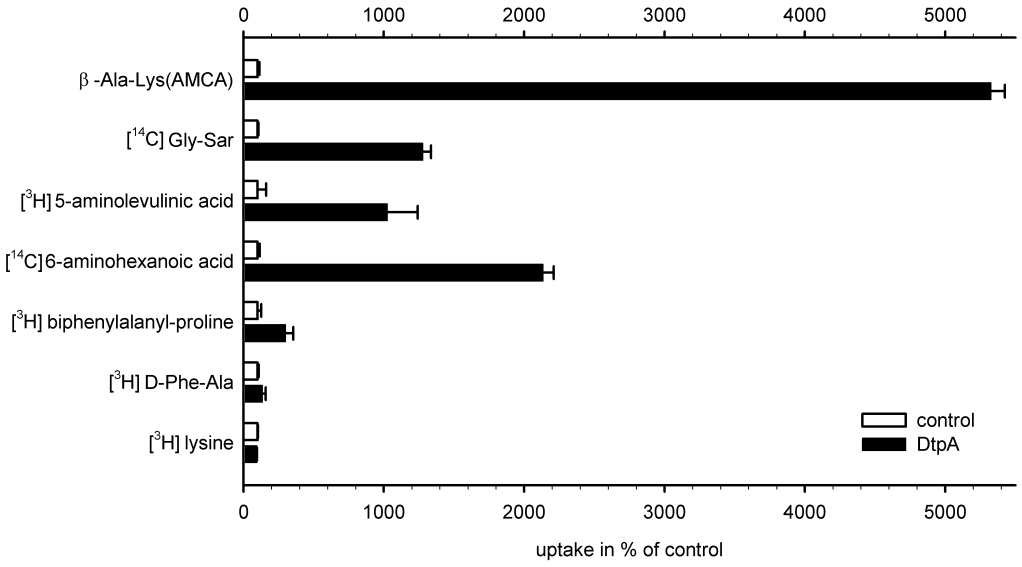

Fig. 14: Uptake of labeled test compounds into DtpA overproducing cells. 100% corresponds to the uptake in control cells. β-Ala-Lys(AMCA) (500 µM), [^{14}C]Gly-Sar (17.5 µM, 0.1 µCi), [^{3}H]5-aminolevulinic acid (3 µM, 1 µCi), [^{14}C]6-aminohexanoic acid (18 µM, 0.1 µCi), biphenylalanyl-[^{3}H]-proline (200 nM, 0.5 µCi), [^{3}H]D-Phe-Ala (250 nM, 1 µCi), [^{3}H]lysine (27 nM, 0.25 µCi).

4.4.1.1.1. β-Ala-Lys(AMCA) as reporter-substrate for DtpA

As β-Ala-Lys(AMCA) appeared as a good substrate of DtpA and can be detected by its fluorescence in whole cells, it was first used to characterize the uptake processes mediated by DtpA in more detail. As given in Fig. 15 A, cells overexpressing *dtpA* showed only minor autofluorescence in the absence of β-Ala-Lys(AMCA) (bar 4), but fluorescence increased significantly after incubation of cells with 50 µM β-Ala-Lys(AMCA) (bar 5). Fluorescence was strongly reduced by addition of an excess amount of the non-labelled dipeptide Gly-Gln

(bar 6). In control cells that carried the empty vector (without the transporter gene) there was no increase of fluorescence above the background (bar 2). Fig. 15 B shows the **time-dependence** of the uptake of β-Ala-Lys(AMCA) by DtpA.

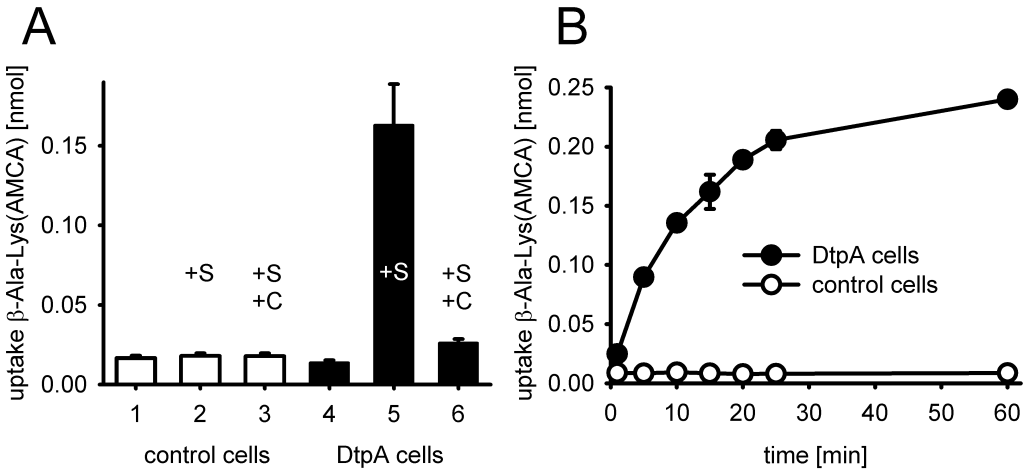

Fig. 15: Uptake of β-Ala-Lys(AMCA) by *dtpA* expressing cells. (A) Control cells (white bars) compared to *dtpA* overexpressing cells (black bars): Incubation with buffer alone (bar 1+4), with the substrate (+S) 50 µM β-Ala-Lys(AMCA) (bar 2+5) or with substrate plus competitor (S+C) 10 mM Gly-Gln. n=3 **(B)** Time-dependent uptake of 50 µM β-Ala-Lys(AMCA). n=2.

Another important parameter in the characterization of transport function is the **apparent substrate affinity**, characterized by the transport constant K_t. Fig. 16 shows its determination with the saturation of transport by increasing concentrations of β-Ala-Lys(AMCA).

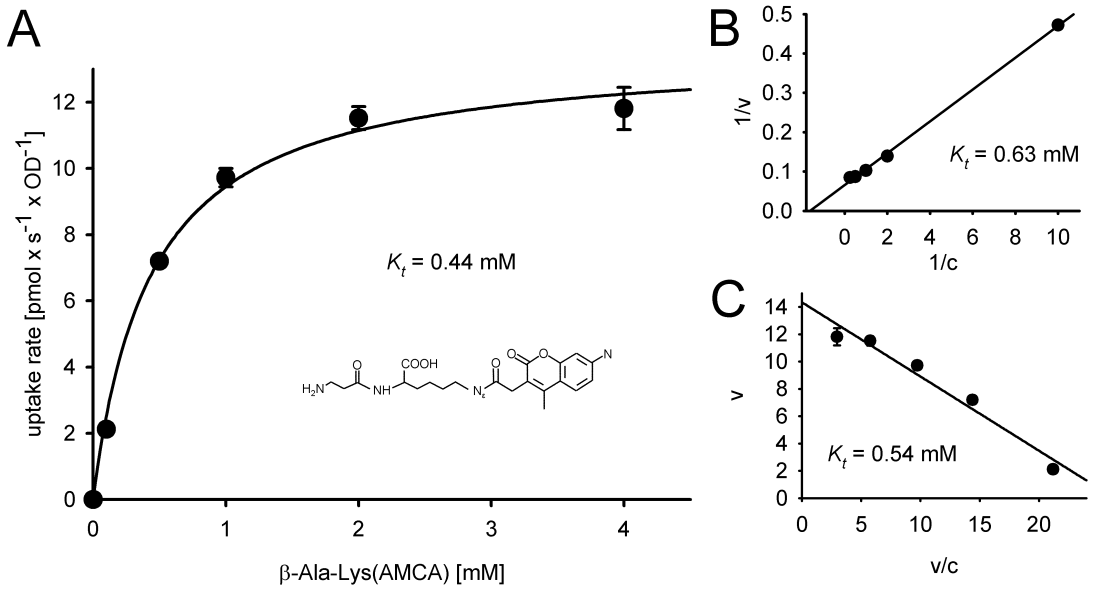

Fig. 16: Determination of the affinity of β-Ala-Lys(AMCA) for uptake via DtpA. (A) Saturation kinetic with increasing substrate concentrations. K_t is 0.44 ± 0.05 mM. The structure of β-Ala-Lys(AMCA) is shown. n=2. **(B)** Lineweaver-Burk linearization of the kinetic from A; K_t is 0.625 mM, v is uptake rate, c is the concentration. **(C)** Eadie-Hofstee linearization of the kinetic from A; K_t is 0.54 mM, v is the uptake rate, c is the concentration.

The concentration corresponding to the half-maximal uptake rate was calculated from Fig. 16 A, resulting in K_t = 0.44 ± 0.05 mM. Panel B shows the Lineweaver-Burk linearization and panel C the of Eadie-Hofstee linearization, which gave similar results with K_t of 0.625 mM and 0.54 mM, respectively. This is not a very high affinity, but as it is below 1 mM it can be considered as good to medium affinity substrate for PTR-family members. Ideally competition experiments should be carried out at concentrations above K_t to be near the maximal transport velocity.

For further characterization of transport, the requirements of **Na^+ and H^+ as cotransport-ions** were studied (Fig. 17 A). The replacement of Na^+ by choline had no significant effect on the uptake of β-Ala-Lys(AMCA), but the presence of CCCP, a proton-ionophore, caused complete inhibition of transport. Thus, peptide uptake via DtpA depends on the proton-motive force and is most likely - as described for the other members of the PTR-family - mediated by a coupled proton-substrate cotransport.

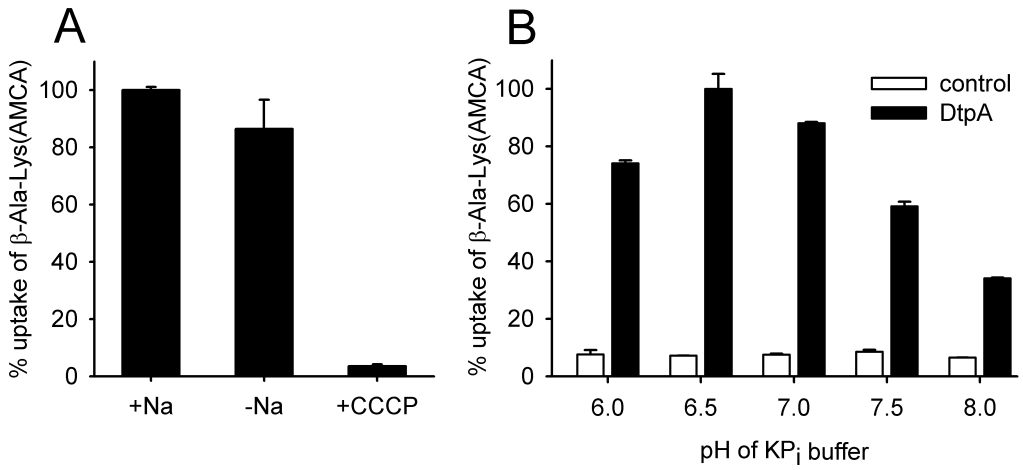

Fig. 17: Na^+-, proton- and pH-dependence of uptake by DtpA. (A) *dtpA* overexpressing *E. coli* were offered 50 µM β-Ala-Lys(AMCA) in buffers containing 150 mM NaCl (bar 1, +Na), 150 mM cholinechloride in exchange for NaCl (bar 2, -Na), or containing the protonophore CCCP (10 µM) (bar 3, +CCCP). n=4. **(B)** *dtpA* overexpressing *E. coli* and control cells were offered 500 µM β-Ala-Lys(AMCA) in potassium phosphate buffers of different pH. n=2, 5 min uptake.

In Fig. 17 B the **pH dependence** of β-Ala-Lys(AMCA) transport is demonstrated. The uptake rate increased from pH 8 to pH 6.5, which goes in line with the proposed proton co-transport, as a higher outside pH means a higher proton gradient from the outside to the inside and therefore an increased driving force for a proton importing system. Nevertheless, here also other factors come into play like the charge modifications of the protein and the substrate and those might explain the decrease of transport rates observed at pH 6.

To determine the transporters **substrate specificity**, *E. coli* cells overexpressing *dtpA* were incubated with 50 µM β-Ala-Lys(AMCA) in the presence of an excess (200-fold) of L-alanine either as free amino acid or in di-, tri- and tetrapeptide form (Fig. 18). Alanine and tetra-alanine did not inhibit uptake of β-Ala-Lys(AMCA), while di- and tri-alanine completely

inhibited β-Ala-Lys(AMCA) uptake. Inhibition of transport by increasing concentrations of di- and tri-alanine allowed apparent affinities (K_i values) of 0.47 ± 0.03 mM and 0.22 ± 0.01 mM to be determined (Fig. 19A) by calculation from the IC_{50} value (concentration of the half-maximal inhibition in the diagram) using the formula from Cheng and Prusoff (Table 3). Stereospecificity of DtpA-mediated flux was assessed by determining IC_{50} values of dipeptides carrying L- or D-alanine residues (Fig. 19 B). Substitution of the N-terminal L-Ala for the D-isomer did not alter affinity significantly, but when the C-terminal L-Ala was replaced by a D-isomer affinity of the competitor was reduced about 8-fold (Table 3). D-Ala-D-Ala did not show detectable affinity for interaction with DtpA.

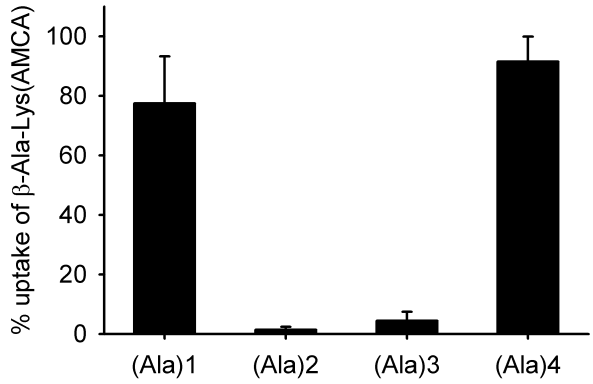

Fig. 18: Chainlength-dependence of uptake by DtpA. Competitive inhibition of β-Ala-Lys(AMCA) uptake (50 µM) by alanine and the di-, tri- and tetrapeptide of alanine (each 10 mM). n=6.

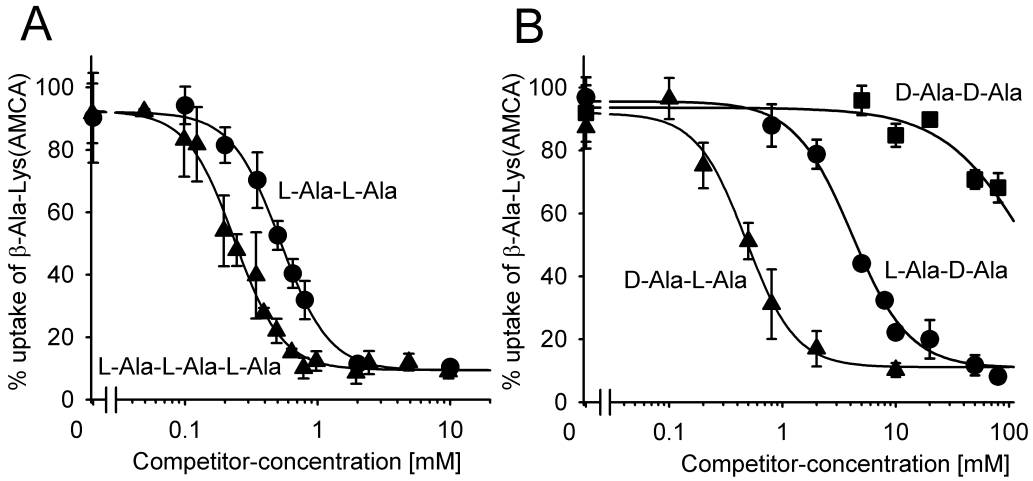

Fig. 19: Competition kinetics with DtpA. (A) Competitive inhibition of β-Ala-Lys(AMCA) uptake (50 µM) by the di- and tripeptide of L-alanine (0.5 - 10 mM). L-Ala-L-Ala (circles) showed an IC_{50} of 0.52 mM and L-Ala-L-Ala-L-Ala (triangles) an IC_{50} of 0.24 mM. n=6. **(B)** Steroselectivity of transport was determined by inhibition of β-Ala-Lys(AMCA) (50 µM) uptake by 0.1 - 10 mM of D-Ala-L-Ala (triangles) with an IC_{50} of 0.48 mM, or 0.8 - 80 mM of L-Ala-D-Ala (circles) with an IC_{50} of 4.1 mM, or 5 - 80 mM of D-Ala-D-Ala (squares). n=4.

To further characterize substrate specificity of DtpA, IC_{50} and K_i values of various other compounds were determined, ranging from differently charged dipeptides consisting of L-amino acids, to ω-amino-fatty-acid and a known inhibitor of mammalian peptide transporters (Fig. 20, Table 3). Neutral dipeptides represented by Gly-Gln or cationic peptides such as Lys-Gly showed relatively high affinities with K_i values of 0.46 ± 0.05 mM and 0.39 ± 0.02 mM, respectively. Introducing the positively charged amino acid at the C-terminal position (Gly-Lys) resulted in a 7-fold reduction of affinity represented by a K_i of 2.54 ± 0.24 mM as compared to 0.39 mM for Lys-Gly. This indicates an asymmetric substrate binding site in DtpA similar to that described for the mammalian peptide transporters (Theis *et al.*, 2002). This observation is strengthened by experiments with the anionic dipeptide Asp-Gly. When Asp instead of Lys is placed in the first position affinity decreases by 10-fold (Asp-Gly, K_i = 4.00 ± 0.40 mM) whereas when placed in the second position affinity increases again when compared to a Lys residue (Gly-Asp, K_i = 1.72 ± 0.12 mM). Modifying the peptide bond nitrogen by a CH_3 group like in glycyl-sarcosine, yielded a moderate affinity (K_i = 1.04 ± 0.08 mM). The highest affinity of all tested compounds displayed the inhibitor of mammalian peptide transporters Lys-Z-Nitro-Pro with a K_i value of 0.03 ± 0.01 mM. Mammalian peptide transporters do not require a peptide bond for recognition of a substrate (Doring *et al.*, 1998). To test whether this holds true also for DtpA, 5-aminolevulinic acid was used as a substrate which carries only the two oppositely charged head groups separated by four carbon units and a backbone carbonyl. Its apparent affinity was 1.52 ± 0.13 mM and therefore higher than that of most charged dipeptides.

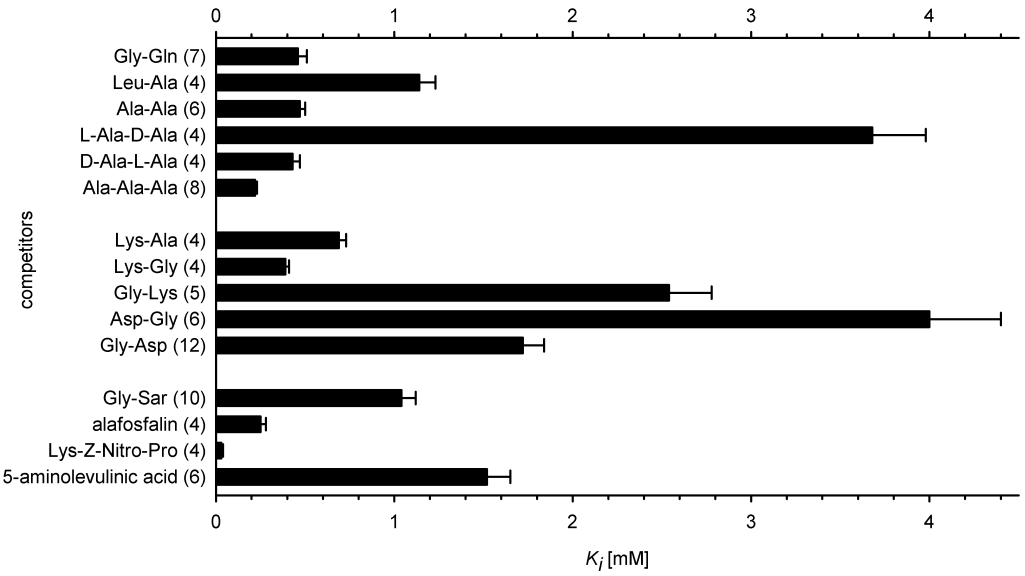

Fig. 20: Apparent K_i values of competitors in DtpA uptake kinetics. *Ki* values were calculated using the equation $K_i = IC_{50}/(1+[substrate]/K_d)$ (Cheng and Prusoff, 1973). IC_{50} values were determined in competition kinetics (usually 0.1 - 10 mM competitor) with 50 µM β-Ala-Lys(AMCA). Values are summarized in Table 3. Number of repeated analysis indicated in parentheses.

Table 3: Summary of IC_{50}-values (mM) and K_i-values

	IC_{50}	K_i
Gly-Gln	0.51 ± 0.06 (7)	0.46 ± 0.05
Leu-Ala	1.27 ± 0.10 (4)	1.14 ± 0.09
Ala-Ala	0.52 ± 0.03 (6)	0.47 ± 0.03
Ala-D-Ala	4.10 ± 0.33 (4)	3.68 ± 0.30
D-Ala-Ala	0.48 ± 0.05 (4)	0.43 ± 0.04
Ala-Ala-Ala	0.24 ± 0.01 (8)	0.22 ± 0.01
Lys-Ala	0.77 ± 0.05 (4)	0.69 ± 0.04
Lys-Gly	0.43 ± 0.02 (4)	0.39 ± 0.02
Gly-Lys	2.83 ± 0.27 (5)	2.54 ± 0.24
Asp-Gly	4.46 ± 0.45 (6)	4.00 ± 0.40
Gly-Asp	1.92 ± 0.13 (12)	1.72 ± 0.12
Gly-Sar	1.16 ± 0.09 (10)	1.04 ± 0.08
alafosfalin	0.28 ± 0.03 (4)	0.25 ± 0.03
Lys-Z-Nitro-Pro	0.033 ± 0.006 (4)	0.03 ± 0.01
5-aminolevulinic acid	1.69 ± 0.14 (6)	1.52 ± 0.13

Numbers in parentheses indicate the number of independent determinations. K_i values were determined by the equation $K_i = IC_{50} / (1 + [substrate] / K_d)$ (Cheng and Prusoff, 1973). All amino acids are L-isoforms unless otherwise indicated. K_i values used for Fig. 20.

Beside di- and tripeptides mammalian peptide transporters accept a broad spectrum of **peptidomimetics** like β-lactam antibiotics and ACE-inhibitors as substrates. Selected peptidomimetics that are known substrates of mammalian peptide transporters were tested for their interaction with DtpA in competition assays (Fig. 21). Compared to the dipeptide Gly-Gln, which inhibited β-Ala-Lys(AMCA) uptake by 97%, similar inhibition rates of 86%, 79% and 79%, respectively were observed for the three aminocephalosporins cefadroxil, cefalexin and cephradine at 10 mM concentration. Cefamandole and cefuroxime showed modest inhibition of only 21% and 32%, respectively, which may result from the lack of an α-amino group.

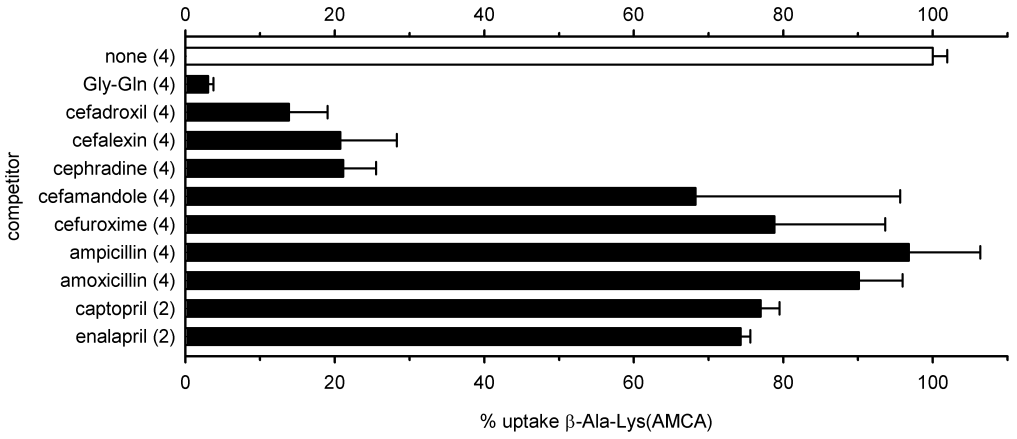

Fig. 21: Petidomimetics as competitors in DtpA uptakes. Uptake of β-Ala-Lys(AMCA) (50 µM) in the absence (none) or the presence of 10 mM indicated substances as competitors (amoxicillin 5 mM). Number of repeated analysis indicated in parentheses.

The two aminopenicillins ampicillin and amoxicillin (5 mM concentration) seemed not to serve as substrates, the ACE-inhibitors captopril and enalapril also showed only low inhibition of β-Ala-Lys(AMCA) uptake.

4.4.1.1.2. Gly-Sar as reporter-substrate for DtpA

For direct comparison with DtpB and for confirmation, also [^{14}C]Gly-Sar was used as reporter substrate. The **time-dependent uptake** in Fig. 22 A shows a fast saturation of the uptake at a concentration of 1 mM Gly-Sar, with the linear initial rate window below 1 minute. Therefore, uptake time was usually 30 seconds. The determination of K_t by uptake kinetics with increasing substrate concentrations resulted in a **K_t of 1 mM** (Fig. 22 B). This confirmed the K_i of 1 mM obtained from β-Ala-Lys(AMCA) competition experiments (Table 3).

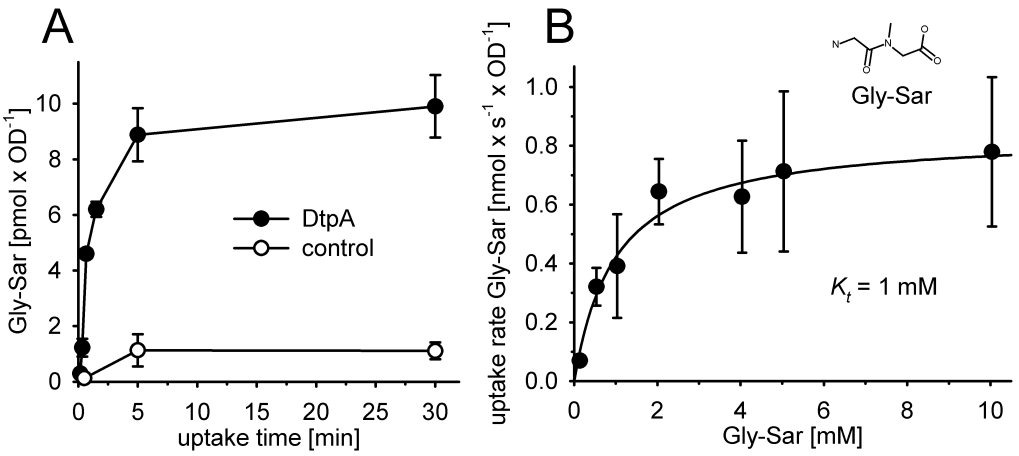

Fig. 22: Uptake of Gly-Sar by DtpA. (A) Time-dependent uptake of [^{14}C]Gly-Sar (1 mM) by *E. coli* cells overexpressing *dtpA*. n=2. **(B)** Saturation kinetics determined by uptake assays with *E. coli* cells overexpressing *dtpA* in the presence of various concentrations of Gly-Sar. The uptake velocities were determined using four time points (10, 20, 40, 60 s). The K_t-value of 1 mM was determined by nonlinear regression analysis of the presented data. n≥2.

Also with Gly-Sar as reporter substrate, the **pH dependence** was tested. Like with β-Ala-Lys(AMCA) higher uptake rates were observed at lower pH (Fig. 23) and with Gly-Sar as substrate uptake rates increased further even at pH as low as 5.

Substrate specificity was assessed using competition experiments with 1 mM Gly-Sar as a substrate and 10 mM of the competitors in *E. coli* cells over-expressing *dtpA*. The uptake rates in the presence of the competitor are presented in Fig. 24. The substrate specificity data essentially match those determined with β-Ala-Lys(AMCA). A difference is that 10 mM Gly-Sar do not inhibit uptake completely as only a 10-fold substrate excess was used in this experiment. Nevertheless substrates with high affinity like Ala-Ala or Ala-Ala-Ala showed total inhibition even at a 10-fold excess. Additionally here the antibiotic chloramphenicol was

tested. This is not a beta-lactam or structurally similar compound and therefore, it was very interesting to find a good inhibition. The possibility that the toxic effect accounts for the reduction of uptake can be excluded because the used *E. coli* strain carries the pLysS plasmid with a *cam* gene (chloramphenicol resistance).

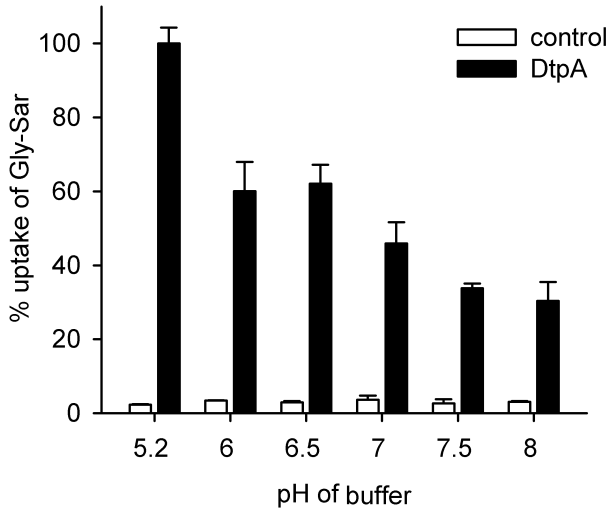

Fig. 23: pH dependence of Gly-Sar uptake by DtpA. *dtpA* overexpressing *E. coli* and control cells were offered 35 µM Gly-Sar in buffers of different pH. n=2, 30 s uptake.

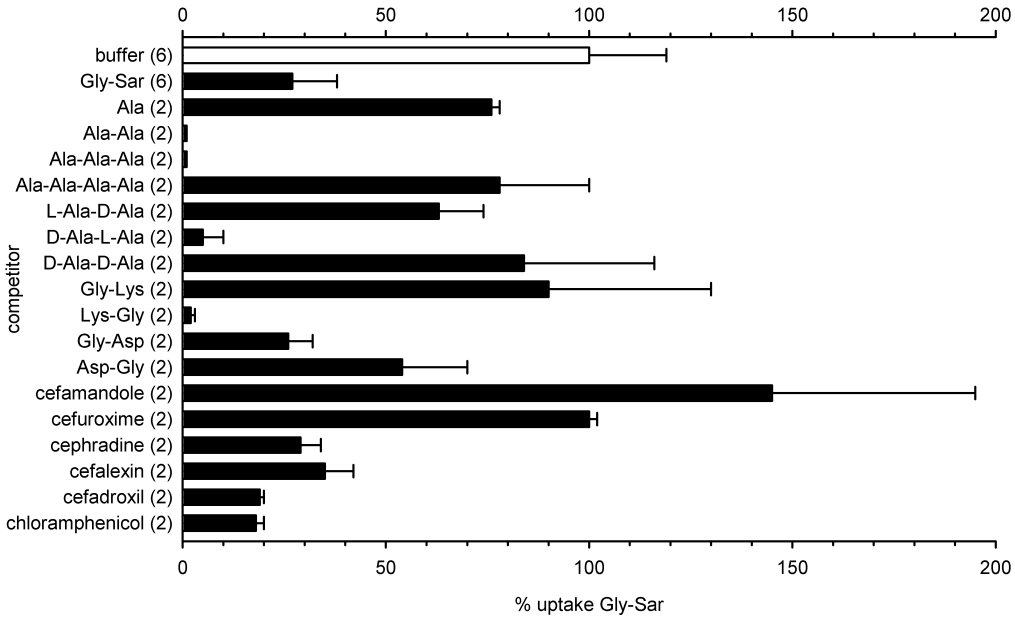

Fig. 24: Competitors for Gly-Sar uptake by DtpA. Uptake of [^{14}C]Gly-Sar (1 mM) in the absence (buffer) or the presence of 10 mM of the indicated substances as competitors (chloramphenicol 5 mM). Number of repeated analysis indicated in parentheses, 30 s uptake.

4.4.1.2. DtpB - transport characteristics and substrate specificity

The compounds tested directly for uptake by DtpB are shown in Fig. 25. β-Ala-Lys(AMCA) only showed low, but Gly-Sar high uptake rates, and appeared therefore suitable for further

characterization of transport function. Also quite good uptake rates were observed for biphenylalanylproline (Bip-Pro).

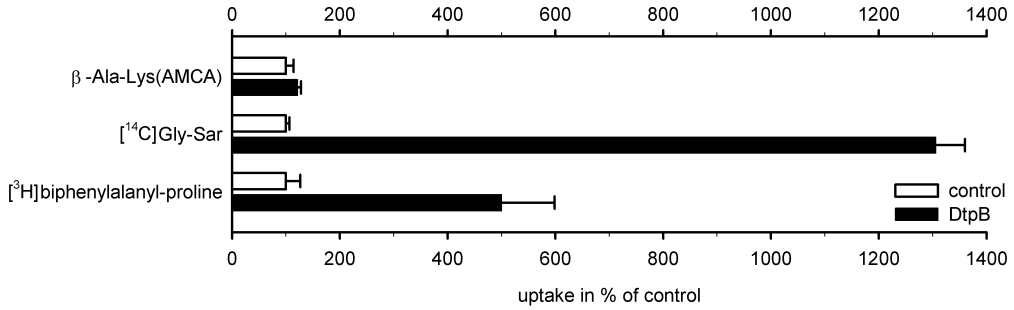

Fig. 25: Uptake of labeled substances by DtpB. 100% corresponds to the signal of control cells that do not overexpress *dtpB*. β-Ala-Lys(AMCA) (50 µM), [^{14}C]Gly-Sar (17.5 µM, 0.1 µCi), biphenylalanyl-[^{3}H]-proline (200 nM, 0.5 µCi).

Gly-Sar as reporter-substrate for DtpB

The **time-dependent uptake** in Fig. 26 A shows saturation at a concentration of 1 mM Gly-Sar, with the linear initial rate window below 1 minute. Therefore, uptake time was usually 30 seconds. The determination of K_t from uptake kinetics with increasing substrate concentrations resulted in a ***K_t* of 6.5 mM** (Fig. 26 B). This is a low affinity what makes it difficult to work at ideal concentrations in competition experiments.

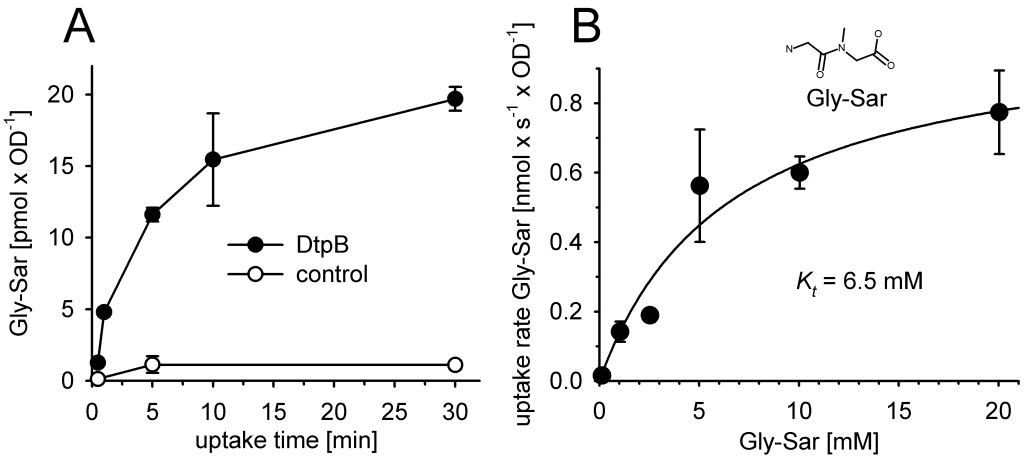

Fig. 26: Uptake of Gly-Sar by DtpB. (A) Time-dependent uptake of [^{14}C]Gly-Sar (1 mM) by *E. coli* cells overexpressing *dtpB*. n=2. **(B)** Saturation kinetics determined by uptake assays with *E. coli* cells overexpressing *dtpB* in the presence of various concentrations of Gly-Sar. The uptake velocities were determined using four time points (10, 20, 40, 60 s). The K_t-value of 6.5 mM was determined by nonlinear regression analysis of the presented data. n≥2.

Like with DtpA, the requirements of **Na^+ and H^+ as cotransport-ions** were studied by replacing Na^+ by choline and by the addition of CCCP, respectively. Na^+ replacement had only a very small effect on the uptake of Gly-Sar, but the presence of CCCP caused

complete inhibition of transport (Fig. 27 A). Thus, peptide uptake via DtpB also depends on the proton-motive force and is most likely also coupled to proton-symport. In Fig. 27 B the **pH dependence** of Gly-Sar transport by DtpB is demonstrated. The uptake rate increased from pH 8 to pH 6. This goes in line with a coupling to proton cotransport, as a lower outside pH means a higher proton gradient.

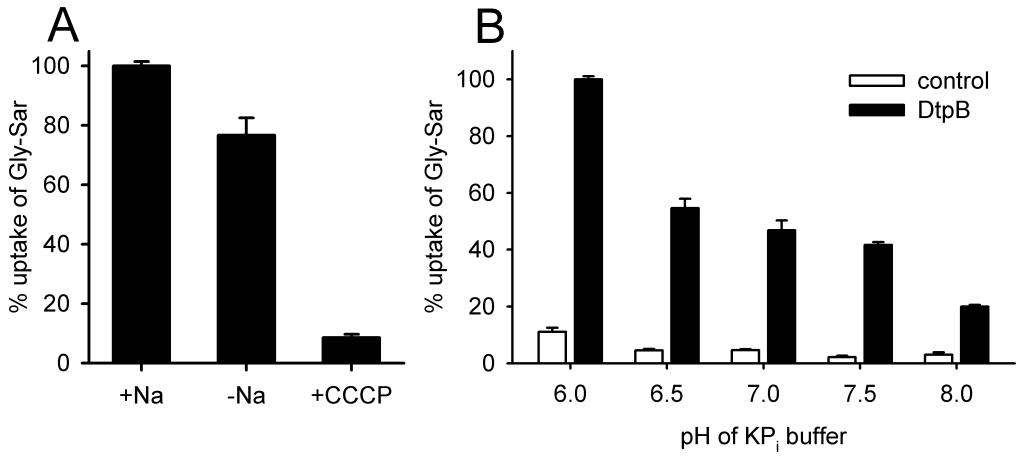

Fig. 27: Na^+-, proton- and pH-dependence of uptake by DtpB. (A) *dtpB* overexpressing *E. coli* were offered 50 µM [^{14}C]Gly-Sar in buffers containing 150 mM NaCl (bar 1, +Na), 150 mM cholinechloride in exchange for NaCl (bar 2, -Na), or containing the protonophore CCCP (10 µM) (bar 3, +CCCP). n=2. **(B)** *dtpB* overexpressing *E. coli* and control cells were offered 35 µM [^{14}C]Gly-Sar in potassium phosphate buffers of different pH. n=2, 5 min uptake.

To assess the substrate specificity of DtpB, competition experiments with 1 mM Gly-Sar as a substrate and 10 mM of the competitors were performed. The uptake rates in the presence of the competitor are presented in Fig. 28. Similar to DtpA, neither the amino acid Ala nor the tetrapeptide Ala-Ala-Ala-Ala caused significant inhibition of DtpB-mediated transport. Compared to the same set of experiments as performed for DtpA (Fig. 24), for DtpB essentially all tested competitors reduced transport to a lower extent than in case of DtpA, which reflects primarily the lower affinity of the reporter-substrate Gly-Sar for DtpB. As the Gly-Sar concentration is with 1 mM below the K_t of 6.5 mM, the 10-fold excess of Gly-Sar is not strong enough for complete inhibition, and even the 100 fold excess with 100 mM causes no complete inhibition (bar 1-3). Despite this, there were differences between DtpB and DtpA when inhibitory effects of individual peptides were compared. In case of DtpB, peptides containing D-stereoisomers of L-Ala essentially failed to inhibit uptake whereas for DtpA strong inhibition was observed with D-Ala when placed in N-terminal position. For peptides containing only D-Ala virtually no competition was seen at all. The effects of charged amino acid residues and their spatial position were similar to DtpA. A positively charged amino acid at the N-terminus caused stronger inhibition than when located in the C-terminus. A negatively charged residue was clearly preferred at the C-terminus. From the selected β-

lactam antibiotics (peptidomimetics) only cephradine and cefalexin significantly reduced Gly-Sar uptake via DtpB.

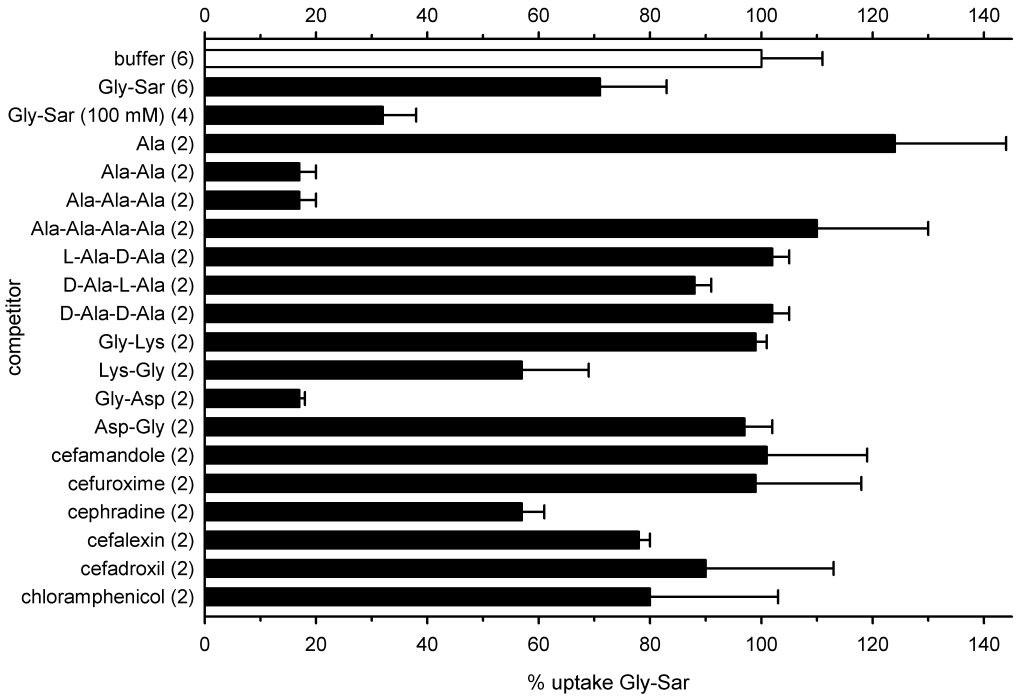

Fig. 28: Competitors for Gly-Sar uptake by DtpB. Uptake of [^{14}C]Gly-Sar (1 mM) in the absence (buffer) or the presence of 10 mM of the indicated substances as competitors (chloramphenicol 5 mM). Number of repeated analysis indicated in parentheses, 30 s uptake.

Competition kinetics were also determined for the phosphonopeptide alafosfalin that is a high affinity substrate for DtpA (K_i = 0.25 mM). For DtpB the affinity was lower with a K_i of 1 mM (Fig. 29).

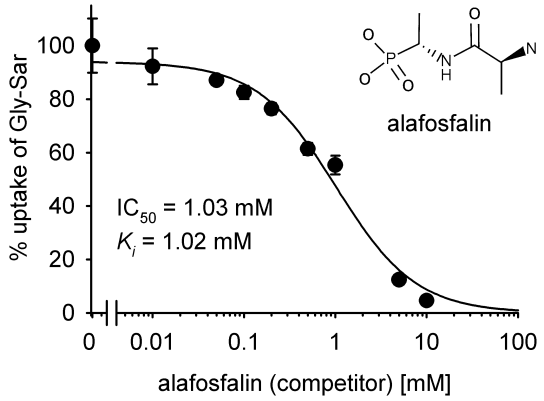

Fig. 29: Competition kinetics with DtpB. Competitive inhibition of Gly-Sar uptake (44 µM) by alafosfalin (0.01 - 10 mM).

Taken together based on data obtained with Gly-Sar and the competition experiments DtpB is a prototypical PTR transporter but compared to DtpA with a lower affinity.

4.4.1.3. DtpC - transport characteristics and substrate specificity

The compounds that were tested for DtpC transport activity are shown in Fig. 30. β-Ala-Lys(AMCA) and Gly-Sar were found to be taken up to some extent but uptake rates were not high enough for comprehensive characterization. In contrast, 5-aminolevulinic acid, 6-aminohexanoic acid (6-AHA), biphenylalanylproline (Bip-Pro) and lysine showed high uptake rates. Minor uptake rates were observed for arginine and histidine, while glycine was not transported at all. Based on this pre-screening lysine was chosen for further characterization as it showed the most robust signals.

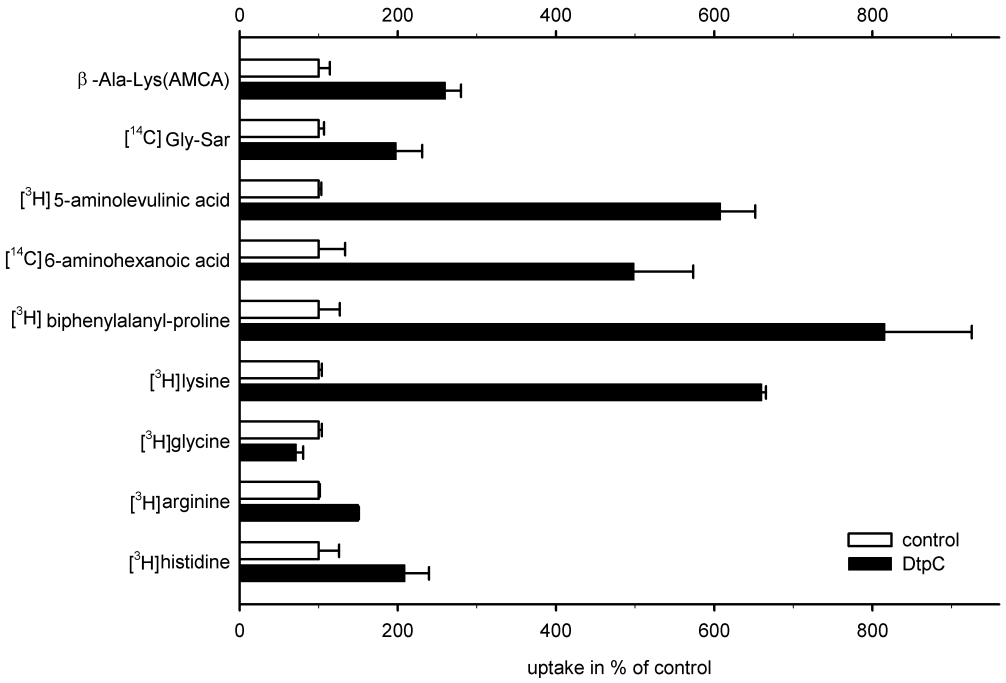

Fig. 30: Uptake of labeled test compounds for DtpC. 100% corresponds to the signal of control cells that do not overexpress *dtpC*. β-Ala-Lys(AMCA) (50 µM), [^{14}C]Gly-Sar (17.5 µM, 0.1 µCi), [^{3}H]5-aminolevulinic acid (3 µM, 1 µCi), [^{14}C]6-aminohexanoic acid (18 µM, 0.1 µCi), biphenylalanyl-[^{3}H]-proline (200 nM, 0.5 µCi), [^{3}H]lysine (27 nM, 0.25 µCi), [^{3}H]glycine (110 nM, 1 µCi), [^{3}H]arginine (34 nM, 0.1 µCi), [^{3}H]histidine (38 nM, 0.1 µCi).

Lysine as reporter substrate

Time-dependence of lysine uptake into cells is shown in Fig. 31 A. Linearity was obtained for time periods of up to 5 minutes and this was the standard uptake time for DtpC transport analysis with lysine. Fig. 31 B shows the determination of K_t from uptake kinetics with increasing substrate concentrations of lysine, which resulted in a **K_t of 31.8 µM**. This is a relatively high affinity compared to affinities of other PTR-transporters to their substrates.

For DtpC as well the requirements of **Na^+ and H^+ as cotransport-ions** were studied by replacing Na^+ by choline and the addition of CCCP, respectively (Fig. 32 A). Here the Na^+ replacement seemed to have an inhibiting effect on the uptake of lysine, but the variance

was too high to judge in a final decision of whether transport is indeed sodium-dependent. The presence of CCCP however caused strong, yet not complete inhibition of transport. Also with respect to the **pH dependence** of lysine transport by DtpC, the data differed substantially from those obtained for DtpA and DtpB. As Fig. 32 B shows, the uptake rate is nearly constant, but decreased towards pH 6. This is unexpected if a proton co-transport is assumed. But as mentioned before, pH changes may also affect protein and substrate charge, which could change uptake characteristic stronger than the effect of the proton-gradient on the driving force.

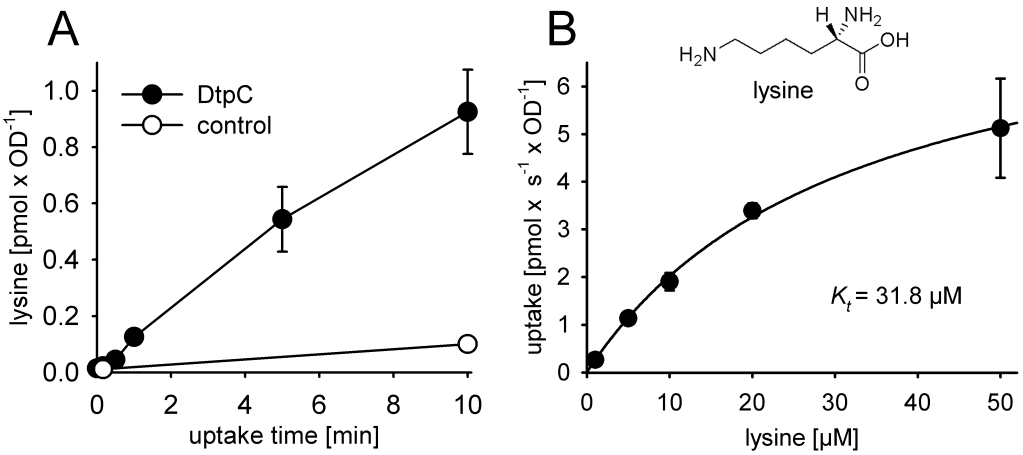

Fig. 31: Uptake of lysine by DtpC. (A) Time-dependent uptake of [^{3}H]Lys (22 nM) by *E. coli* cells overexpressing *dtpC*. n=2. **(B)** Saturation kinetics determined by uptake assays with *E. coli* cells over-expressing *dtpC* in the presence of various concentrations of Lys. The uptake velocities were determined using four time points (10, 20, 40, 60 s). The K_t-value of 31.8 µM was determined by nonlinear regression analysis of the presented data. n≥2.

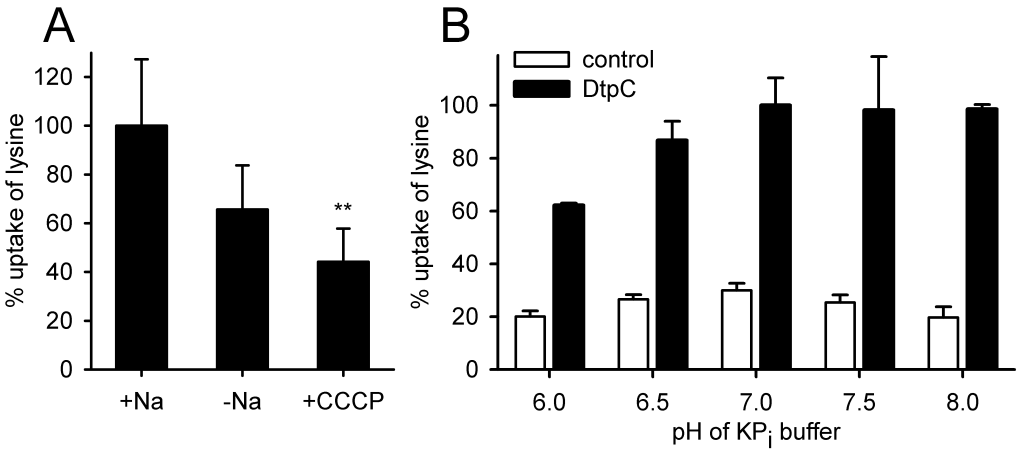

Fig. 32: Na^+-, proton- and pH-dependence of uptake by DtpC. (A) *dtpC* overexpressing *E. coli* were offered 22 nM [^{3}H]Lys in buffers containing 150 mM NaCl (bar 1, +Na), 150 mM cholinechloride in exchange for NaCl (bar 2, -Na), or containing the protonophore CCCP (10 µM) (bar 3, +CCCP). n=4. **significant: p=0.011. **(B)** *dtpC* overexpressing *E. coli* and control cells were offered 50 µM [^{3}H]Lys in potassium phosphate buffers of different pH. n=2.

Competition experiments were also performed to determine the transporter's **substrate selectivity** in *E. coli* cells overexpressing *dtpC*. In a first series of experiments all 20 proteinogenic amino acids were used as competitors and, as shown in Fig. 33, only lysine and arginine and to a lesser extent histidine, were able to significantly reduce lysine influx. Transport of these amino acids was also observed by direct uptake of [^{3}H]Arg and [^{3}H]His (Fig. 30).

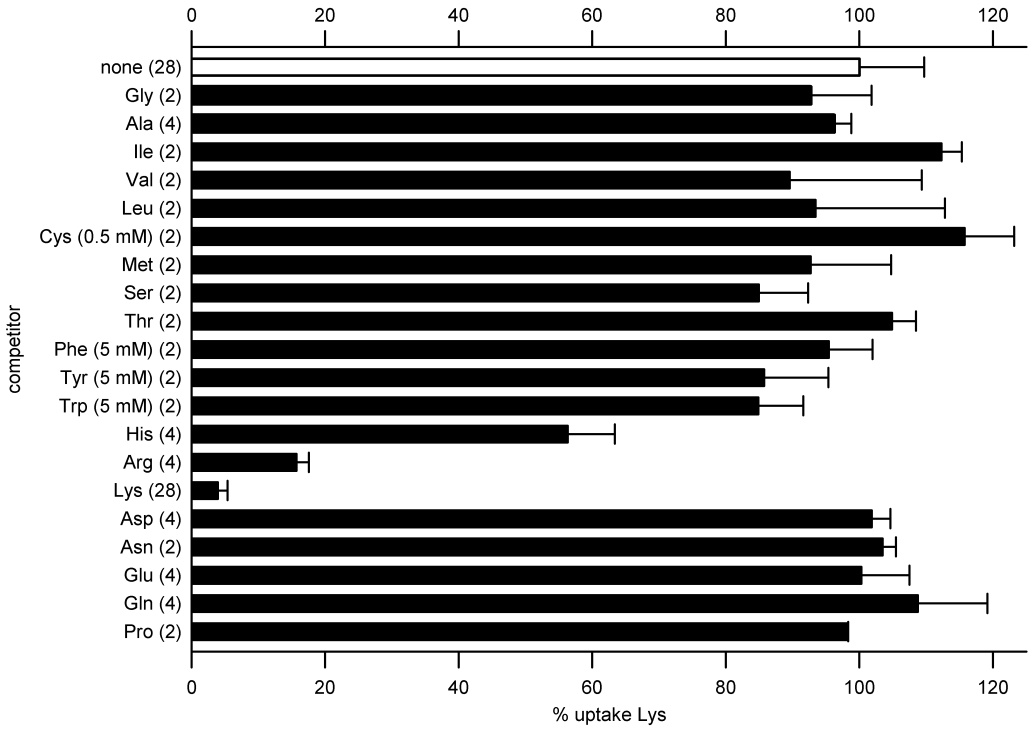

Fig. 33: Amino acids as competitors for Lys uptake by DtpC. Uptake of [^{3}H]lysine (22 nM) in the absence (none) or the presence of 10 mM (except otherwise indicated) of the indicated substances as competitors. Number of repeated analysis indicated in parentheses.

Next, a large number of different dipeptides, tripeptides and derivatives was tested for inhibition of lysine influx in cells over-expressing *dtpC* (Fig. 34). Essentially only di- and tripeptides carrying at least one cationic side chain significantly reduced lysine uptake. In contrast to the peptides containing a Lys or Arg residue, dipeptides containing negatively charged or neutral amino acids did not show competition. To determine the preferred chain length, omega-amino fatty acids with different lengths were used, from which only 5-aminopentanoic acid and 6-AHA showed significant competition.

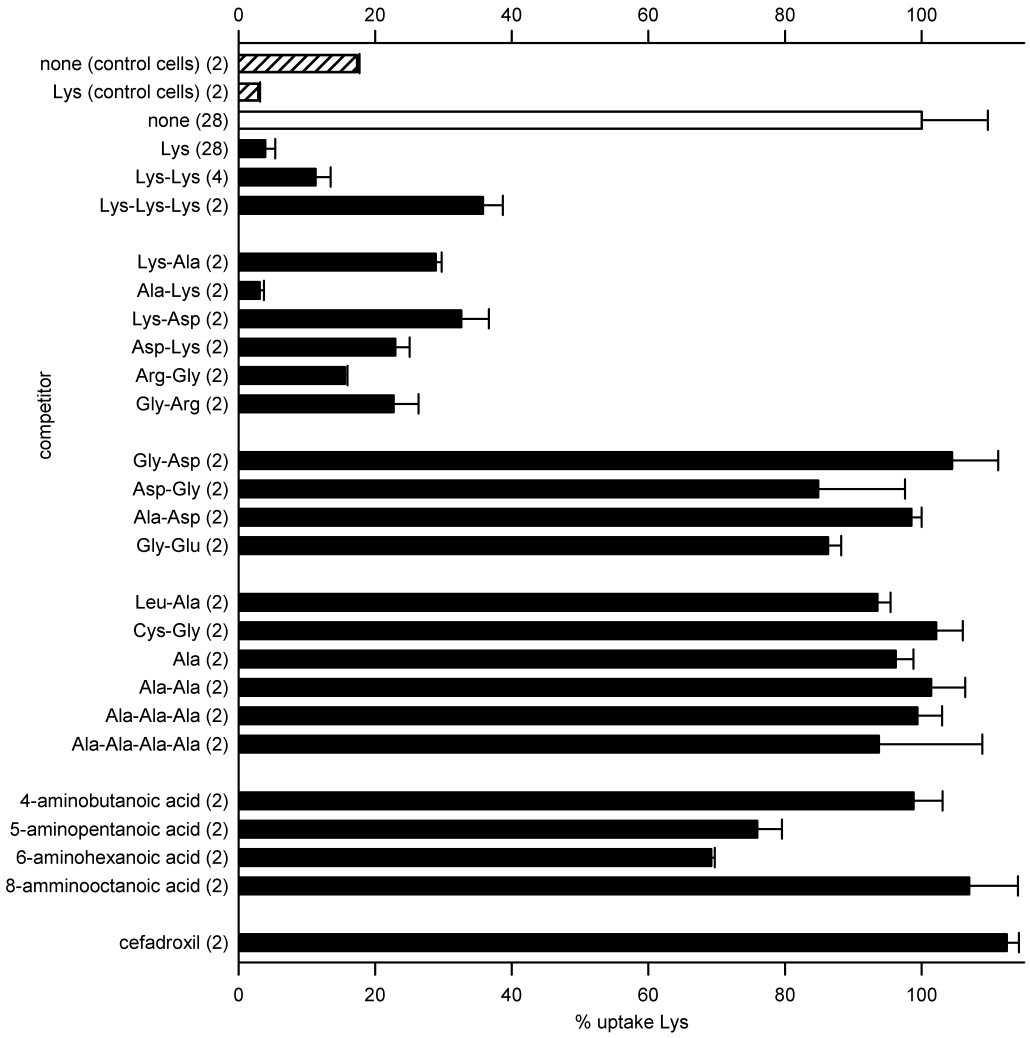

Fig. 34: Peptides as competitors for Lys uptake by DtpC. Uptake of [^{3}H]lysine (22 nM) with control cells or *dtpC* overexpressing cells, in the absence (bar 1 and 3, none) or the presence of 10 mM of the indicated substances as competitors. Number of repeated analysis indicated in parentheses.

An additional series of experiments employed substrates, in which different amino groups were blocked. Results are demonstrated in Fig. 35, where also the competitor excess was reduced to 10-fold to achieve a better differentiation. Like in the first set of experiments the tripeptide Lys-Lys-Lys showed less inhibition as compared to the Lys-dipeptide and the other tested lysine containing tripeptides appeared not to serve as substrates. Ornithine, that just has a shorter side chain than lysine, has substrate character and is transported, whereas 1,5-diaminopentane or hexanoic acid did not show good competition. When the α-amino group of lysine was modified as in α-N(Z)-Lys, it was unable to compete for uptake and similarly, when the ε-amino group in Ala-Lys was blocked as in Ala-Lys-Z-Nitro, no inhibition of lysine transport was observed.

Since the human PEPT1 and PEPT2 proteins, but also the *E. coli* DtpA protein, was shown to transport β-lactam (aminocephalosporin) antibiotics such as cefadroxil, the capability for

cefadroxil to compete with lysine for uptake via DtpC was also tested, but no transport inhibition was observed (Fig. 34). Also carnitine seems to be no substrate of DtpC (Fig. 35).

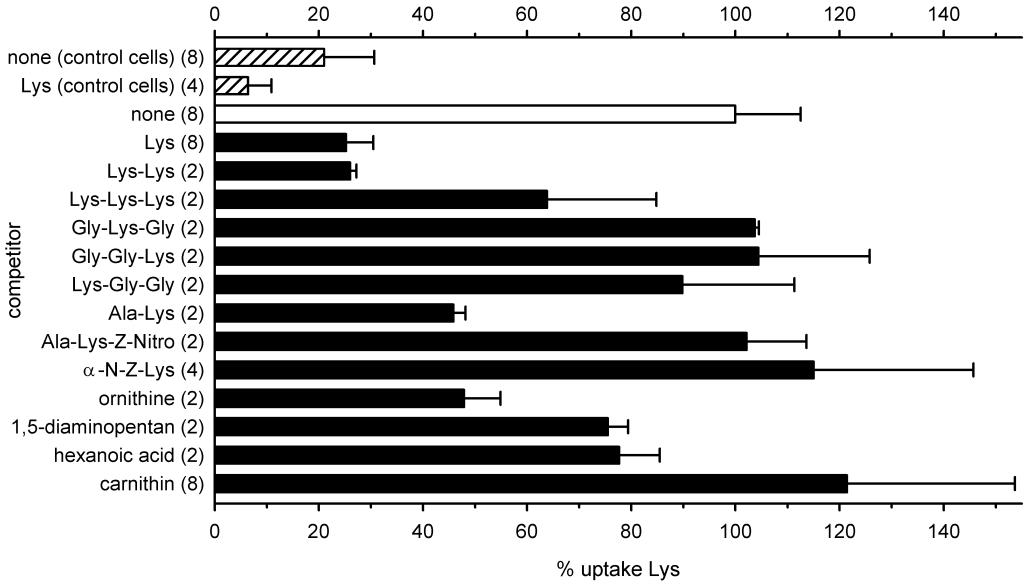

Fig. 35: Peptides as competitors (with 10-fold excess) for Lys uptake by DtpC. Uptake of [^{3}H]lysine (50 µM) with control cells or *dtpC* overexpressing cells, in the absence (bar 1 and 3, none) or the presence of 500 µM (10-fold excess) of the indicated substances as competitors. Number of repeated analysis indicated in parentheses.

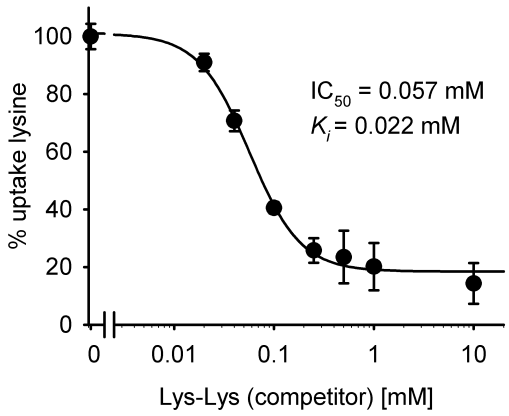

Fig. 36: Competition kinetics of DtpC. Competitive inhibition of [^{3}H]lysine (50 µM) uptake in *dtpC* overexpressing cells by increasing concentrations of Lys-Lys.

An inhibition kinetic was performed for Lys-Lys and is shown in Fig. 36. Here an IC_{50} of 57 µM corresponding to a K_i of 22 µM was determined suggesting that this dipeptide has the same high affinity for transport as free lysine with 32 µM.

As all peptides that showed competition contained lysine, the question arose of whether a cleavage of the peptides could have occurred by extracellular peptidases, with the released free amino acid then competing with labeled lysine for uptake. Therefore, **experiments with peptidase inhibitors** were conducted with the data shown in Fig. 37. Bestatin is a highly

effective aminopeptidase inhibitor and was proven not to interfere with lysine uptake and inhibition (Fig. 37 A, bar 2). The same inhibition was observed for Lys-Lys in the absence and in the presence of very high (200 µM) concentrations of bestatin. If in case of Lys-Lys competition would have been due to free lysine from cleavage, inhibition of cleavage should have reduced transport inhibition. Therefore, Lys-Lys seems to be transported by DtpC as dipeptide. This was confirmed using a different inhibitor of peptide hydrolysis, the sigma protease inhibitor cocktail (PIC) that contains 4-(2-aminoethyl)benzenesulfonyl fluoride (AEBSF), bestatin, pepstatin A, E-64, and phosphoramidon. A concentration 1000-fold higher than suggested by the manufacturer was used here. Fig. 37 B shows that PIC has no major influence on lysine uptake and competition, and also does not prevent the ability of Lys-Lys to inhibit lysine uptake. Here additionally the competitor concentration was reduced to 1 mM to lower the possibility that the small fraction of Lys-Lys that still might be cleaved produces sufficient lysine for effective competition.

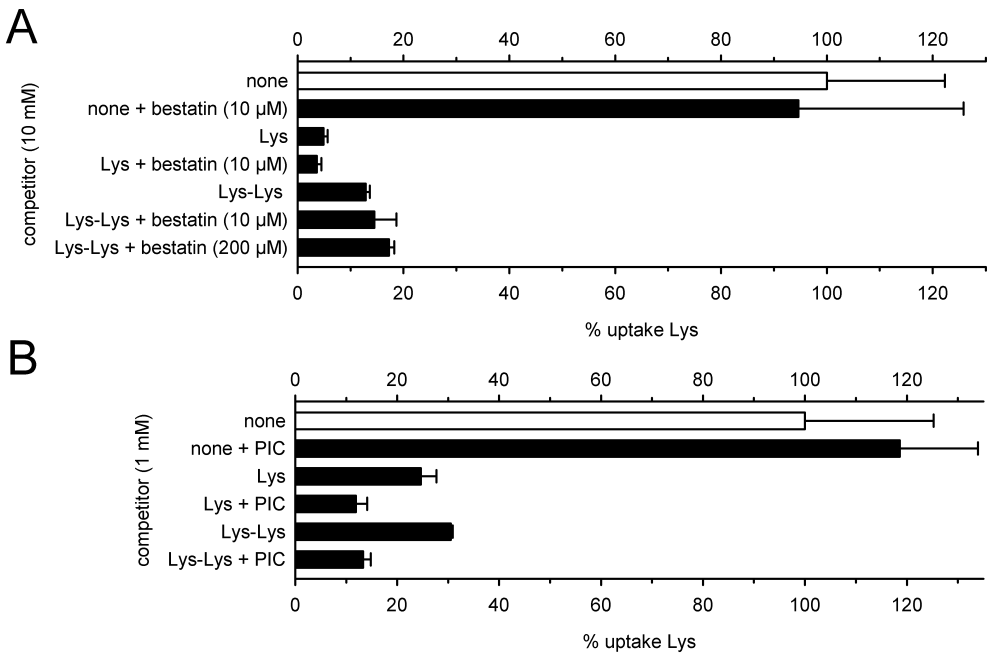

Fig. 37: Control of Lys-Lys degradation. (A) Uptake of [^{3}H]lysine (22 nM) with *dtpC* overexpressing cells and inhibition by 10 mM Lys or Lys-Lys, in the presence or absence of 10 µM (200 µM) of the aminopeptidase inhibitor bestatin. **(B)** Uptake of [^{3}H]lysine (600 nM) with *dtpC* overexpressing cells and inhibition by 1 mM Lys or Lys-Lys, in the presence or absence of protease inhibitor cocktail (PIC) 1:50 (1000 fold of the recommended concentration). n=2.

Bip-Pro

Biphenylalanyl-proline (Bip-Pro) is a known high-affinity but low transport rate substrate of the mammalian PTR transporters PEPT1 and PEPT2 (Knutter *et al.*, 2007). Its interaction with DtpC was tested in more detail as demonstrated in Fig. 38. Panel A shows the time-

dependent uptake characteristic with a linear initial rate region up to ~20 minutes and determination of the apparent affinity resulted in a mean K_t of 1.4 mM (panel B).

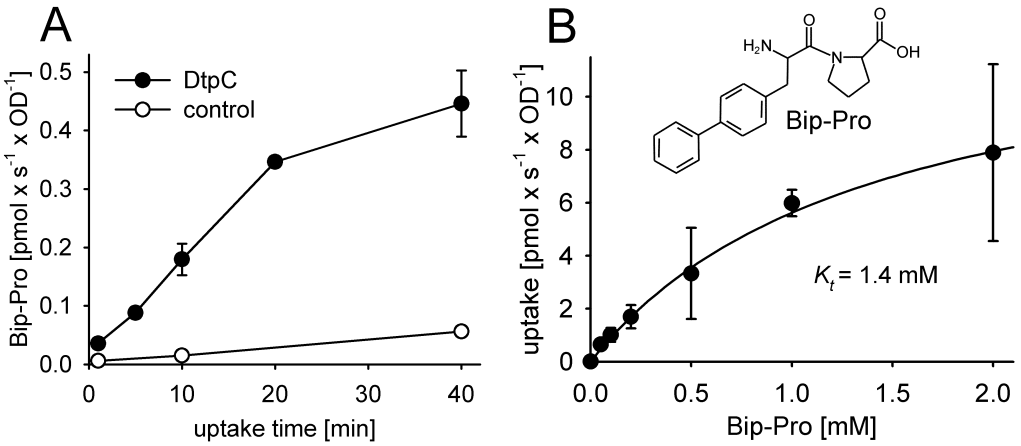

Fig. 38: Uptake of biphenylalanyl-[^{3}H]proline by DtpC. (A) Time-dependent uptake of Bip-[^{3}H]Pro (40 µM) by *E. coli* cells overexpressing *dtpC*. n=2. **(B).** Saturation kinetics was performed with *E. coli* cells overexpressing *dtpC* in the presence of various concentrations of Bip-Pro. The uptake velocities were determined at 30 s. The K_t-value of 1.4 mM was determined by nonlinear regression analysis of the presented data. n≥2.

4.4.1.4. DtpD - transport characteristics and substrate specificity

Directly tested compounds for uptake by DtpD are shown in Fig. 39. β-Ala-Lys(AMCA) is taken up at low levels while Gly-Sar and 5-aminolevulinic seem not to serve as substrates. In contrast 6-aminohexanoic acid (6-AHA) and biphenylalanylproline (Bip-Pro) show solid uptake rates and 6-AHA was used for further characterization (because of commercial availability of the compound). For D-Phe-Ala and the free amino acids no uptake was observed.

6-aminohexanoic acid as a reporter substrate

The time-dependence of 6-AHA uptake by DtpD is shown in Fig. 40 A. Only around 30 seconds linearity was observed and therefore 30 seconds were chosen for further transport experiments. A kinetics of uptake with increasing substrate concentrations is shown in Fig. 40 B and revealed a low affinity with a ***K_t* of 10.6 mM**. Despite the fact that 6-AHA has to be classified as low affinity substrate it was used as a tool for screening for better substrates.

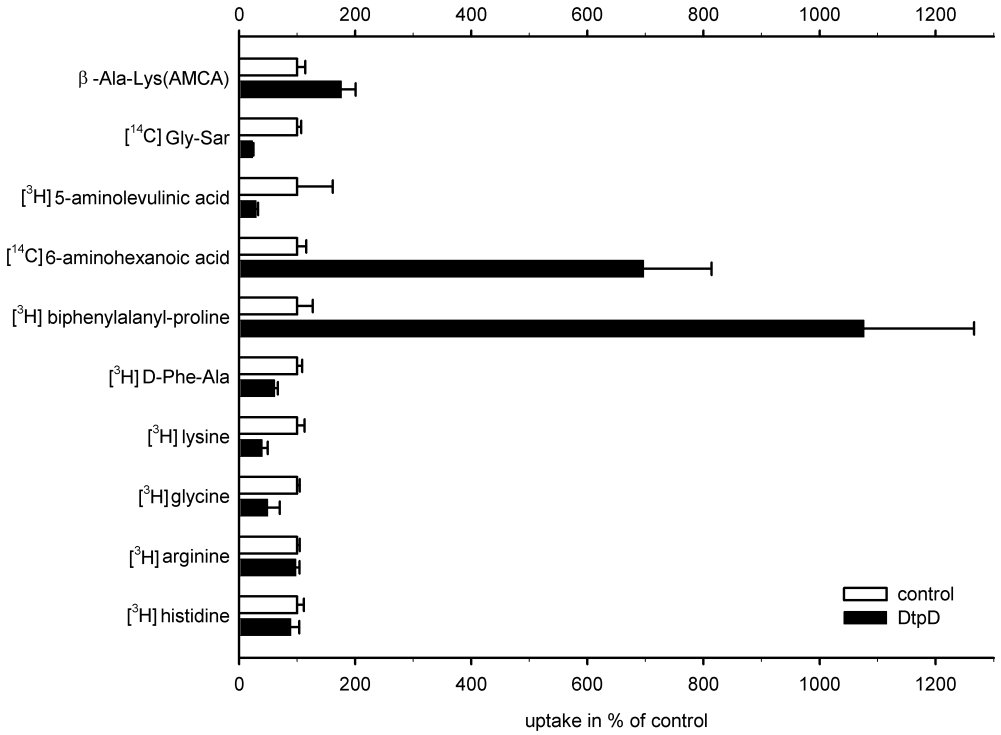

Fig. 39: Uptake of labeled test compounds by DtpD. 100% corresponds to the signal of control cells that do not overexpress *dtpD*. β-Ala-Lys(AMCA) (50 µM), [^{14}C]Gly-Sar (17.5 µM, 0.1 µCi), [^{3}H]5-aminolevulinic acid (3 µM, 1 µCi), [^{14}C]6-aminohexanoic acid (18 µM, 0.1 µCi), biphenylalanyl-[^{3}H]-proline (200 nM, 0.5 µCi), [^{3}H]D-Phe-Ala (250 nM, 1 µCi), [^{3}H]lysine (110 nM, 1 µCi), [^{3}H]glycine (110 nM, 1 µCi),. [^{3}H]arginine (64 nM, 0.2 µCi), [^{3}H]histidine (76 nM, 0.2 µCi).

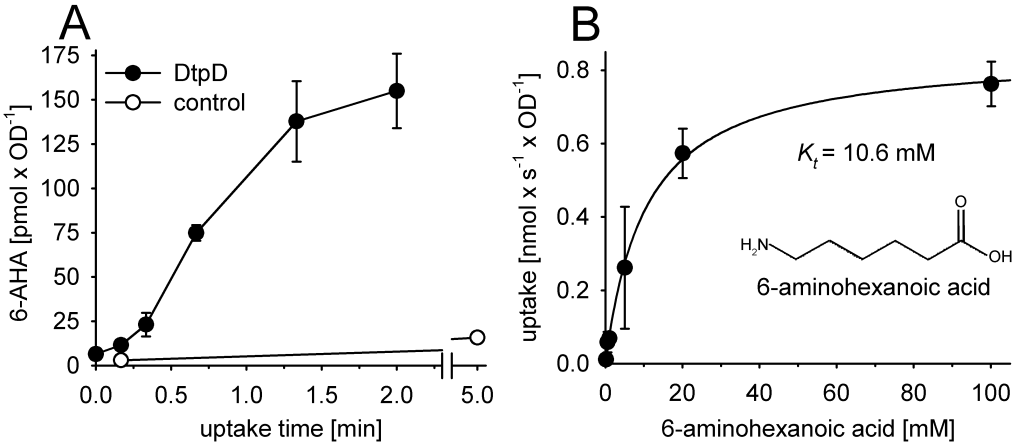

Fig. 40: Uptake of 6-aminohexanoic acid by DtpD. (A) Time-dependent uptake of [^{14}C]6-aminohexanoic acid (72 µM) by *E. coli* cells overexpressing *dtpD*. n=2. **(B).** Saturation kinetics was performed with *E. coli* cells overexpressing *dtpD* in the presence of various concentrations of 6-AHA. The uptake velocities were determined using four time points (10, 20, 40, 60 s). The K_t-value of 10.6 mM was determined by nonlinear regression analysis. n≥2.

The requirements of **Na^+ and H^+ as cotransport-ions** were also for DtpD studied by replacing Na^+ by choline and the addition of CCCP, respectively (Fig. 41 A). Here the Na^+ replacement had a strong inhibitory effect on the uptake of 6-AHA but also the presence of CCCP caused strong inhibition of transport. From these results it is not possible to conclude a proton-dependence, because a collapse of the proton gradient could cause secondarily also the loss of the Na^+ gradient, which would impede uptake as well. The **pH dependence** however showed a clear increase of 6-AHA transport in acidic buffer (Fig. 41 B), which would be typical for a proton-coupled process.

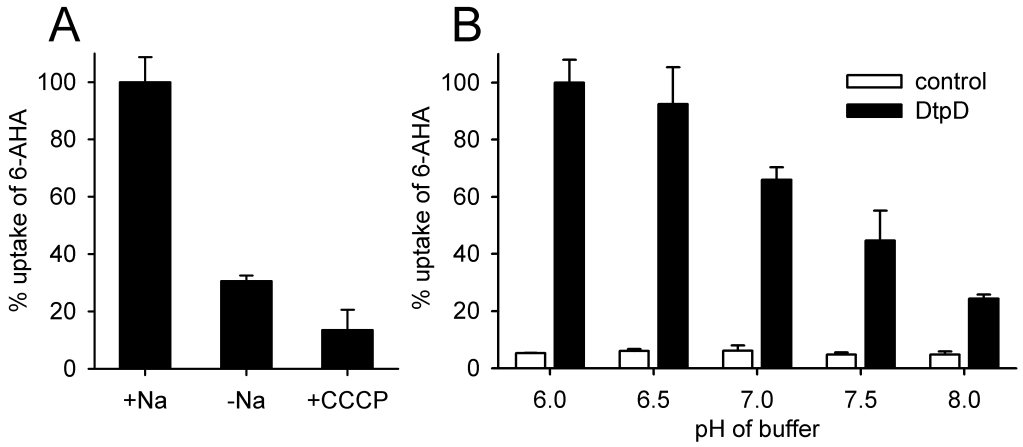

Fig. 41: Na^+-, proton- and pH-dependence of uptake by DtpD. (A) *dtpD* overexpressing *E. coli* were offered 72 µM [^{14}C]6-aminohexanoic acid in buffers containing 150 mM NaCl (bar 1, +Na), 150 mM cholinechloride in exchange for NaCl (bar 2, -Na), or containing the protonophore CCCP (10 µM) (bar 3, +CCCP). n=4. **(B)** *dtpC* overexpressing *E. coli* and control cells were offered 72 µM [^{14}C]6-aminohexanoic acid in Tris/HCl buffers of different pH. n=2.

Competition experiments with *E. coli* cells overexpressing DtpD were used to determine the **substrate specificity**. The data of the first set of compounds tested are shown in Fig. 42. Peptides consisting of 1 to 5 glycine residues did not reduce but seemed to slightly increase the uptake. Also Peptides consisting of 1 to 4 alanine residues showed only in case of the di- and the tetrapeptide a moderate inhibition, as did the uncharged dipeptide Gly-Gln. When charged amino acids were present in peptides, competition was very strong as in case of a C-terminal Lys or Arg but no competition was seen when the Lys or Arg was placed in the N-terminal position. This charge position selectivity was stronger in DtpD than in DtpA or DtpB and showed a reversed orientation. The competition experiment confirmed also that lysine alone is not a substrate. Peptides containing the negatively charged Asp residue showed low competition and here the preferred position appeared to be amino-terminal.

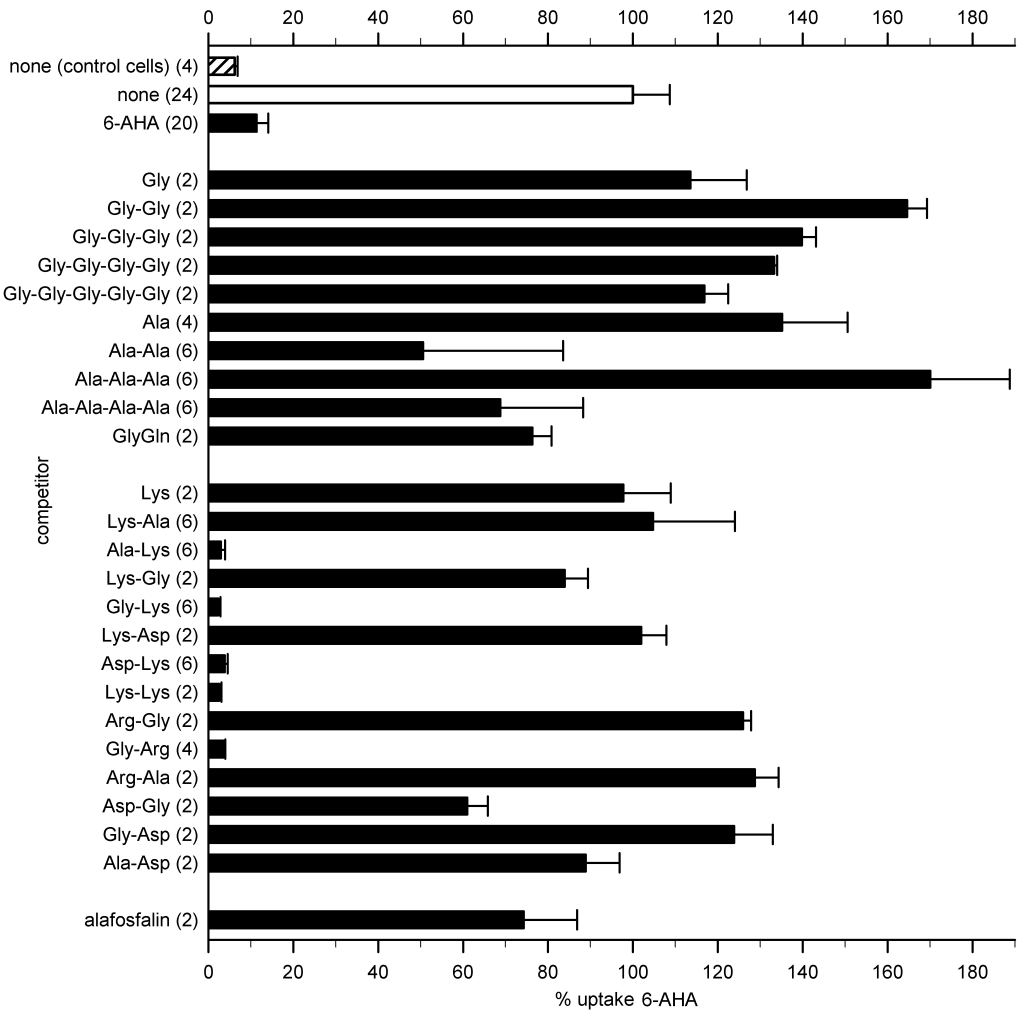

Fig. 42: Competitors for 6-aminohexanoic acid uptake by DtpD. Uptake of [^{14}C]6-AHA (72 µM) in the absence (bar 1 and 2, none) or the presence of 10 mM of the indicated substances as competitors. Number of repeated analysis indicated in parentheses, 30 s uptake.

In a second set of experiments the excess of competitor was reduced to 10-fold for better differentiation (Fig. 43). Two of the four tested lysine containing tripeptides (Lys-Lys-Lys and Gly-Lys-Gly) showed considerable competition, while another uncharged dipeptide, Gly-Gly, did not inhibit uptake. Of the peptidomimetics, the angiotensin converting enzyme (ACE) inhibitors (captopril and enalapril) showed very strong, and the β-lactam antibiotics cefuroxime and ampicillin only weak uptake inhibition. The antibiotic chloramphenicol showed significant inhibition. Hexanoic acid was obviously no substrate while 1,5-diaminopentane (cadaverine) with two amino groups but no carboxy group, showed some competition. The efficiency of lysine for competition increased slightly when the α-amino group was blocked with an uncharged group like in α-N(Z)-Lys or Nα-t-BOC-Lys. Blocking of the ε-amino group of Ala-Lys like in Ala-Lys-[Z(NO_2)] led to a loss of competition efficiency.

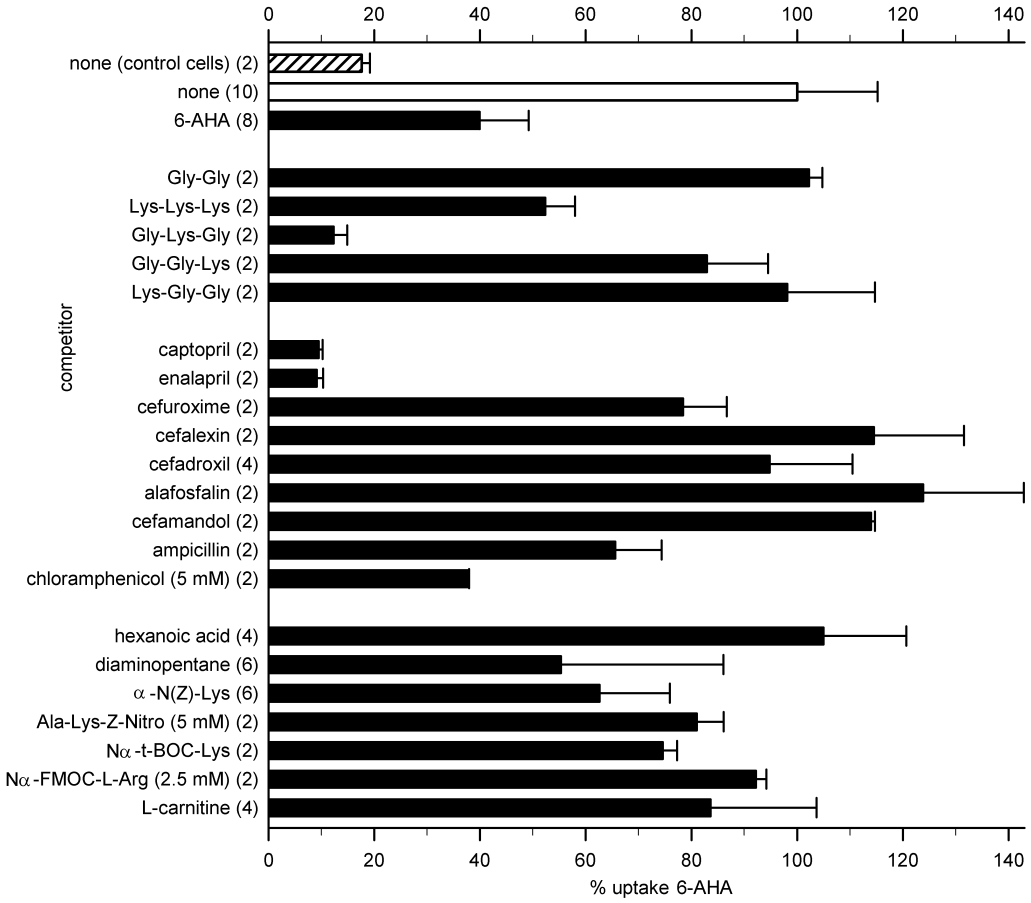

Fig. 43: Peptides and peptidomimetics as competitors (10-fold excess) for 6-aminohexanoic acid uptake by DtpD. Uptake of [^{14}C]6-AHA (1 mM) with control cells or *dtpD* overexpressing cells, in the absence (bar 1 and 2, none) or the presence of 10 mM (10 x excess, except otherwise indicated) of the indicated substances as competitors. Number of repeated analysis indicated in parentheses.

For some compounds the competition was examined closer by kinetic analysis with increasing competitor concentrations (Fig. 44). The dipeptide Lys-Lys showed high affinity with an EC_{50} of 0.0322 mM corresponding to a K_i of 0.0295 mM.

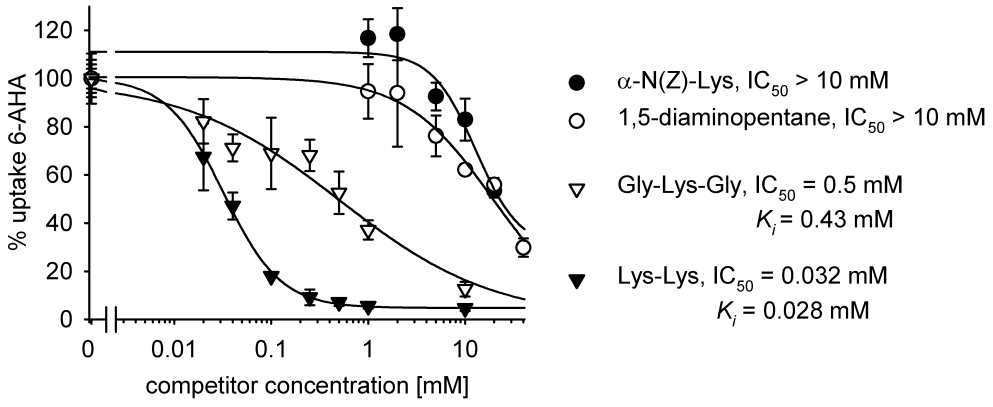

Fig. 44: Competition kinetics of DtpD. Competitive inhibition of [^{14}C]6-aminohexanoic acid (1 mM) uptake in *dtpD* overexpressing *E. coli* by increasing concentrations of potential substrates.

Also the tripeptide Gly-Lys-Gly with an EC_{50} of 0.502 mM corresponding to a K_i of 0.459 mM has high affinity. Rather low affinities revealed α-N(Z)-Lys and 1,5-diaminopentane with EC_{50} values above 10 mM.

Bip-Pro

Bip-Pro was the second compound that was accessible for direct studies as labeled compound. Uptake was characterized and Fig. 45 A shows the **time-dependence** of Bip-Pro uptake, which did not reach saturation even after 40 minutes. The kinetics of flux with increasing substrate concentrations was measured at short time intervals of 30 seconds (Fig. 45 B) and revealed a rather low affinity with a K_t of 5.2 mM. Nevertheless, the total amount of Bip-Pro taken up was higher than with any other overexpressed PTR transporter of *E. coli*, with DtpA possessing 300%, DtpB 500%, DtpC 816% and for DtpD 1077% of uptake as compared to control cells.

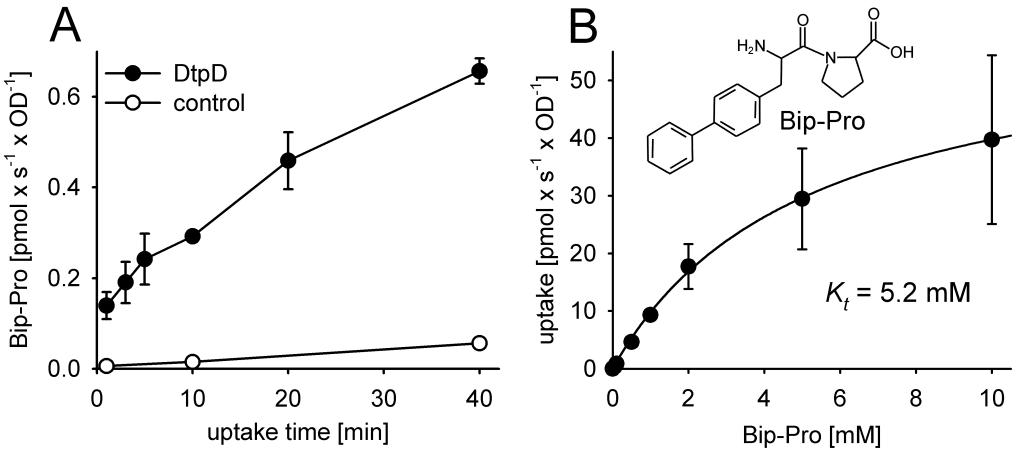

Fig. 45: Uptake of biphenylalanyl-[^{3}H]proline by DtpD. (A) Time-dependent uptake of Bip-[^{3}H]Pro (40 µM) by *E. coli* cells overexpressing *dtpD*. n=2. **(B).** Saturation kinetics was performed with *E. coli* cells overexpressing *dtpD* in the presence of various concentrations of Bip-Pro. The uptake velocities were determined at 30 s. The K_t-value of 5.2 mM was determined by nonlinear regression analysis of the presented data. n≥2.

4.4.2. *In vitro* uptake studies

To examine the role of the proton-gradient as a driving force more thoroughly, several *in vitro* systems were employed. Membrane vesicles were used for uptake experiments and the purified transporter proteins were reconstituted into proteoliposomes and tested for uptake and finally proteoliposomes containing the transporters were tested for function in a novel chip-based sensor system that uses current measurements. With the proteoliposome based techniques it could be shown that the purified proteins are still active after purification which is a prerequisite for further crystallization attempts.

4.4.2.1. Transport in membrane vesicles

Isolated membranes of *E. coli* containing the overproduced transport proteins were fused with proteoliposomes containing bovine cytochrome *c* oxidase. A transmembrane proton-gradient (inside negative) is generated when cytochrome *c* oxidase is supplied with electrons, which are transferred from reduced ascorbate via TMPD and cytochrome *c* (methods section 7.12, p. 92). Before addition of ascorbate, there was generally only a slow influx of radiolabeled substrates into the vesicles (Fig. 46). Addition of ascorbate however caused a marked increase in Gly-Sar influx into vesicles containing either DtpA or DtpB, but not into control vesicles (Fig. 46 A/B). There was also an increased uptake of lysine after ascorbate addition in case of DtpC (Fig. 46 C), although here control vesicles showed a modest increase in uptake. For DtpD no increase in uptake of 6-AHA after addition of ascorbate could be observed (Fig. 46 D).

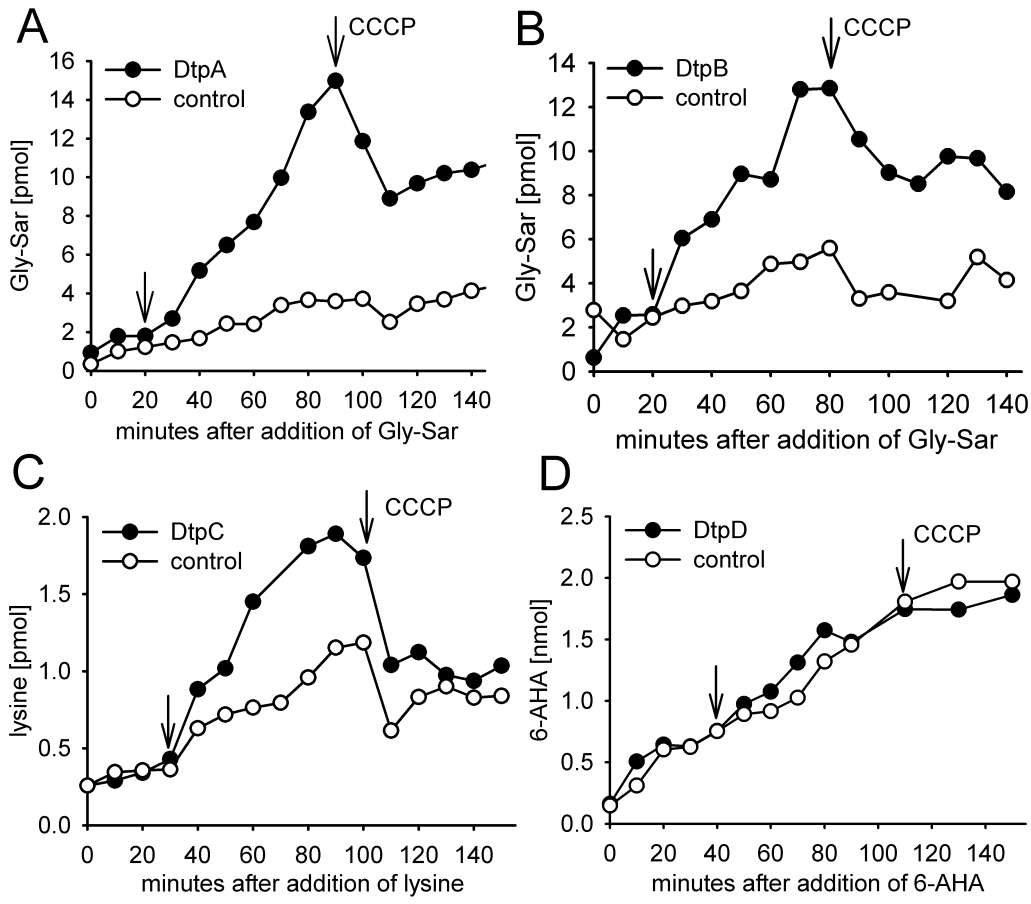

Fig. 46: *In vitro* transport studies with membrane vesicles. Vesicles from membranes of transporter overexpressing *E. coli* were fused with cytochrome *c* oxidase containing proteoliposomes. After 20 min (arrow), a proton gradient was established by addition of a mix of ascorbate/TMPD/cytochrome *c* and destroyed by addition of 10 µM CCCP as indicated. **(A)** DtpA: uptake of Gly-Sar (175 µM). **(B)** DtpB: uptake of Gly-Sar (175 mM). **(C)** DptC: uptake of [^{3}H]lysine (110 nM). **(D)** DtpD: uptake of [^{14}C]6-aminohexanoic acid (181 µM).

Because of a possible Na^+ dependence of DtpC and DtpD experiments were also carried out in the presence of Na^+ ions (150 mM NaCl, 25 mM HEPES pH 7.4) but the generation of a Na^+ gradient by addition of 100 mM NaCl to the outside medium did also not increase the uptake of 6-AHA into DtpD-containing vesicles (data not shown).

A collapse of the proton-gradient was induced by 10 µM carbonyl cyanide m-chlorophenoxylhydrazone (CCCP) addition, which caused efflux of radiolabeled substrates out of the vesicles containing either DtpA, DtpB or DtpC, indicating that the accumulation of substrate above the extra-vesicular concentration was occurring only in the presence of the proton-gradient. For these three transporters a proton-dependence of peptide influx therefore is most plausible.

4.4.2.2. Uptake into proteoliposomes

In a separate series of experiments the purified transporter proteins were reconstituted into proteoliposomes. Membranes of transporter-overexpressing *E. coli* cells were solubilized with the detergent n-dodecyl-β-D-maltoside (DDM) and the proteins were purified by Ni^{2+}-affinity chromatography making use of the C-terminal His-tag, with purity data and yields described before (see Fig. 12). For reconstitution into liposomes the detergent was removed by adsorption onto Bio Beads. Subsequently the liposomes containing the transporters were fused with vesicles containing cytochrome *c* oxidase using a freeze-thaw-sonication cycle and a proton-gradient was generated as described (methods section 7.12, p. 92). After initiation of the proton-gradient, Gly-Sar uptake increased around 60-fold in case of DtpA and almost 10-fold in case of DtpB (Fig. 47 A/B) and substrate efflux was observed after addition of CCCP. DtpC proteoliposomes did not show any increased lysine uptake (Fig. 47 C). Also with a NaCl gradient or in HEPES or TRIS buffer with addition of NaCl, no increased uptake was detectable (data not shown). With DtpD proteoliposomes there was no increased uptake of 6-AHA either. Fig. 47 D shows such an experiment without or with a NaCl gradient and later an application of a proton-gradient, but under none of the conditions a significant uptake of 6-AHA was observed.

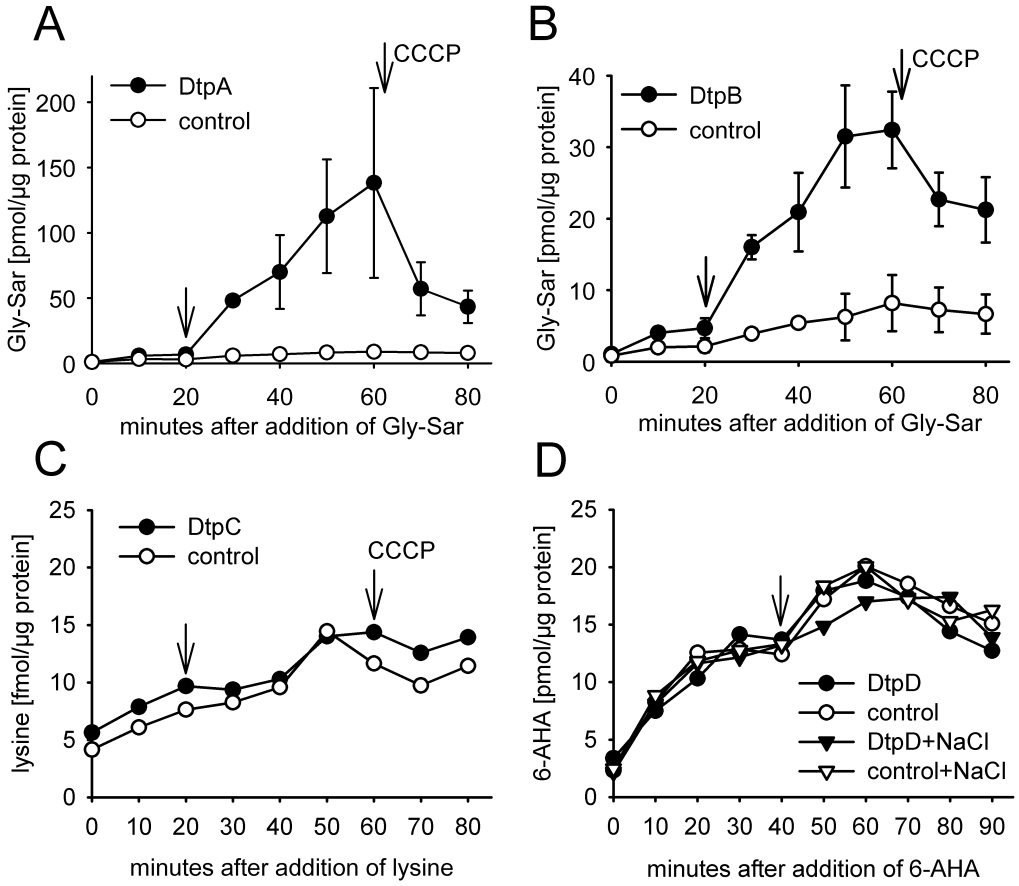

Fig. 47: *In vitro* transport studies with proteoliposomes. Proteoliposomes with purified transporter proteins were fused with cytochrome *c* oxidase containing proteoliposomes. After 20 min (arrow), a proton gradient was established by addition of a mix of ascorbate/TMPD/cytochrome *c* and destroyed by addition of 10 µM CCCP as indicated. **(A)** DtpA: uptake of Gly-Sar (175 µM). n=2. **(B)** DtpB: uptake of Gly-Sar (175 mM).n=2 **(C)** DtpC: uptake of [^{3}H]lysine (110 nM). **(D)** DtpD: uptake of [^{14}C]6-aminohexanoic acid (181 µM). +NaCl: 20 mM NaCl gradient from outside.

4.4.2.3. Electrical measurements employing proteoliposomes

As additional technique and for unequivocally demonstrating the electrogenic nature of the transport process a chip-based assay system was used. Here proteoliposomes containing DtpA or DtpB were adsorbed onto the gold-surface of the SURFE^{2}R^{one} system (IonGate Biosciences GmbH). This system uses a solid-support membrane technology and allows detection of capacity-coupled currents induced by movement of charged molecules across a lipid bilayer or natural membrane (methods section 7.13, p. 93). After adsorption of the proteoliposomes on the gold surface, the SURFE^{2}R^{one} chip is perfused with different buffers either containing the test compounds or a reference compound. In the transport studies employing the proteoliposomes with the *E. coli* transporters the chips were first perfused with a buffer containing glycine (glycine was included for charge and osmotic equilibration only) and then exchanged for buffers containing the dipeptide glycyl-glycine (Gly-Gly). Fig. 48 demonstrates that Gly-Gly induced significant currents in DtpA- or DtpB containing

proteoliposomes but not in control liposomes lacking the transport proteins. The initial short current spikes are artifacts induced by buffer changes. The negative current peaks observed after changing back to the glycine-containing washing buffer represent most likely the backflow of charges (Gly-Gly with protons) out of the liposomes as now the substrate gradient is reversed. Since the transport studies were performed in Na^+-free buffers at pH 7.0, the observed currents must originate from proton-movement coupled to dipeptide translocation in a symport mechanism.

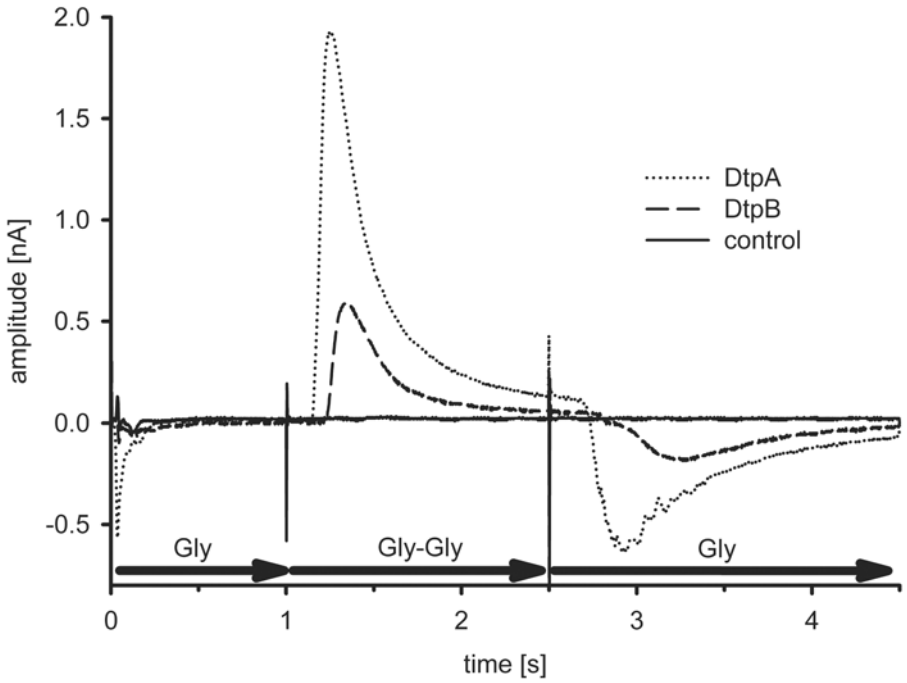

Fig. 48: Electrical measurements with proteoliposomes using the SURFE^{2}R^{one} setup. Electrical response of liposome-reconstituted DtpA (dotted line) or DtpB (dashed line) to a change from a solution without substrate (Gly) to a solution with substrate (Gly-Gly). The solid line shows the recording from a sensor loaded with protein-free liposomes. The current peaks indicate proton co-transport; the negative peak is backflow of charges out of the liposomes. (One of >10 similar experiments using ≥2 sensors)

Like in the cytochrome *c* oxidase energized vesicles, DtpA caused higher signals than DtpB, suggesting that DtpA has a higher turn-over rate or higher stability *in vitro* but it might also be just by variance in the sensor preparation.

DtpC and DtpD could not yet be tested with adequate substrates. Early experiments with Gly-Gly were unsuccessful, but studies in the cells already indicated that Gly-Gly may be unsuitable for transport characterization.

4.4.3. Analysis of KO-strains

To assess whether PTR transporter genes of *E. coli* are expressed under standard growth conditions, uptake experiments were performed also with knockout strains from the Keio

collection (Baba *et al.*, 2006) and substrates specific for each transporter (Fig. 49) were employed. There was a clear reduction of Gly-Sar uptake in the *dtpA* knockout strain (Fig. 49 A), but the *dtpB* knockout did not differ in Gly-Sar uptake from a wild type strain (Fig. 49 B). Thus, under standard growth conditions, *dtpB* seems not to be expressed and Gly-Sar uptake seems mainly to be catalysed by DtpA. In uptake experiments performed with lysine, *dtpC* deletion mutants showed after some time reduced uptake (Fig. 49 C). A reduced uptake relative to wild type controls was also observed for 6-AHA uptake in cells lacking *dtpD* (Fig. 49 D). Thus, of the four Dtp proteins in *E. coli*, DtpA, DtpC and DtpD appear to be expressed under standard culture conditions to provide nutrient/peptide uptake.

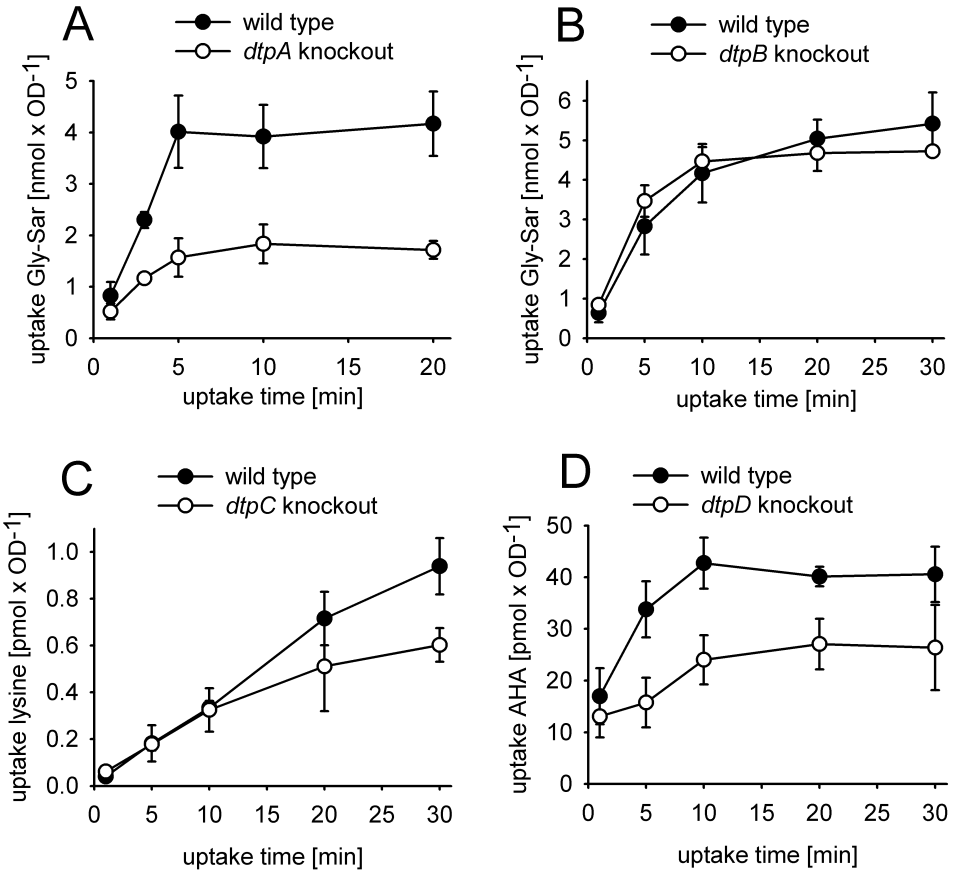

Fig. 49: Uptake experiments with knockout strains of the *E. coli* PTR transporter. (A) Uptake of [^{14}C]glycyl-sarcosine (35 µM) by wild type *E. coli* cells and the *dtpA* knockout strain. n=4. **(B)** Uptake of [^{14}C]glycyl-sarcosine (35 µM) by wild type *E. coli* cells and the *dtpB* knockout strain. n=4. **(C)** Uptake of [^{3}H]lysine (20 nM) by wild type *E. coli* cells and the *dtpC* knockout strain. n=4. **(D)** Uptake of [^{14}C]6-aminohexanoic acid (73 µM) by wild type *E. coli* cells and the *dtpD* knockout strain. n=4.

For the *dtpC* knockout strain additionally the uptake of arginine or histidine was examined. Fig. 50 shows that it is essentially unchanged after 30 minutes of incubation suggesting that DtpC does not play a prominent role in overall uptake of arginine and histidine in *E. coli*.

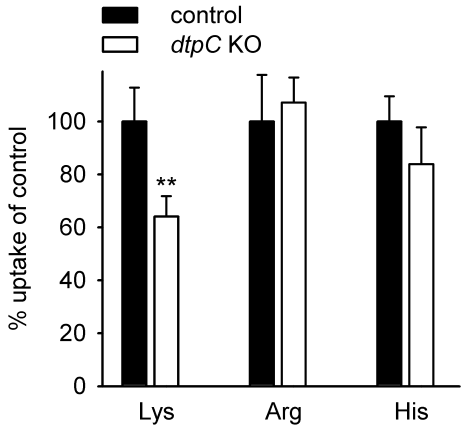

Fig. 50: Uptake of amino acids by the *dtpC* knockout strain or control *E. coli*. 30 min uptake with 22 nM [^{3}H]lysine present. 100%= 0.52 fmol × s^{-1} × OD^{-1}. Arg: [^{3}H]arginine (34 nM), 100%=0.38 fmol × s^{-1} × OD^{-1}. His: [^{3}H]histidine (38 nM), 100%=0.076 fmol × s^{-1} × OD^{-1}. n=4, **: significant reduction ($p<0.01$)

4.4.4. Growth curves

With growth curves a second *in vivo* technique was applied for testing the functional expression of the transporters. This growth assay is based on the use of toxic substrates that can impair proper growth of the *E. coli* cells. One is the phosphonopeptide alafosfalin and the other compound is the antibiotic chloramphenicol. For the growth curves *E. coli* cells carrying the overexpression vector for a transporter were grown in the presence of a non-lethal concentration of alafosfalin and expression of the transporter was induced at the OD_{600} of 1. The effect on the growth was observed by OD_{600} measurements.

4.4.4.1. Growth curves - alafosfalin

Alafosfalin is an antibacterial agent that acts by inhibition of cell wall biosynthesis. After uptake it is cleaved to alanine and aminoethylphosphonic acid, which disrupts various steps in cell wall biosynthesis (Maruyama *et al.*, 1979). Fig. 51 shows the growth curves with alafosfalin and the four PTR transporters of *E. coli*. In Fig. 51 A the growth curve for cells overexpressing *dtpA* is demonstrated. Growth rates were slightly reduced in the presence of 200 µg/ml alafosfalin as compared to *E. coli* grown in the absence of alafosfalin. When expression of *dtpA* was induced at an OD_{600} of about 1, alafosfalin now caused cell death. This indicates that DtpA was functionally expressed in the membrane and thereby loaded the cells with the toxic agent. Fig. 51 B shows the relevant curve for DtpB. Here the alafosfalin concentration was increased to 500 µg/ml to observe a defined effect. Additionally control cells carrying the empty expression vector were grown to survey the effect of IPTG on growth. Panel C demonstrates the effect of *dtpC* overexpression with the same alafosfalin

concentration demonstrating only a small effect. The *dtpD* overexpression produced effects (Fig. 51 D).

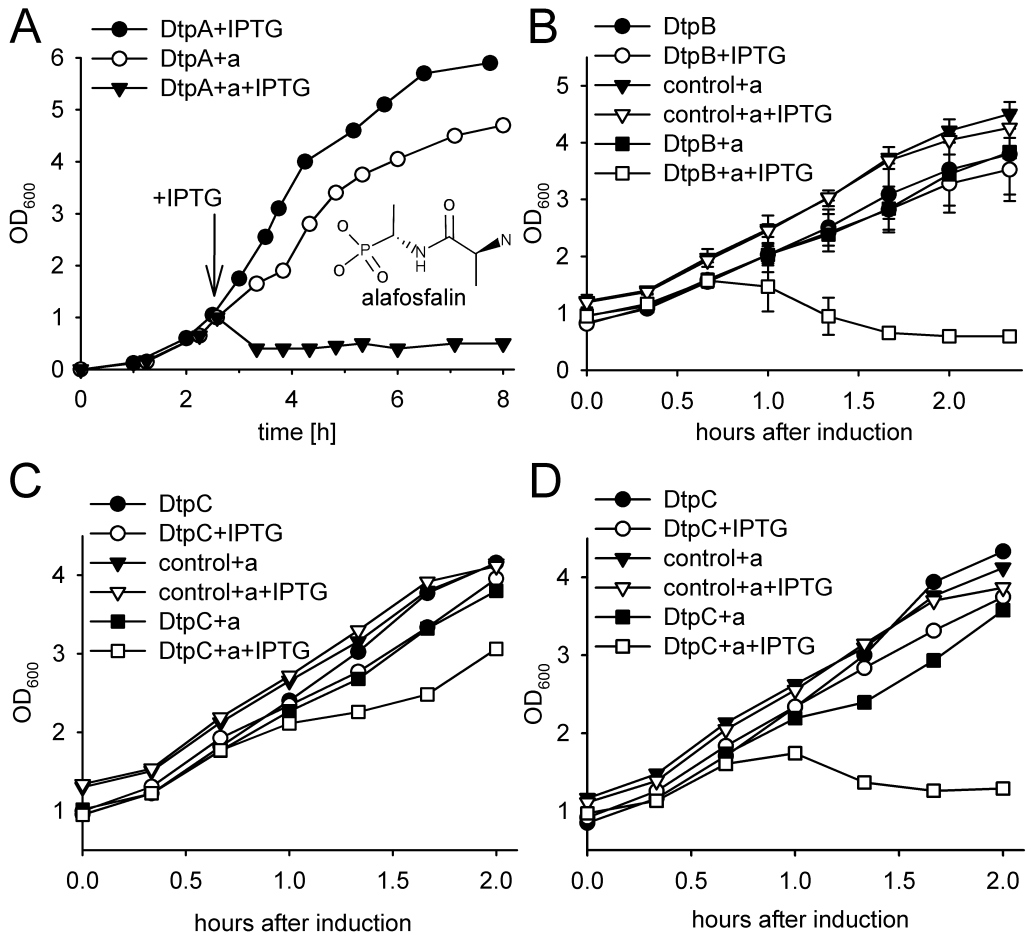

Fig. 51: Growth curves in the presence of alafosfalin. *E. coli* cells carrying the overexpression vector for the transporters or the empty vector were grown in the absence or presence of the toxic substrate alafosfalin. At OD_{600}= 1 expression was induced by 0.1 mM IPTG, or not induced. **(A)** DtpA; 200 µg/ml (1 mM) alafosfalin. **(B)** DtpB; 500 µg/ml (2.55 mM) alafosfalin. **(C)** DtpC; 500 µg/ml alafosfalin. **(D)** DtpD; 500 µg/ml alafosfalin.

4.4.4.2. Growth curves - chloramphenicol

Chloramphenicol is a antibiotic agent that acts as an inhibitor of protein biosynthesis by binding to the ribosome and blocking of the peptide bond formation (Nierhaus and Nierhaus, 1973). Chloramphenicol was used at a concentration of 1 ng/ml for all four transporters and the *E. coli* BL21 strain without pLysS was used, because pLysS carries a chloramphenicol resistance gene.

Fig. 52 demonstrates that the overexpression of each of the four transporters resulted in growth inhibition, but with differing efficacy. Clearly *dtpA* and *dtpD* overexpression inhibited cell growth most; in case of *dtpD* even the uninduced background expression seemed to have an effect. Generally weaker was the effect in case of DtpB and DtpC. The growth

inhibition caused by *dtpB* overexpression appeared to be slightly stronger than that with *dtpC* overexpression. Beside the different expression levels of the proteins, these differences might also reflect differing binding/transport affinities.

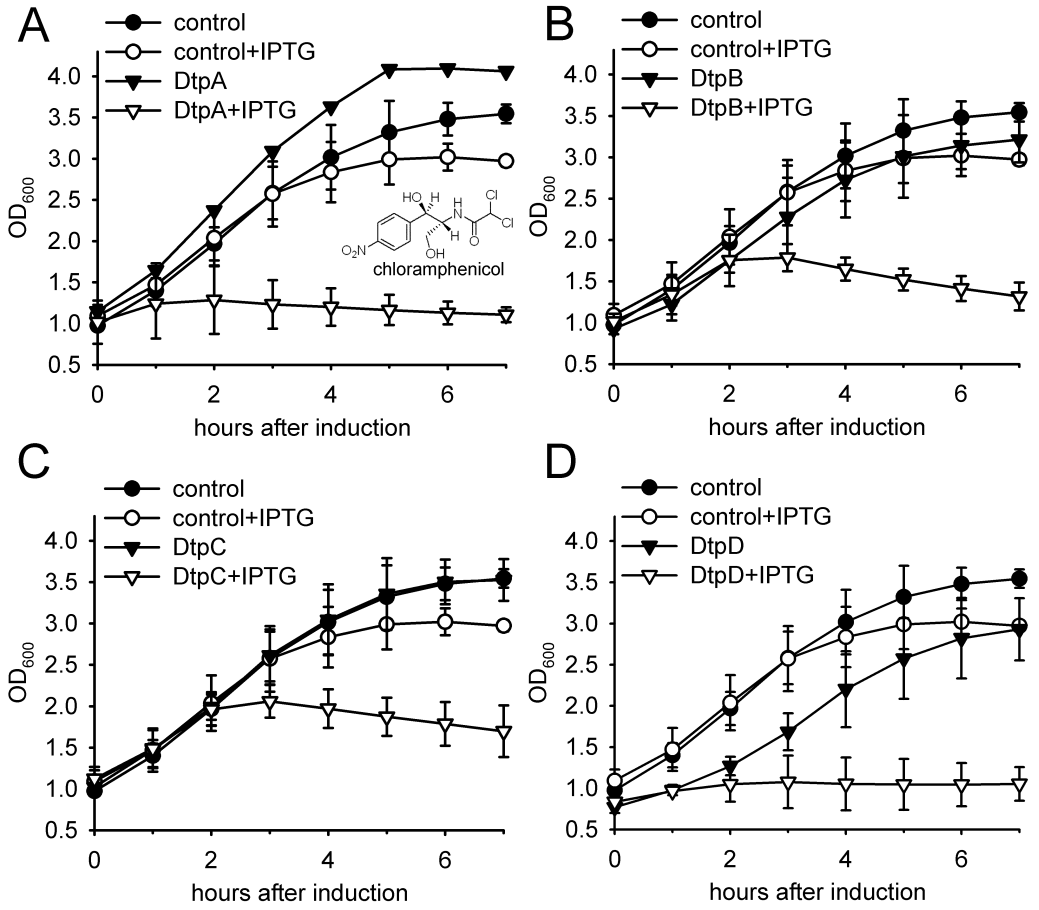

Fig. 52: Growth curves in the presence of chloramphenicol. *E. coli* cells carrying the overexpression vector for the transporters or the empty vector were grown in the presence of the toxic substrate chloramphenicol (1 ng/ml, 3.1 nM). At OD_{600}= 1 expression was induced by 0.1 mM IPTG, or not induced. **(A)** DtpA. **(B)** DtpB. **(C)** DtpC. **(D)** DtpD.

4.5. Expression of the transporters in *Xenopus* oocytes

Expression in oocytes was performed because it would enable the characterization of current-coupled transport via the two electrode voltage clamp technique. For expression the DtpA mRNA was injected into *Xenopus laevis* oocytes and 3 days after injection current measurements were performed. Unfortunately no currents were detected when the substrates Gly-Sar or Gly-Gln were offered for uptake. When different injection volumes and concentrations of cRNA or different incubation temperatures or a modification of the RNA with a eukaryotic Kodzack sequence were introduced (see methods section 7.14.1, p. 95) still no currents could be recorded. A Western blot with oocyte membranes obtained after injection of the mRNA (see methods section 7.14.3, p. 96) revealed (Fig. 53) a protein band at similar height as the purified control DtpA (lane 2, 3) whereas control oocytes did not have

this band (lane 1). The presence of the DtpA band indicated a normal translation and protein stability in *Xenopus* oocytes; however, the localization of the protein within the cell remained to be determined. If not integrated into the plasma membrane, no functional transport currents would result.

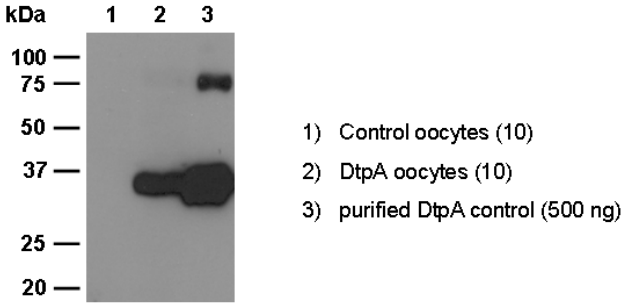

Fig. 53: Western blot of *X. laevis* oocytes with *dtpA* mRNA injected. 10 oocytes were lysed two days after mRNA-injection and trition-x-100-solubilized proteins were loaded on the gel. The His-tag antibody was used for detection.

The localization was addressed by immunohistochemistry on sections of *dtpA*-expressing oocytes (see methods section 7.14.4, p. 96). Visualization of the protein was performed using the His-tag antibody and a secondary antibody with the fluorophore Alexa 488 by fluorescence microscopy. Representative examples of the results are shown in Fig. 54. Obviously DtpA is present in the oocyte and also in (or near) the plasma membrane. Therefore the question arose if a more sensitive method than electrophysiology could detect functionality of the expressed protein. Uptake of radiolabeled substrate (see methods section 7.14.5, p. 97) can be used for this purpose and the first results are shown in Fig. 55.

About half of the injected oocytes showed stronger signals than the relatively homogenous control group oocytes. This indicated that some – yet only a small amount of functional DtpA resided in the membrane. However, in course of this study a useful electrophysiological assay system in oocytes could not be established.

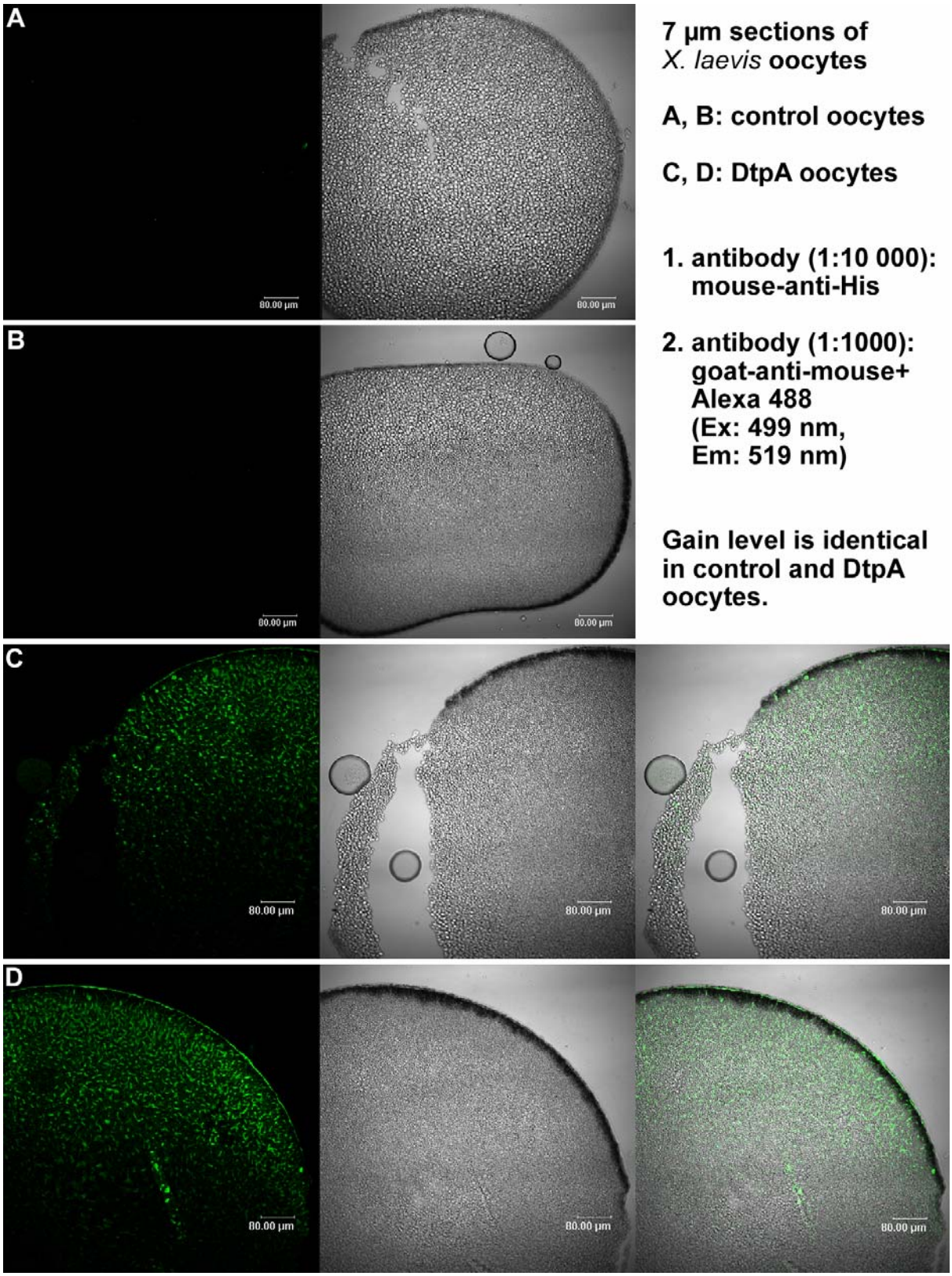

Fig. 54: Immunohistochemistry of oocytes expressing *dtpA*. The left panel shows fluorescence, the center panel the light microscopic picture and right panel the overlay.

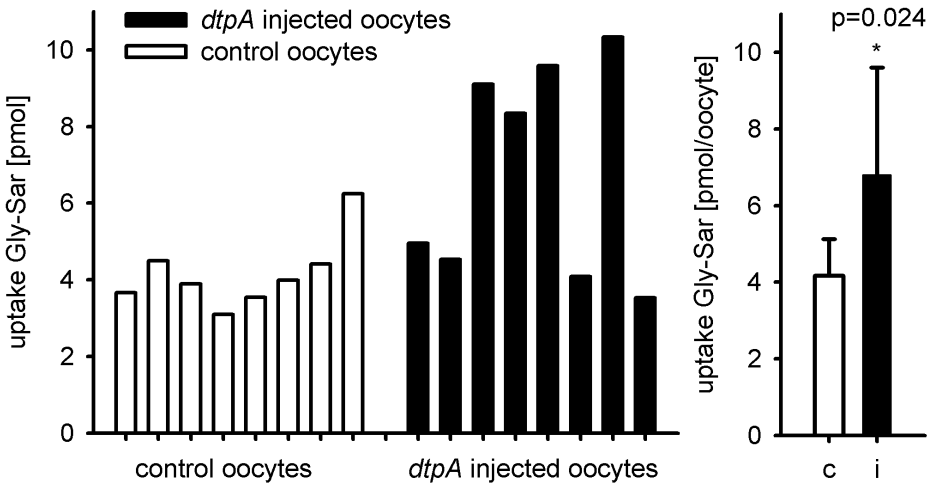

Fig. 55: Radiolabeled uptake in oocytes. [^{14}C]Gly-Sar was offered for uptake with control oocytes and *dtpA*-injected oocytes. The bars represent individual oocytes. The right panel shows the same data as mean +SD. The difference is significant by t-test ($p<0.05$).

4.6. Structural characterization

4.6.1. Crosslink experiments

To assess the quaternary structure of the proteins, chemical crosslinking experiments were conducted. As described in the methods section (7.15, p. 97), the crosslinker substances are able to connect subunits of a multimeric protein (Fig. 73, p. 98), which can be detected in Western blot analysis in a SDS-polyacrylamid gel. Crosslinking was performed for DtpA, DtpB, DtpC and DtpD using membrane preparations of transporter overexpressing *E. coli*. As the protein is still in the membrane without prior denaturation, a potential multimer should still be intact and the crosslinking of the subunits should be enabled. Additionally Ni^{2+}-affinity purified proteins were used and solubilized in the mild, non denaturing detergent DDM, assuming also here the quaternary structure to be intact. As a control a purified aldolase (from rabbit muscle, Sigma) was used, which forms a tetramer of 39 kDa monomers after crosslinking. However, in contrast to the peptide transporters it is not a membrane protein. Fig. 56 shows that with increasing crosslinker concentration and incubation time the amount of monomeric aldolase in the gel decreases and simultaneously bands of higher molecular mass appeared at ~75 kDa, ~100 kDa and at the beginning of the gel that can be interpreted as the dimer, trimer and higher multimers. This demonstrated the feasibility of the approach.

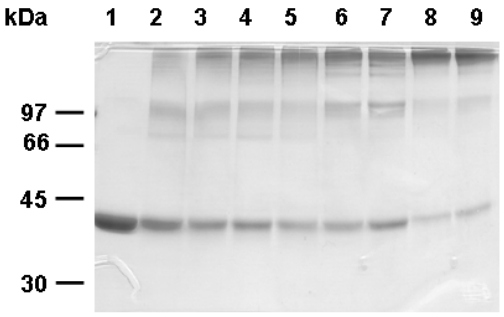

1)	Aldolase	10 µg		
2)	Aldolase	BS^3	0.5 mM	10 min
3)	Aldolase	BS^3	1 mM	10 min
4)	Aldolase	BS^3	0.5 mM	30 min
5)	Aldolase	BS^3	1 mM	30 min
6)	Aldolase	DSS	0.5 mM	10 min
7)	Aldolase	DSS	1 mM	10 min
8)	Aldolase	DSS	0.5 mM	30 min
9)	Aldolase	DSS	1 mM	30 min

Fig. 56: Coomassie stained SDS gel of aldolase crosslink experiments. 10 µg aldolase were treated for indicated times with indicated concentrations of the chemical crosslinker BS^3 or DSS. After SDS polyacrlylamid (12.5 %) gel electrophoresis the monomer at about 40 kDa plus bands of crosslink products of higher molecular mass are visible.

Crosslinking of DtpA did not reveal evidence for a multimeric state. Fig. 57 shows the experiments with BS^3 and DSS where only a faint band of higher molecular mass appeared, corresponding to a very small amount of the protein. Some unspecific multimers are common with membrane proteins that stick together because of their hydrophobicity. In case of DtpA there was additionally glutaraldehyde tested as a crosslinker with a shorter chain length. It is not ideally suitable as crosslinker because it has also effects on proteins. Also here no convincing bands indicating higher multimeric states were found (Fig. 58). The triton purified DtpA has from the beginning a distinct multimeric fraction, but this does not increase upon crosslinking although the monomeric form decreases. So it might be more of a stability problem and unspecific dimerisation. With DDM purified and membrane localized DtpA the dimer band is only very faint, but glutaraldehyde influences the monomer band of DDM-purified DtpA to appear with higher mass. An explanation for this might be an intramolecular crosslinking.

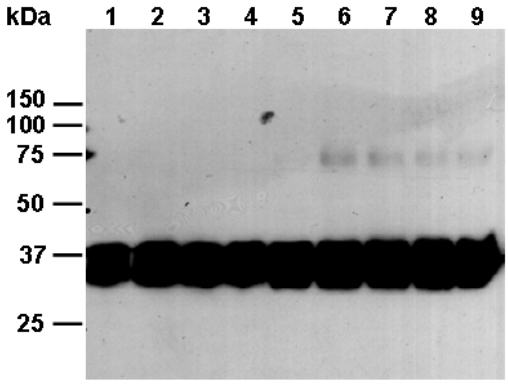

1)	DtpA	membrane		
2)	DtpA	membrane	BS^3	0.5 mM
3)	DtpA	membrane	BS^3	1 mM
4)	DtpA	membrane	DSS	0.5 mM
5)	DtpA	pure		
6)	DtpA	pure	BS^3	0.5 mM
7)	DtpA	pure	BS^3	1 mM
8)	DtpA	pure	DSS	0.5 mM
9)	DtpA	pure	DSS	1 mM

Fig. 57: Anti His-tag Western blot of DtpA crosslink experiments: 600 ng purified DtpA and membranes containing about 600 ng DtpA were treated for 30 min with indicated concentrations of the chemical crosslinker BS^3 or DSS. After SDS polyacrlylamid (12.5 %) gel electrophoresis a Western blot with detection of the His-tag was performed.

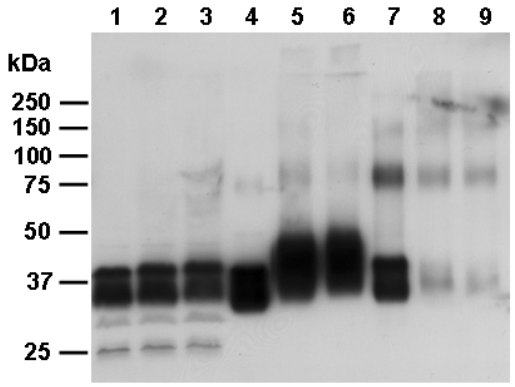

	glutaraldehyde
1) DtpA membrane	
2) DtpA membrane	0.5 mM
3) DtpA membrane	1 mM
4) DtpA pure (DDM)	
5) DtpA pure (DDM)	0.5 mM
6) DtpA pure (DDM)	1 mM
7) DtpA pure (triton)	
8) DtpA pure (triton)	0.5 mM
9) DtpA pure (triton)	1 mM

Fig. 58: Anti His-tag Western blot of DtpA crosslink experiments with glutaraldehyde: 600 ng purified DtpA (with triton or DDM as detergent) and membranes containing about 600 ng DtpA were treated for 30 min with indicated concentrations of the chemical crosslinker glutaraldehyde.

A similar picture appears with DtpB, where also no convincing crosslinking band was obtained (Fig. 59). This also was the case for DtpC (Fig. 60) and DtpD (Fig. 61).

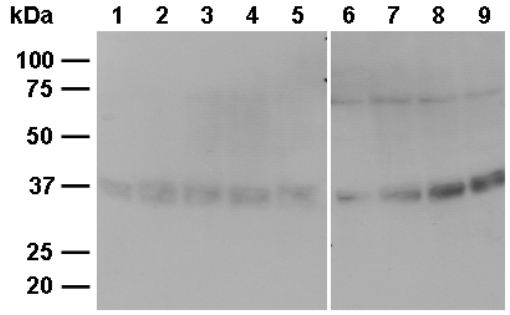

1) DtpB	pure	1 µg	
2) DtpB	pure	BS^3 1 mM	10 min
3) DtpB	pure	BS^3 1 mM	30 min
4) DtpB	pure	DSS 1 mM	10 min
5) DtpB	pure	DSS 1 mM	30 min
6) DtpB	membrane		
7) DtpB	membrane	BS^3 1 mM	30 min
8) DtpB	membrane	DSS 1 mM	10 min
9) DtpB	membrane	DSS 1 mM	30 min

Fig. 59: Anti His-tag Western blot of DtpB crosslink experiments: 1.6 µg purified DtpB and membranes containing about 2 µg DtpB were treated for indicated times with 1 mM of the chemical crosslinkers BS^3 and DSS.

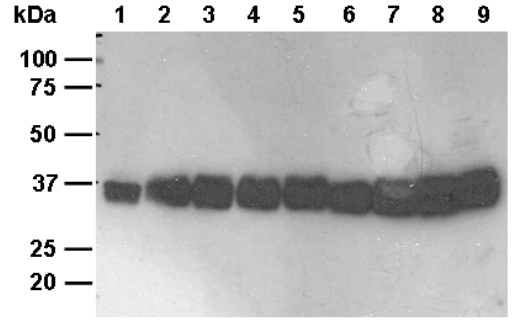

1) DtpC			
2) DtpC	BS^3	0.5 mM	10 min
3) DtpC	BS^3	1 mM	10 min
4) DtpC	BS^3	0.5 mM	30 min
5) DtpC	BS^3	1 mM	30 min
6) DtpC	DSS	0.5 mM	10 min
7) DtpC	DSS	1 mM	10 min
8) DtpC	DSS	0.5 mM	30 min
9) DtpC	DSS	1 mM	30 min

Fig. 60: Anti His-tag Western blot of DtpC crosslink experiments: 1.6 µg purified DtpC were treated for indicated times with the indicated concentrations of the chemical crosslinkers BS^3 and DSS.

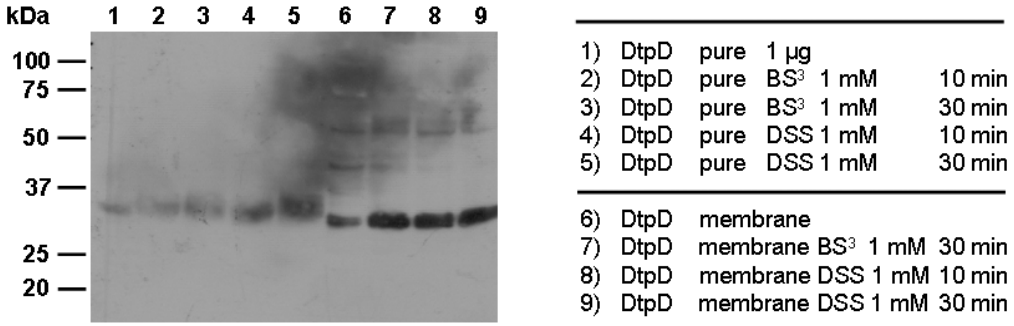

Fig. 61: Anti His-tag Western blot of DtpD crosslink experiments: 1.6 µg purified DtpD and membranes containing about 2 µg DtpD were treated for indicated times with 1 mM of the chemical crosslinkers BS^3 and DSS.

Although it would be expected that crosslinking is successful if proteins form multimers, it can not be concluded that the transporter do not form multimers or act as multimers from the negative results obtained here.

4.6.2. Gel filtration

Another method that was used to elucidate the oligomeric state of the proteins was by analytical gel filtration. The principle of the method is the differential mobility of particles according to their size in the column. Large particles pass rapidly while smaller particles enter the pores of the column material and are delayed. Therefore solutions of purified proteins that were solubilized in the non-denaturing detergent DDM were loaded onto a gel filtration column. By comparison to standard proteins the molecular mass of the proteins or protein complexes can be estimated and conclusions about the multimeric state can be drawn. In Fig. 62 the results for the four transporters are shown. DtpA and DtpD show a narrow relatively high single peak. This reflects the high purity in nickel affinity chromatography and a high stability after purification as the proteins are monodisperse with only one size fraction. In contrast, the peaks of DtpB and DtpC are smaller, broader and with various sidepeaks. There are also aggregated protein particles that elute in the void volume (8 ml fraction) of the column. These findings suggest that here a lower purity and possibly also a lower stability of these two proteins cause the sidepeaks. The calculated masses are relatively high in comparison to the predicted monomer masses of about 55 kDa that are also seen in Western blot analysis with about 40 kDa. Therefore a di- or trimeric form seems probable based on these experiments. But it has to be taken into account that the detergent micelle of DDM is carried with all membrane proteins, which makes them bigger and allows them to move faster, which can lead to an overestimation of their molecular mass. This is especially critical with DDM, which forms relatively big micelles. Therefore, the size exclusion chromatography does also not allow solid conclusions to be drawn on the oligomerization

state of the proteins. Nevertheless, the data are valuable as a measure for protein quality, which is important for successful crystallization.

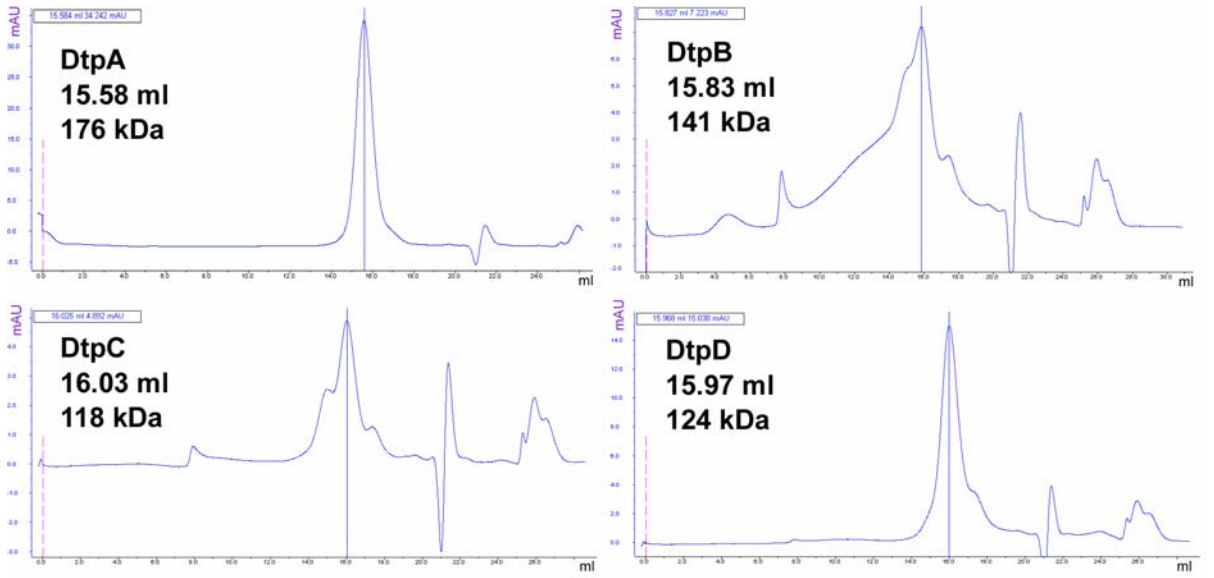

Fig. 62: Gel filtration of purified transporter proteins. The y-axis is UV absorption and indicates protein. The x-axis is the elution volume from the sepharose 6 column. 200 µl protein solution was loaded that contained in case of DtpA 70 µg, DtpB 100 µg, DtpC 40 µg and DtpD 93 µg protein. The late negative-positive signal and the following three peaked signal are salt peaks. The small peaks at 8 ml are denatured/aggregated proteins.

4.6.3. Dynamic light scattering

Another technique for estimating the hydrodynamic radius of the particles, and by that on the probable oligomeric state, is the dynamic light scattering. Measurements are based on the dependence of light scattering fluctuations on the mobility and thereby the size (hydrodynamic radius) of particles in solution. This was done as an example for DtpA as described in the methods section (7.17, p. 99). The results are shown in Table 4 with a mean molecular mass derived with 113.4 kDa - but like in gel filtration here also the DDM micelle is measured that makes the protein to appear in larger size. However, like in gel filtration analysis, only one particle species (monodispersity) can be observed with high percentage in the fraction. Only about 1% of the particles appeared as aggregates what indicated a high stability of the protein. The buffer alone was also measured and only when DDM is present, there appear particles with a size of 5.3 nm corresponding to a mass of 36 kDa. This represents the DDM micelles and provides a measure for DDM mass addition to the mass of the solubilized proteins. In conclusion, no final judgement on the oligomerization state of DtpA can be made from lightscaattering either.

Table 4: Dynamic light scattering of DtpA

sample		particle diameter	percentage	corresponding kDa
DtpA	(1)	8.55 nm	98.7 %	100.8 kDa
DtpA	(2)	8.82 nm	98.8 %	108.4 kDa
DtpA	(3)	9.39 nm	99 %	125.5 kDa
DtpA	(4)	9.24 nm	98.8 %	120.9 kDa
buffer		0.829 nm	100 %	0.4 kDa
buffer with DDM (0.03%)		5.53 nm	100 %	36.4 kDa

4.6.4. Circular dichroism spectrometry

For DtpA the secondary structure was analyzed via circular dichroism (CD) spectrometry. As described in the methods section (7.18, p. 99) a DtpA solution analyzed showed the typical shape of a high alpha-helical protein content (Fig. 63). The determining features are the strong negative minima at ~208 nm and ~222 nm that are caused by alpha-helical structures. A positive maximum is present at 199 nm, which is more typical for β-sheet structures and might indicate also some β-sheet areas in the protein. For comparison with typical CD-spectra for α-helical and β-sheet structures see methods section Fig. 75, p. 100.

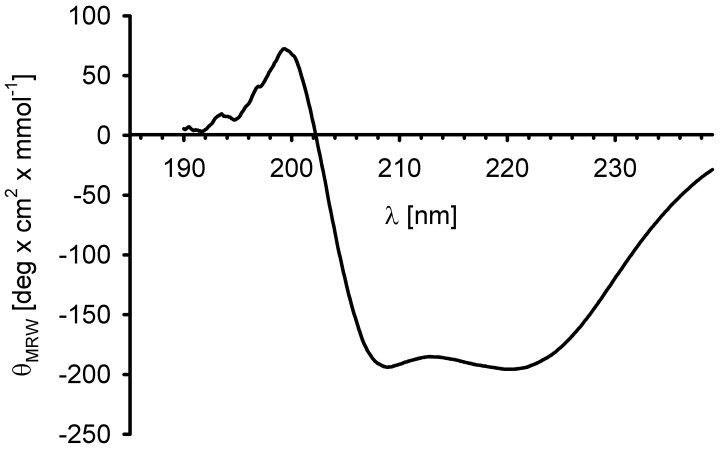

Fig. 63: CD-spectrum of DtpA. Normalized to the molar ellipticity per amino acid θ_{MRW}

4.6.5. MALDI-TOF mass spectrometry

Matrix assisted laser desorption/ionization time of flight (MALDI-TOF) mass spectrometry was used to demonstrate that the protein is of full length after overproduction, because the band in the gel had indicated a smaller molecular mass than expected (~40 kDa instead of ~55 kDa). Two strategies were followed: 1) to analyze the undigested protein 2) to digest the purified protein (directly or out of a SDS-gel) with trypsin and to analyze the fragments. This would additionally have allowed experiments to map the substrate binding site by

crosslinking substrates during transport and identifying the fragments with the additional labeled mass of the substrate. Experiments with the undigested protein as described in the methods section (7.19, p. 100) were unsuccessful in producing any signal what might be attributed to the high hydrophobicity of the membrane protein. Digestion with trypsin was either done directly with purified DtpA or with protein that was excised from a SDS-gel. The 2D-gel of purified DtpA showed a prominent smeared spot and several minor spots (Fig. 64) that probably reflect the impurities after nickel-affinity elution. After trypsination and MALDI-TOF analysis, none of the peptide masses could be assigned with significance to predicted fragments by database search. It was quite surprising that none of the spots could be identified; one explanation is that all of them are probably membrane proteins (because of the purification procedure) and therefore problematic candidates (for trypsination as well as desorption/ionization). Also from the direct digestion and the 1D-gel excised protein there were fragment masses detected with witch the database search could not identify a corresponding protein. Table 5 shows detected masses and compares them to the theoretically expected masses of fragments from trypsin digested DtpA. There are at least three masses detected that mach to an expected fragment (in bold type) including the C-terminal His-tag region, which was detected with all three methods. Nevertheless most of the expected masses are absent, some are only similar and some of the detected masses don't mach to any expected fragment. The reason for these inconclusive results may again be the high hydrophobicity that could account for incomplete trypsination and problems in the desorption/ionization.

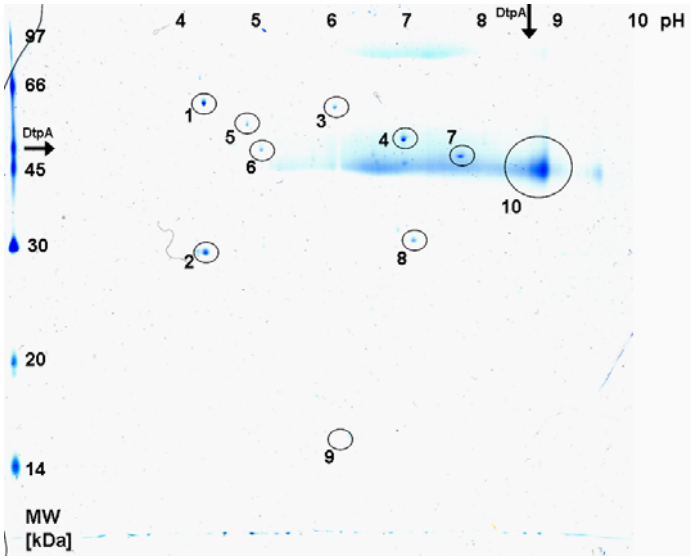

Fig. 64: 2D-SDS-PAGE of purified DtpA. 150 µg purified DtpA were separated by isoelectric focusing and afterwards according to molecular mass in the SDS-PAA-gel. The theoretical values for the isoelectric point and the molecular mass of DtpA are indicated by arrows.

Table 5: MALDI-TOF analysis of trypsinated DtpA (YdgR)

DtpA trypsinated MALDI-TOF analyzed*			Theoretical fragments of trypsinated DtpA [Theoretical pI: 8.73 / Mw (average mass): 55056.26]		
directly	1D-gel	2D-gel			
mass	**mass**	**mass**	**mass**	**position**	**peptide sequence**
			4766.3198	415-459	LMGFIMGSWFLTTAGANLIG GYVAGMMAVPDNVTDPLMSLEVYGR
			4334.2926	373-414	FASDAGIVSVSWLVASYGLQ SIGELMISGLGLAMVAQLVP QR
			4133.2151	90-130	VIMLGAIVLAIGYALVAWSG HDAGIVYMGMAAIAVGNGLF K
			4121.2109	306-342	NVEHSILGLAVEPEQYQALN PFWIIIGSPILAAIYNK
			3638.9591	275-305	MIVAFILMLEAIIFFVLYSQ MPTSLNFFAIR
			3432.7395	51-83	QLGMSEADSITLFSSFSALV YGLVAIGGWLGDK
			3232.5555	148-176	LDGAFTMYYMSVNIGSFFSM IATPWLAAK
			2954.7553	220-246	NLLLTIIGVVALIAIATWLL HNQEVAR
		2807.37	2874.5374	177-202	YGWSVAFALSVVGLLITIVN FAFCQR
2225.03	2225.13		2268.3763	460-481	VFLQIGVATAVIAVLMLLTA PK
			2039.089	353-372	FAIGMVMCSGAFLILPLGAK
	1940.9		1952.9746	1-18	MSTANQKPTESVSLNAFK
	1821.92		**1821.9607**	**35-50**	**FGYYGLQGIMAVYLVK**
	1700.12		1713.8231	206-219	QYGSKPDFEPINYR
1696.78	1696.78		1686.889	22-34	AFYLIFSIELWER
			1620.9545	247-262	MALGVVAFGIVVIFGK
1433.65		1488.05	1412.6726	131-143	ANPSSLLSTCYEK
1395.69	**1395.67**	**1395.74**	**1395.6777**	**497-508**	**AAVALEHHHHHH**
1150.57	1150.58	1066.11	1090.5271	343-352	MGDTLPMPTK
1060.05		1050.11			
994.43			**994.4146**	**485-493**	**MTQDDAADK**
967.55	967.57	914.58			
			696.3385	263-268	EAFAMK
			517.3344	84-88	VLGTK
			501.2416	144-147	NDPR

*Only matching or similar experimental masses are shown. Total number of obtained masses was each about 15-20

4.6.6. Protein crystallization

Crystallization experiments were performed at the M. E. Müller Institute for Structural Biology of the University of Basel, Switzerland, during a 3 month period in the host lab. Additional experiments were conducted by the local project partner PhD student Fabio Casagrande and are reported in his dissertation (http://pages.unibas.ch/diss/) and a corresponding manuscript (Casagrande *et al.*, 2009).

4.6.6.1. 2D crystallization

The reconstitution of high protein content containing proteoliposomes with the purified transporter proteins via dialysis was performed as described in the methods section (7.20, p. 102). Table 16 in the methods section shows the factors that were varied during the crystallization attempts. Table 6 shows the relevant features of the proteins for crystallization and the outcome from the various trials performed. None of the proteins was stable enough in a high critical micelle concentration (CMC) detergent what would have allowed a faster

dialysis and that would have increased the probability for proper crystallization. DtpC failed to yield sufficiently high protein concentrations while DtpB was not pure enough and may therefore not have formed crystals. Only DtpD, which could be dialyzed rapidly at 37 °C, and to some extent also DtpA, successfully showed 2D crystal formation in the membrane of the proteoliposomes. The conditions that led to successful small tubular crystals in case of DtpA were: detergent DDM, lipid dimyristoylphosphatidylcholine (DMPC), standard dialysis buffer, room temperature and various LPR (lipid to protein ratio). DtpD showed medium tubular or variable shaped crystals with the detergent DDM or Cymal-7, *E. coli* lipid, standard dialysis buffer (but also with betaine or KCl) and 37 °C at LPR of 0.25. Some of the DtpD vesicles with crystalline regions are shown in Fig. 65. When crystalline regions in the proteoliposomes were present, this was usually already indicated by the shape of the proteoliposomes, which were not round but angular. 2D crystals are visible in negative stain EM pictures of proteoliposomes as grids in the membrane. They represent regularly arranged protein particles in the membrane (scheme in Fig. 76, p. 104).

The problem with these proteoliposomes was that there was always an unordered region in the middle but no large continuous crystal grid. Fabio Casagrande optimized the 2D crystallization further in his PhD project and obtained first information from diffracting crystals about unit cell dimensions and packing order on DtpA and DtpD.

Table 6: 2D crystallization results (-: negative feature, +: positive feature)

transporter	high CMC detergent	relatively pure	high yield	dialysis at 37 °C	vesicles with crystal-grids
DtpA (YdgR)	-	+	+	-	+/-
DtpB (YhiP)	-	+/-	+	-	-
DtpC (YjdL)	-	-	-	n.d.	-
DtpD (YbgH)	-	+	+/-	+	+

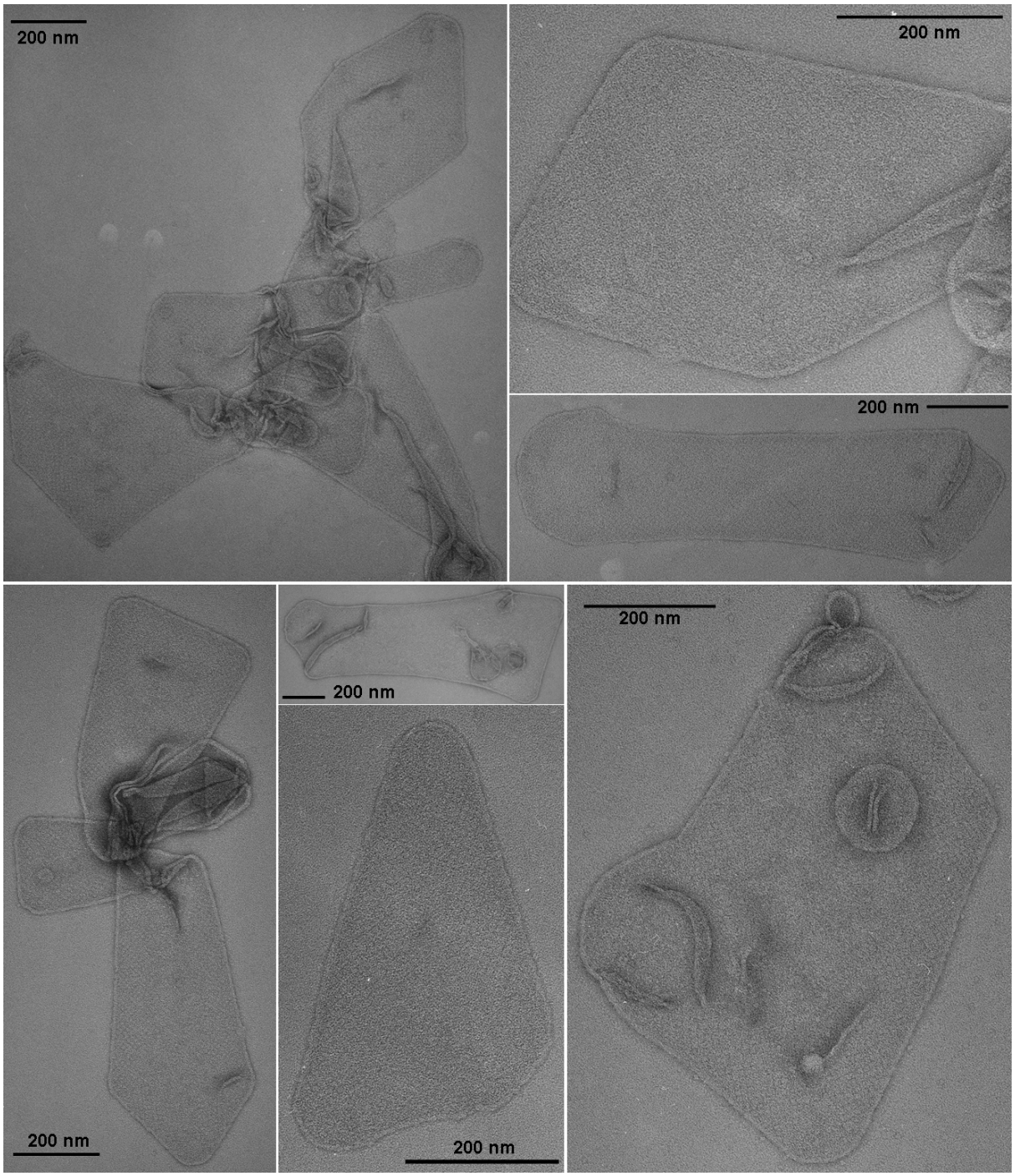

Fig. 65: DtpD vesicles with visible 2D crystal-grids: Negative stain electron microscopic pictures of proteoliposomes (*E. coli* lipid, DtpD) with a LPR of 0.25. Dialysis of the detergent DDM was performed at 37 °C.

4.6.6.2. 3D crystallization

For 3D crystallization trials (methods section 7.20, p. 102) the protein was exposed to different buffers under conditions leading to supersaturation and subsequently to the possibility of crystallization. This was initially done for DtpA and DtpB and the various conditions tested are listed in Table 7. Protein concentrations were raised to ~10 mg/ml with

spin-columns, which is considered as a minimum concentration for crystallization. As concentrating could have negative effects on protein quality, directly eluted proteins were used as well. Since the detergent can have a major influence on protein stability and conformation and therefore on crystal forming, beside DDM also Cymal-7 was used. Other factors that were modified in the crystallization trials were buffer substances (and pH), ionic strength (NaCl concentration) and different types and concentrations of precipitants (polyethylene glycols (PEG)). Some minor crystal forming with DtpA was observed after some weeks but the size of the crystals was too small and tests did not show diffraction. Further experiments (also with DtpD) were carried out by Fabio Casagrande (PhD thesis) but yet not with ordered crystals.

Table 7: 3D-crystallization conditions

Feature	Tested range
Protein:	direct (4-7 mg/ml), concentrated (~10 mg/ml)
Detergent:	DDM, Cymal-7
Buffer and pH:	Na-cacodylate pH 5.5, ME pH 6.5, Mops pH7.5, Tris pH 8.5 (each 50 mM)
Ionic strength:	NaCl (mM): 100, 250, 400, 550, 700, 850
Precipitant:	PEG 200, PEG 300, PEG 400, PEG 1000, PEG 4000 (each 30-55 %)

5. DISCUSSION

5.1. Sequence analysis

The PTR family in *E. coli* is represented by the four genes *ydgR*, *yhiP*, *yjdL* and *ybgH* which were renamed here *dtpA*, *dtpB*, *dtpC* and *dtpD*. Dtp stands for di- and tripeptide permease in analogy to DtpT, which is used for the homologue in *Lactococcus lactis* and other bacteria. At this time all of the four genes were classified as hypothetical transporter proteins. By locus analysis, *ydgR* then was identified to be the *E. coli* homologue of *tppB* from *Salmonella typhimurium* (Goh *et al.*, 2004), which had been described in early studies in 1984 (Gibson *et al.*, 1984; Higgins and Gibson, 1986). Also in *E. coli* some work was done with deletion mutants of *tppB* (Payne *et al.*, 2000a; Payne *et al.*, 2000b), but leaving many aspects like transport mode or biochemical analysis unaddressed.

After identification by BLAST search using PEPT1 as template in the *E. coli* genome, the degree of sequence similarity was investigated in more detail using multiple sequence alignments. The sequence identity between the functionally similar PEPT1 and PEPT2 transporters is nearly 50% plus 20% similarity, while the *E. coli* transporters share with PEPT1 only about 20% identity and 30% similarity. Highest sequence identity between the *E. coli* transporters and PEPT1 and PEPT2 can be found in the first half of the proteins especially in the transmembrane regions (TM) 1-6 and the first extracellular loop. A modest sequence identity is also found in TM 10–12 and, as suggested by functional analysis of mammalian PEPTs based on chimeric proteins and by site directed mutagenesis, these regions are involved in substrate binding and transport (Bolger *et al.*, 1998; Doring *et al.*, 1996; Fei *et al.*, 1997; Terada *et al.*, 1996; Yeung *et al.*, 1998; Zhu *et al.*, 2000). Some of the amino acid residues in these regions were identified as essential for transport by PEPT1 and are well conserved in the *E. coli* transporters including Tyr_{64} in TM 2 and Glu_{595} in TM 10. The amino acid His_{121} at the beginning of TM 4 is not conserved (except DtpD), and only in case of DtpA there is an alternative His residue nearby. Surprisingly the His_{57} residue that is described as essential for proper function in the mammalian peptide transporters is not conserved in any of the *E. coli* transporter and is replaced by a serine residue (or Gly in DtpB). The region with the lowest homology is found around TM 7–9. These regions are thought to contribute to the different kinetic phenotypes of PEPT1 and PEPT2 (Fei *et al.*, 1998). Most strikingly, the *E. coli* transporters do not possess the large extracellular loop between TM 9 and TM 10 found in PEPT1 and PEPT2, which suggests that the loop domain is not important at all for the transport process.

Graphically the overall sequence similarity together with some additional PTR family members is displayed in the dendrogram (Fig. 5). The distances indicate the closest relation of PEPT1 and PEPT2 to DtpA and DtpB, then DtpC followed by DtpD. This was also the basis for the order of naming from A-D. From the prokaryotic species, DtpT from *L. lactis* is slightly closer to PEPT1 and PEPT2 than the *E. coli* transporters.

Transmembrane domain predictions for the PTR transporter result in very different numbers of TM, depending on the program used. It is generally assumed that the PTR transporter possess 12 TM. By using the most sophisticated TMHMM program for all 13 examined PTR members, only for PEPT1 12 TM were predicted whereas for the *E. coli* transporters 14 TM were predicted. This suggests that the number of TM in this family is quite variable or that the prediction tools in this family may not work sufficiently.
The distribution of the four genes in the *E. coli* genome appears to be homogenous. The genetic neighbors are only in case of the lysine-transporting *dtpC* functionally related, with the cadaverine operon (lysine catabolism) upstream and a lysine t-RNA gene downstream in the same reading direction. Because of a strong transcriptional terminator located after *cadA* (Meng and Bennett, 1992) it is however not probable that *dtpC* belongs to the *cad* operon.

5.2. Overexpression

All four transporters were already cloned and expressed in a global membrane proteome analysis approach of *E. coli*, where by GFP and PhoA fusion constructs the C-terminus of all four proteins was found to be localized in the cytoplasm (Daley *et al.*, 2005). In the present project all four transporters were overexpressed in *E. coli* using the pET-21 vector, which adds a hexahistinde tag to the C-terminus. All four proteins could be detected in Western blots with a molecular weight of about 40 kDa, while their calculated masses are about 55 kDa. Most likely, the increased mobility with the underestimation of mass is caused by excess SDS binding, which is not unusual for highly hydrophobic membrane proteins. Proteolysis could be excluded – at least in case of DtpA by adding a second N-terminal tag (T7-tag) and probing the intact protein by Western-blotting that demonstrated that both termini were present.
At the expression level DtpA was found to yield high protein quantities, slightly less was found for DtpB and DtpD, whereas DtpC yielded lowest levels. The reason might be that DtpC is toxic as protein or via its function when inserted in higher amounts in the membrane, or that there is a more rapid degradation of DtpC or its mRNA due to sequence characteristics. It was tried to overcome the weaker expression of DtpC by varying the induction- and expression-conditions, but without success. The low expression level however

was not a problem for the functional characterization, as uptake was still detectable, but crystallization attempts seem impracticable without a further increase of *dtpC* expression level. However, the expression levels obtained here for the four membrane proteins were around 1 mg/l culture after purification and this corresponds to similar values reported in literature (Wang *et al.*, 2003).

The different efficiency of recognition of the proteins by the His-tag antibody was quite surprising, but persistent in many experiments. Based on the same protein quantities DtpA was detected with prominent bands compared to DtpD, with DtpB and DtpC in between. The reason might be that amino acids near the His-tag either favor or hinder the binding of the tag-specific antibody or that the secondary structure, despite SDS denaturation, impairs blotting efficiency, reduces the adsorption to the PVDF membrane or blocks antibody binding.

5.3. Purification

The purification by the His-tag of all four proteins was possible but with different purities. The yield corresponded to the expression level, with highest yields for DtpA, followed by DtpB and DtpD, and with lowest yields for DtpC. The quantity of purified protein per liter culture was about one third of the estimations derived from by Western blot with cell membranes and was with up to 8 mg/l culture for DtpA exceptionally high for membrane proteins (Wang *et al.*, 2003). The purity was highest with DtpA and DtpD, intermediate with DtpB and lowest with DtpC. At least in case of DtpC this reflects as well the low expression level: the contaminating proteins appear to be the same as in purifications with the other transporters, but in case of DtpC the ratio of contaminants to DtpC is markedly higher. A further purification step like gel filtration or ion exchange chromatography seemed necessary but would have reduced the yield further.

5.4. Functional characterization: substrate specificity

For functional characterization, uptake experiments were conducted in cells overexpressing the different proteins by using prototypical substrates generally employed for characterization of mammalian proteins. This approach was successful in case of DtpA with β-Ala-Lys(AMCA) and for DtpB with [^{14}C]Gly-Sar. The reporter substrates [^{3}H]lysine for DtpC and [^{14}C]6-aminohexanoic acid (6-AHA) were identified by screening available different radiolabeled compounds structurally similar to dipeptides. 6-AHA resembles the minimal structure of a peptide with amino- and carboxyterminus separated by an appropriate intramolecular distance (structure in Fig. 40, p. 43), and was found to be transported as well by DtpA, DtpC

and by the human PEPT1 protein (Doring *et al.*, 1998). Lysine is also an aminohexanoic acid, namely 2,6-diaminohexanoic acid and therefore resembles also a dipeptide in structure. Apparent substrate affinities for the test compounds varied considerably (Table 8). Highest affinity with a K_t of 0.032 mM was observed with lysine for DtpC. The K_t of β-Ala-Lys(AMCA) for DtpA was around 0.5 mM followed by Gly-Sar in case of DtpA with a K_t of 1 mM. In the same range was the K_t of 1.4 mM for Bip-Pro in case of DtpC, while for DtpD a K_t of 5.2 mM here revealed low affinity. Similar low affinity with a K_t of 6.5 mM was found for Gly-Sar in case of DtpB and a K_t of 10.6 mM with 6-AHA represented lowest affinity in case of DtpD. Values above 1 mM are generally considered to represent low affinity substrates and in case of values above 15 mM compounds are no longer classified as substrates in case of the mammalian transporters (Biegel *et al.*, 2006; Brandsch *et al.*, 2004).

Table 8: Affinities of the reporter substrates in mM

Substance	DtpA	DtpB	DtpC	DtpD
[^{3}H]lysine	-	-	0.032	-
β-Ala-Lys(AMCA)	0.5	-	-	-
[^{14}C]Gly-Sar	1	6.5	-	-
Bip-[^{3}H]Pro	-	-	1.4	5.2
[^{14}C]6-AHA	-	-	-	10.6

Importance of backbone length

It has been shown for the mammalian PTR transporters, that a certain backbone distance in a peptide that separates a negatively and a positively charged terminus is sufficient for substrate recognition (Doring *et al.*, 1998). Resolving similar chain length restrictions for peptides in case of the four *E. coli* transporters was more difficult. For **DtpA** and **DtpB** it became obvious when using alanine-based di-, tri- and tetrapeptides that only di- and tripeptides bound to the transporters. In case of **DtpC** neither peptides consisting of alanine nor of glycine showed any competition. The fact that lysine was transported and also arginine and more weakly histidine, suggested DtpC to be an amino acid transporter. However, peptides containing specifically cationic residues in the side chain did compete with lysine for uptake. By using peptidase and protease inhibitors, it was found no evidence for hydrolysis of the peptides with the release of cationic amino acids that then could compete with lysine for uptake. When long-chain omega-amino acids were employed, no binding was observed. But the 5 and 6 carbon unit omega amino fatty acids 5-aminolevulinic acid and 6-AHA, which resemble the backbone-length of a dipeptide, showed specific transport. Taken together this indicates that DtpC possesses a similar backbone chain length restriction like DtpA and DtpB. Interestingly the side chain of the amino acid lysine (and to some extent also arginine

and histidine) represents the same charge-distance structure except that here an amino-group is placed next to the carboxygroup at the α–carbon. Therefore, it may actually be the side chain in all of these lysine/arginine containing peptides that confers the affinity. With **DtpD**, again uncharged alanine- and glycine-peptides did not show competition whereas charged di- and tri-peptides, containing lysine or arginine were shown to compete. But in case of DtpD the free amino acids lysine or arginine alone are not transported.

Substrate selectivity

Beside the overall chain length of substrates, also the amino acid composition is a factor that was shown to influence affinity in mammalian peptide transporters. Therefore, peptides consisting of different amino acids and with altered positions of amino acids were examined. In case of **DtpA** the competition experiments were carried out kinetically with increasing inhibitor concentrations, and from the IC_{50} value the system-independent affinity constant K_i was calculated. K_i values of substrates for DtpA were compared to literature values reported for mammalian PEPT1 and PEPT2 and those are shown in Fig. 66.

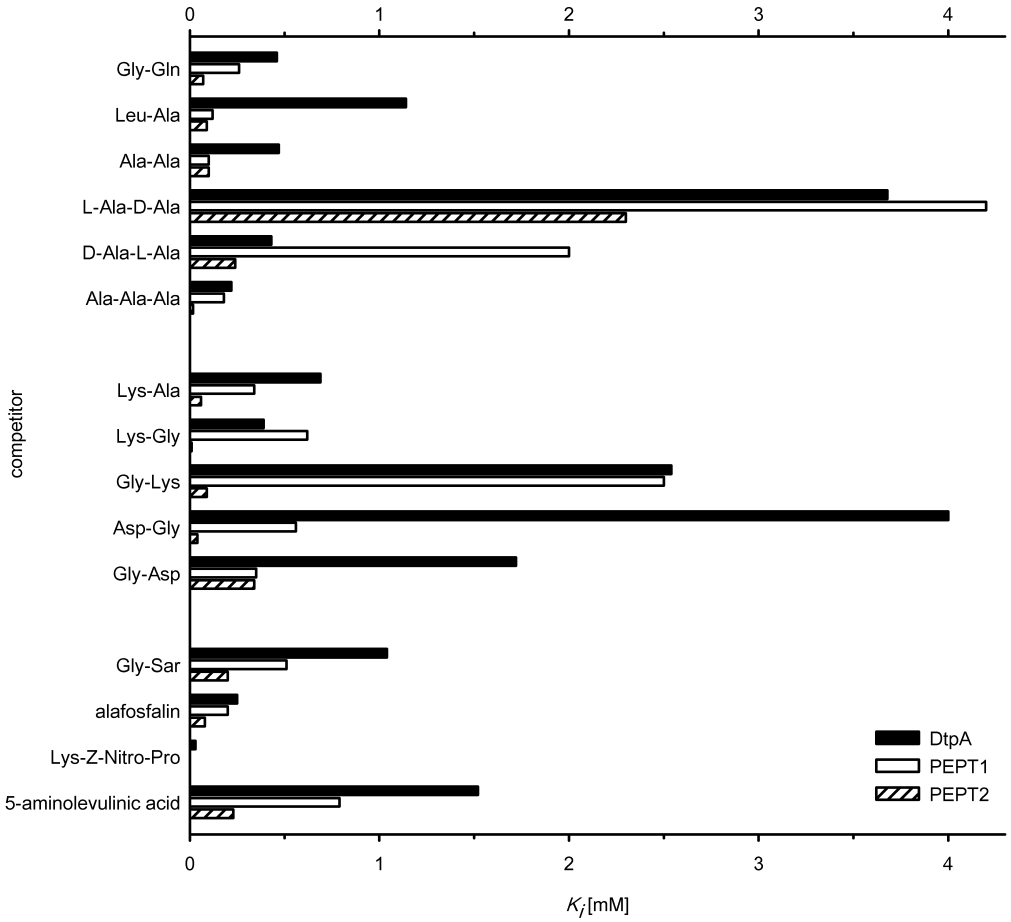

Fig. 66: Comparison of K_i of PEPT1, PEPT2 and DtpA. Values for hPEPT1 (Caco-2 cells/Gly-Sar) and hPEPT2 (*Pichia pastoris* expression/D-Phe-Ala) taken from (Biegel *et al.*, 2006).

The affinities measured are in general in the same range as those found for PEPT1, whereas PEPT2 always has clearly higher affinities. The substrate recognition pattern of DtpA shows a remarkable similarity to the mammalian PEPT1 in various aspects. All known substrates of PEPT1 that were tested with DtpA also interacted with the substrate binding site of the bacterial protein with very similar affinities. Moreover, the observed stereoselectivity of transport and differences in affinities of charged peptides with identical side chains but in different spatial position (N- versus C-terminal) are also characteristic for PEPT1. Finally, even peptidomimetics such as the aminocephalosporins showed a similar fingerprint in competition experiments with DtpA as described in literature for PEPT1. DtpA represents therefore in its substrate recognition pattern in all aspects a mammalian PEPT1-phenotype and suggests that DtpA possesses a similar architecture in the substrate binding domain.

DtpB, like DtpA, has a clear preference for di- and tripeptides composed of L-amino acids. The chain length restriction and some other features match well with data of mammalian PEPT1 and PEPT2 proteins (Biegel *et al.*, 2006; Terada *et al.*, 2000). DtpB, like DtpA, discriminates dipeptides based on the position of charges within the substrate. Peptides containing a positively charged side chain in N-terminal position are good competitors, but the ability to compete is lost when the side chain charge is present in the C-terminus. The reversed pattern was observed for negatively charged side chains, which were generally better tolerated at the C-terminal position. A similar charge preference is found in the mammalian peptide transporters (Daniel *et al.*, 1992; Kottra *et al.*, 2002). Of the ß-lactam antibiotics tested, only cephradine and cefalexin showed modest inhibition of Gly-Sar influx via DtpB whereas for DtpA best inhibition was seen with cefadroxil followed by cephradine and cefalexin. The mammalian peptide transporter PEPT1, which is expressed in the intestine, also clearly prefers those substrates but does not transport cefamandole or cefuroxime that are considered to be inactive when administered orally (Bretschneider *et al.*, 1999). Taken together, DtpB also shows essentially the prototypical substrate characteristics of a di-/tripeptide transporter of the PTR-family. Despite its lower affinity for Gly-Sar and alafosfalin, it is similar to DtpA in the substrate recognition pattern and also shows similarities to the mammalian transporters of the PEPT-subgroup.

Whereas all tested zwitterionic or anionic di- and tripeptides failed to show binding to **DtpC**, lysine turned out to be high-affinity substrate. Similarly, all lysine-containing di- and tripeptides - regardless of the position of the side chain were effective competitors. With its capability to transport also arginine, arginine-containing dipeptides and histidine, DtpC has a distinct selectivity for substrates containing one, two or even three cationic amino acids. Genetically this transporter is different from all described systems of *E. coli* that can transport

lysine, arginine or histidine (*lysP*, *argT-hisJQMP*, *artPIQM-artJ*), and therefore DtpC represents an additional lysine transport system, which seems to be active under standard growth conditions, as suggested by lysine transport experiments with a *dtpC* knockout strain. The feature of transporting lysine as well as only cationic di- and tripeptides makes DtpC unique amongst the di- and tripeptide transporters characterized so far. None of the other three PTR members of *E. coli* is capable to transport α-amino acids and so are PEPT1 and PEPT2 of mammals unable to bind any of the free amino acids. Phenomenological DtpC seems similar to the histidine transporting PTR transporters PHT1 and PHT2 cloned from mammalian cells (Sakata *et al.*, 2001; Yamashita *et al.*, 1997) that also transport selected dipeptides, or to the plant PTR transporter BnNTR1;2, which was shown to transport nitrate and histidine but only weakly lysine and arginine (Zhou *et al.*, 1998). However, in contrast to PHT1 and PHT2, for which zwitterionic dipeptides displayed a high affinity interaction with histidine influx, DtpC failed to show any affinity for zwitterionic di- and tripeptides.

Despite the fact that 5-ALA and 6-AHA, in analogy to other PTR members (Doring *et al.*, 1998), and also Bip-Pro show some affinity to DtpC, only di- and tripeptides with at least one cationic side chain are potent competitors. Since 6-AHA is similar in overall length to lysine, its amino-group may mimic the ε-amino group of lysine allowing it to fit into the substrate binding pocket. In a similar fashion, 5-ALA mimics ornithine in overall chain length. That the cationic groups are crucial for binding was demonstrated by loss of competition when these functional groups were blocked in lysine or lysine-containing dipeptides. A terminal carboxy-group at the α-position seems also important since 1,5-diaminopentane showed only weak competition with lysine for uptake. The apparent affinity for lysine transport was 32 µM and for Lys-Lys uptake 22 µM, classifying DtpC as the transporter with the highest affinity amongst all characterized *E. coli* PTR transporters, where most substrates have affinities in the millimolar range. The affinity of DtpC for lysine is in the same range as the affinities of other transport systems for cationic amino acids in *E. coli* (Rosen, 1971), such as the lysine transporter LysP (K_d=10 µM) and the LAO system binding protein ArgT (for Lys K_d=0.5 µM and for Arg K_d=1.5 µM). A second binding protein is HisJ, which has a K_d of 10 µM for Arg and of 0.1 µM for His (Caldara *et al.*, 2007).

DtpD also showed a high affinity for Lys-Lys with a K_i of 0.03 mM, which is substantially better than its K_t of 10.6 mM for 6-AHA, and also some of the tested dipeptides show stronger inhibition of 6-AHA uptake than 6-AHA itself, indicating higher affinities than 6-AHA. This implies that DtpD is a high affinity dipeptide transporter, even compared with DtpA, where most substrates have a K_i of 0.3-2 mM. The competition experiments revealed selectivity for the position of charged amino acids in the dipeptides: carboxy terminal positive charges and amino terminal negative charges were preferred by DtpD, which is opposite to

what was found for DtpA and DtpB (DtpC showed no clear selectivity). This is a very interesting finding because it implies a different structure within the substrate binding site. Another difference to DtpA and DtpB is that DtpD (like DtpC) efficiently only transports peptides with charged side-chains. Also the tested β-lactam antibiotics, from which cefadroxil and cefalexin show inhibition for DtpA, showed none here. In contrast, the ACE inhibitors captopril and enalapril, which show no competition for DtpA, showed good competition for DtpD, like in mammalian PTR transporters (Zhu *et al.*, 2000). Concerning minimal substrate features, it was found that the terminal amino group is needed, because hexanoic acid alone showed no competition. The α-amino group of lysine also plays an important role in substrate recognition: For DtpD lysine shows some competitive inhibition only if the α-amino group was blocked like in α-N(Z)-Lys, what led to a loss of competition for DtpC. For DtpD like DtpC, the competition decreased if the ε-amino group of a lysine containing dipeptide was blocked as in Ala-Lys[Z(NO_2)], indicating the crucial side chain charge and position in substrate recognition.

5.5. Functional characterization: transport mode

Members of the PTR family such as PEPT1 or PEPT2 operate as electrogenic proton-coupled symporters with a variable flux-coupling stoichiometry for proton to substrate cotransport and the main driving force is provided by membrane voltage (Kottra *et al.*, 2002). To investigate the transport mode of the *E. coli* PTR transporters, several experimental approaches were used. In intact cells, a collapse of the proton gradient by CCCP and the pH dependence suggested proton-coupling. However, only uptake studies in membrane vesicles and proteoliposomes with an applied artificial proton gradient and electrical measurements of proton-cotransport and charge movement into proteoliposomes allowed a more detailed analysis.

When the proton-gradient was abolished in whole cell uptake experiments in all four cases a loss of uptake was observed, suggesting a proton-coupling of substrate transport. The effect was less pronounced in case of DtpC. Only with DtpD (and to some extent also with DtpC) a dependence on Na^+ for uptake activity was observed. Therefore, here the CCCP experiment does not necessarily reflect proton-dependence, as the loss of the proton-gradient would secondarily also cause a loss of the Na^+ gradient (Bassilana *et al.*, 1984). The pH dependence expected for proton-coupled cotransporters is higher uptake at lower extracellular pH. DtpA, DtpB and DtpD showed increased transport at lower pH but not DtpC. However, beside the proton-gradient, the pH also influences substrate charges and the charge of the transporter proteins. Since pK_a values of carboxy- and amino-groups in

peptides are typically around 3 and 10, alterations in pH can lead to different affinities of substrates. In addition, the protein may partially or completely be denaturated at lower pH. This could be the case for example in case of DtpA at pH 6 in which β-Ala-Lys(AMCA) uptake decreased when pH was lowered further or in case of DtpC with a lack of a typical pH dependency. However, the proton-dependence of DtpC uptake was shown in membrane vesicles when an artificial proton-gradient was imposed. Similarly, DtpA and DtpB, but not DtpD showed increased substrate influx into membrane vesicles when a proton-gradient was applied.

Reconstitution of the purified proteins into proteoliposomes, previously shown for the *Lactococcus lactis* orthologue DtpT (Hagting *et al.*, 1997a), was only successful in case of DtpA and DtpB. Transport was clearly demonstrated to be energized in the presence of a proton-gradient generating system and proved the functionality of the proteins after solubilization and purification. In case of DtpC and DtpD additionally experiments with Na+ gradients were undertaken but without success and therefore for these two transporters proteoliposome experiments were not conclusive. It might have been that reconstitution had failed (for example the purification for DtpC was rather poor) or that the proteins may have lost function.

The second technique applied to proteoliposomes was based on electrical measurements via the SURFE^{2}R^{one} chip system. For DtpA and DtpB, here capacity-coupled currents were obtained with immobilized proteoliposomes on the SURFE^{2}R^{one} chip, which documents the electrogenic nature of DtpA and DtpB mediated transport process in similarity to on-chip recordings with membranes containing the mammalian PEPT transporters (Kelety *et al.*, 2006). In case of DtpC and DtpD these experiments could not yet establish the electrogenic nature of transport. However, for DtpA and DtpB it was unequivocally established that dipeptide transport by these two bacterial transporters occurs by H^+-symport and is not dependent on any other cellular component. What remains as a problem in all studies employing proteoliposomes and membrane vesicles is the orientation of the transporters within the membrane that can not be controlled. But tracer influx as well as transport charges on the chip system proved that at least a certain proportion of the transporters was in the proper orientation.

5.6. Studies with deletion mutant *E. coli* lines

Knockout mutants obtained from the Keio-collection were used to determine the natural abundance of transport by the four PTR family members of *E. coli*. DtpA and DtpB

functionally and genetically cluster together, but in wild type cells, only DtpA seems to be expressed. DtpB might serve as a backup system of DtpA but is not needed under normal culture conditions. DtpC and DtpD are different both, functionally and genetically, and are both expressed in levels high enough to detect specific substrate transport in wild-type cells as compared to KO mutants. They therefore might have specialised tasks, for which in case of the lysine transporting DtpC system its genetic localisation might provide a hint. It is flanked by the lysine-related genes *lysU*, a lysyl-t-RNA synthetase (VanBogelen *et al.*, 1983) and the *cadBA* operon, which is involved in lysine decarboxylation and lysine/cadaverine antiport for pH regulation (Soksawatmaekhin *et al.*, 2004). The experiment with the *dtpC* KO strain showed additionally that DtpC contributes to overall lysine uptake under normal culture conditions. Uptake of cationic amino acids in *E. coli* was described to be mediated in case of lysine by LysP (Steffes *et al.*, 1992) and the lysine arginine ornithine (LAO) system encoded in the *argT-hisJQMP* locus (Caldara *et al.*, 2007; Rosen, 1973), an ABC transporter system with the binding protein ArgT for lysine, arginine and ornithine and HisJ for histidine and arginine uptake. Arginine and ornithine are additionally transported by a similar system encoded by the *artPIQM-artJ* locus. As *dtpC* is genetically different from all those systems, it represents a novel aspect in lysine uptake into *E. coli* cells whereas its contribution to arginine and histidine uptake seems negligible under standard culture conditions.

5.7. Growth curves

Independent from the different uptake assays the functionality of the transporters was also demonstrated based on growth curves in the presence of toxic compounds that are taken up by the overproduced proteins. This was performed for all four candidates with alafosfalin and chloramphenicol. The degree of growth inhibition correlated again with the protein expression level in which high levels of DtpA caused stronger growth inhibition than the low levels in case of DtpC. DtpD with chloramphenicol showed highest sensitivity despite the fact that protein levels were generally not the highest. Here even the background-expression without induction caused an inhibitory effect and suggests that different affinities for this substrate also contribute to growth inhibition. Alafosfalin is structurally similar to a peptide (structure in Fig. 51, p. 54), is a known substrate of PEPT1 and PEPT2 and is a known intracellular active antibiotic for *E. coli*. It has also been described as substrate for TppB (=DtpA) earlier (Gibson *et al.*, 1984). In contrast, chloramphenicol is structurally (structure in Fig. 52, p. 55) not similar to β-lactam antibiotics which are known substrates of the mammalian PTR transporters. Its identification as a putative substrate for the peptide transporters is highly interesting. Although chloramphenicol is an important anti-bacterial drug, its transport into the cell is not well understood. Its hydrophobicity may allow some diffusion through the

membrane, but resistance mechanisms against chloramphenicol include active export systems (Moreira *et al.*, 2005). Chloramphenicol uptake by different organisms was compared and differs markedly between bacteria and even *E. coli* strains (Vazquez, 1964) and this is hard to understand assuming diffusion as upatke route. A high accumulation (1000 fold above the extracellular concentration) of chloramphenicol was observed for example in *Haemophilus influenzae* and *E. coli* and this was found to be dependent on a proton-gradient (Abdel-Sayed, 1987; Burns and Smith, 1987). The PTR-transporters therefore could be an important system for chloramphenicol uptake. Although chloramphenicol does not possess a prototypical dipeptide structure, inspection of its structure reveals a peptide bond in the backbone next to the carbon unit that carries the two chloride substituents that may allow binding to and transport by the peptide transporters.

5.8. Protein structural information

Various attempts employing crosslinking for obtaining information on the proteins quaternary structure all did not reveal any evidence for a multimeric state. Analytical gel filtration was not informative since the DDM micelles, which increase mass by around 70 kDa (Strop and Brunger, 2005) masked the true particle size. The same problem occurred with dynamic light scattering, where also larger particle sizes were detected as expected for a monomeric form. But it could be revealed from dynamic light scattering as well as from gel filtration that the particle size is highly homogenous. This monodispersity indicated a high stability of the proteins after purification in DDM in the solubilized state and this is desirable for crystallization trials. The gel filtration chromatograms in case of DtpB and DtpC revealed that the proteins may have lower stability than DtpA and DtpB, but here preparations also showed lower purity after Nickel-affinity purification. Information on DtpA from the CD-spectrum confirmed the expected protein nature with high alpha-helical content suggesting also that denaturation or improper folding is not a serious problem with DtpA.

Additional experiments to elucidate the structure of DtpA from our cooperation partners have already been reported (Weitz *et al.*, 2007). BN-PAGE of purified DtpA displayed a strong band with a M_{obs} of ~85 kDa. This M_{obs} is composed of the molecular mass of DtpA (~55 kDa) and the mass of the DDM-Coomassie brilliant blue G-250 micelle and lipids attached to the protein. Thus the M_{obs} indicated that DtpA exists as a monomer. The use of the conversion factor determined by Heuberger et al. 2002 (Heuberger *et al.*, 2002) to estimate the mass of membrane proteins from the M_{obs} also supports the monomeric nature of DtpA. Transmission electron microscopy (TEM) of negatively stained DDM-solubilized DtpA revealed a crown-like structure with a central density (Weitz *et al.*, 2007). The measured diameter of the DtpA

particles was ~8 nm. This is very close to the 9 nm that were obtained with DLS. Assuming a boundary layer of ~1.5 nm (Dekker *et al.*, 1988) for DDM attached to the hydrophobic part of the protein the resulting diameter is similar to that of the red permease monomer when embedded into the lipid bilayer – Red permease is a lactose permease fusion protein which forms monomers and trimers. It consists of twelve transmembrane helices and has a similar molecular weight as DtpA (Zhuang *et al.*, 1999).

Crystallization

There is not much known on the 3D structure of any peptide transporter protein of the PTR family. Protein expression is low in native cells and tissues, and heterologous expression of mammalian PEPT1 in *Pichia pastoris* did not yield enough protein for structural analysis (Theis *et al.*, 2001). The discovery of bacterial homologues with similar transport characteristics to the mammalian proteins that can be expressed and purified with high yield represents therefore an important step towards structural analysis of the protein and insights into the transport mechanism. High amounts of pure and stable membrane protein solubilized with suitable detergents are crucial for structural characterization by crystallization (Chayen and Saridakis, 2008; McPherson, 2004). Crystallization attempts for the four *E. coli* PTR members yielded quite different results. Since none of the proteins was stable in a high critical micelle concentration (CMC) detergent like octylglycoside that would have speeded up the reconstitution step and improved crystallization probability, we had to apply other detergents. DtpC expression was too low and purification also was not satisfactory for any crystallization attempts. For DtpC it will be necessary to improve expression and purity, for example by adding another purification step like gel filtration or ion-exchange chromatography. Improving purity appears also necessary in case of DtpB, which did not yet form 2D crystals, but here extensive screening for better crystallisation conditions needs also to be done. DtpA formed proteoliposomes with 2D crystals, but the narrow tubular shape hampered appropriate diffraction. A similar problem occurred with DtpD, which showed the advantageous feature of being stable at 37°C during dialysis. DtpD formed either also tubes, or other vesicles with crystalline patches but no homogeneous crystals were obtained yet. If there are breaks or holes in the grid no diffraction analysis is possible. To overcome these problems all processes were optimized for DtpD by partner Fabio Casagrande to a degree where fist information about unit cell dimensions and molecular orientation could be drawn from diffraction images (Casagrande *et al.*, 2009) (Dissertation Fabio Casagrande). All experiments performed for 3D crystallization were not yet successful for any of the four proteins either. Nevertheless, the expression, purification, functional reconstitution and first biochemical characterisation of the four PTR transporters from *E. coli* described here

represents an important step towards the crystallisation attempts to finally solve one of the structures of this unique class of membrane transporter proteins.

6. OUTLOOK

Based on the present findings there are a number of future research lines that should be followed:

Crystallization trials have to be continued with different conditions and with improved purification for DtpC and DtpD proteins. Another possibility to obtain better crystals might be via the generation of mutant proteins, for example by selection for loss of transport function mutants that would confer resistance to the toxic peptide alafosfalin.

Characterization of the transport mode of DtpC and DtpD could be extended by employing the Surfe^{2}r technology with suitable substrates or via TEVC measurements. For TEVC, oocyte expression needs to be modified with either higher amount of injected RNA or by co-expression of bacterial chaperones. In case of DtpD a high affinity reporter substrate would be needed and could be represented by a radiolabeled Lys-Lys.

What is highly interesting and has to be examined in more detail is the transport of chloramphenicol by the PTR transporters. The use of radiolabeled chloramphenicol would enable to study its transport by the bacterial transporters.

Also the physiological roles of the four PTR members of *E. coli* need to be elucidated by carrying out for example growth experiments under different environmental conditions and/or by using the different mutant lines.

7. MATERIALS AND METHODS

If not otherwise indicated, chemicals were from Sigma, Roth or Merck. Non-standard laboratory equipment is described in the method where it is used.

7.1. Protein sequence analysis

Sequences were compared using Blast (Altschul *et al.*, 1997), in particular protein blast (http://blast.ncbi.nlm.nih.gov/Blast.cgi). Multiple sequence comparison was performed with Clustal W (Chenna *et al.*, 2003) (http://www.ebi.ac.uk/Tools/clustalw/). Sequence identity and similarity was calculated from a Clustal W alignment by counting the identical and the conserved residues. This number was divided by the length of the protein for which the statement was made (for example from DtpA is X% similar to PEPT1). Transmembrane domain prediction was preformed with TMHMM 2.0 (Krogh *et al.*, 2001) or the indicated programs. The genetic loci were analyzed using the EcoGene Database (Rudd, 2000). The ProtParam program (http://www.expasy.org/tools/protparam.html) was used to calculate mass, isoelectric point and other parameters from the protein sequence.

7.2. Statistical data analysis and calculation

All experiments were performed for the indicated number of observations (n) and are presented as mean ± standard deviation. IC_{50} values were obtained by nonlinear regression using SigmaPlot and the value is given ± standard error. The K_i were calculated from the IC_{50} using the equation from Cheng and Prusoff (Cheng and Prusoff, 1973):

$$K_i = \frac{IC_{50}}{1 + \frac{[s]}{K_D}}$$

K_i = inhibition constant (=affinity) of the competitor
IC_{50} = concentration of the competitor at 50% inhibition
[s] = concentration of the substrate; K_D = affinity of the substrate

Significance was determined by t-test using SigmaPlot and by t-test (1way ANOVA plus Dunnett's multiple comparison test) using GraphPad Prism 4.

7.3. Cloning

Cloning was performed in *E. coli* TOP10F' (Novagen/Merck). Genomic DNA from *E. coli* strain O157:H7 was prepared with the Qiagen DNeasy Kit and the transporter genes were obtained by PCR using primers that add Hind III and Xho I for cloning (Table 9).

Table 9: Primers

Gene name	Primers forward (Fw, + Hind III) and reverse (Rev, + Xho I)
ydgR (*tppB*, *dtpA*)	Fw: AAAAAGCTTATGTCCACTGCAAACCAAAAAC
	Rv: AAACTCGAGCGCTACGGCTGCTTTCGC
yhiP (*dtpB*)	Fw: AAAAAGCTTATGAATACAACAACACCCATG
	Rv: AAACTCGAGATGGCTTTCCGGCGTCGC
yjdL (*dtpC*)	Fw: AAAAAGCTTATGAAAACACCCTCACAGCC
	Rv: AAACTCGAGATCGTTGCTCTCCTGTATCAT
ybgH (*dtpD*)	Fw: AAAAAGCTTATGAATAAACACGCATCACAG
	Rv: AAACTCGAGAGACTCCAGCGCCAGCGC
Primer annealing for rbs integration	Fw: AATTCTTGTTTAACTTTAAGAAGGAGAA
	Rv: AGCTTTCTCCTTCTTAAAGTTAAACAAG

PCR products were digested with Hind III and Xho I and ligated into pET-21 vector (T7 promoter, C-terminal hexahistidine-tag, Novagen). A ribosomal binding site (rbs) (AAGGAG) was added 7 bases 5' of the coding region to improve translation of the protein. This was done by primer annealing where two oligonucleotides are used, which form an insert with compatible ends for ligation into the vector digested with Eco RI and Hind III.

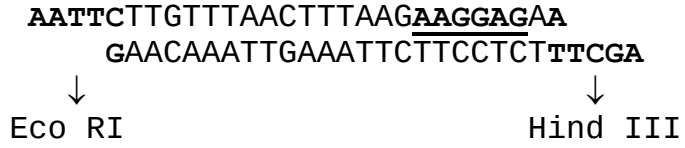

DNA constructs were verified by sequencing. For DtpA, a second expression vector (pET-21b-rbs-T7-YdgR-His) was constructed by cutting pET-21-rbs-YdgR-His with Hind III and Xho I and ligating the insert into pET-21b vector. All used constructs are summarized in Table 10.

Table 10: Plasmids

Name	Features
pET-21+	*amp*
pET-21-rbs-YdgR-His	*amp,* ribosomal binding site+ *ydgR-his*$_6$
pET-21-rbs-YhiP-His	*amp,* ribosomal binding site+ *yhiP-his*$_6$
pET-21-rbs-YjdL-His	*amp,* ribosomal binding site+ *yjdL-his*$_6$
pET-21-rbs-YbgH-His	*amp,* ribosomal binding site+ *ybgH-his*$_6$
pET-21b+	*amp*
pET-21b-T7-YdgR-His	*amp, T7tag-ydgR-his*$_6$

7.4. Overexpression in *E. coli*

For Overexpression *E. coli* BL21(DE3)pLysS (Novagen/Merck, Darmstadt, Germany) was used, which carries the gene for the T7-polymerase gene under the control of the *lac* operator. Therefore with IPTG the potent T7-polymerase is present and transcribes the target gene on the expression plasmid. Expression experiments were carried out with freshly transformed *E. coli* BL21(DE3)pLysS or freshly streaked glycerin stocks. Cultures were grown in LB Medium supplemented with 100 µg/ml ampicillin to OD_{600} of about 0.8 and protein production was induced by adding 0.1 mM IPTG (final concentration). Following 3 h incubation at 37 °C cells were harvested by centrifugation (8 000 x g, 8 min) for biochemical or functional analysis.

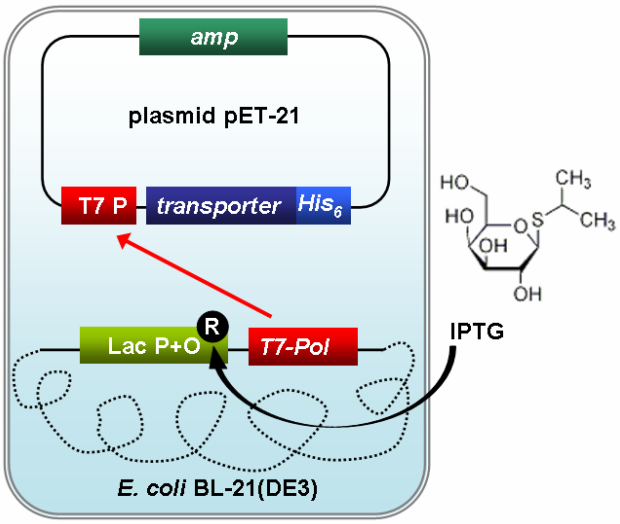

Fig. 67 Expression system in *E. coli*: The host strain carries the gene for the T7 polymerase under control of the *lac* promoter and operator on the chromosome. IPTG removes the *lac*-repressor, the T7 polymerase is made and transcribes the gene on the expression plasmid.

7.5. Growth experiments

Cells were grown in LB to OD_{600}=1 and transferred to a 12 well plate (1 ml/well) and IPTG (0.1 mM) and alafosfalin (500 µg/ml) were added. Growth was continuously recorded by measuring the OD_{600} while shaking at 37 °C in a plate reader (Varioscan, Thermo). For conversion to standard OD_{600}-units a calibration curve was used (Fig. 68) that was generated by measuring the same sample in a standard photometer (diluted if OD_{600} > 1).

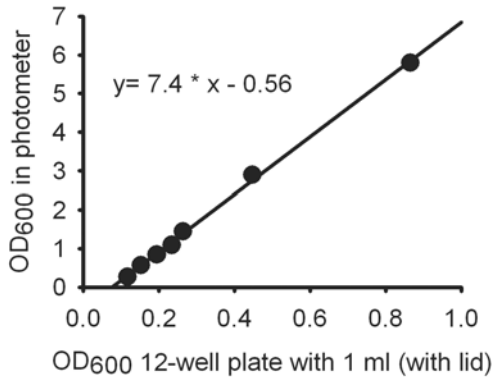

Fig. 68 OD_{600} calibration curve for conversion of measurements from the multi-plate reader to standard OD_{600} values.

7.6. Western blot analysis

For Western blot analysis, cells from 1 ml culture were pelleted and resuspended in lysis buffer (10 mM Hepes-NaOH pH 7.4, 0.5 mM EDTA, 1 mM DTT and protease inhibitor cocktail 1:500 (Sigma)) with lysozyme (1 µg) added. After 1 h of incubation on ice, bacterial DNA was degraded for 30 min by 1 unit benzonase in the presence of 3 mM $MgCl_2$. Membranes were pelleted by centrifugation at 18 000 x g for 30 min and solubilized in a buffer containing 10 mM Hepes-NaOH pH 7.4, 150 mM NaCl, 0.5 mM EDTA, 1 mM DTT and 1% n-dodecyl-β-D-maltoside (DDM). After 15 min on ice, not solubilized material was removed by centrifugation at 40 000 x g for 45 min. Alternatively there was *E. coli* inner membrane used as prepared for purification.

Proteins were separated by SDS-PAGE (12.5 % acryl amide) with a Biometra mini gel chamber at 25 mA, and blotted onto PVDF membranes (Millipore, Bedford, MA, USA) with a semi dry blotter (Amesham/GE) for 1 h with 120 mA using Towbin buffer (25 mM TRIS, 192 mM Gly, 20% methanol). Filters were blocked by incubation for 1 h with 1% (w/v) milk powder in TRIS-buffered saline (TBS; 137 mM NaCl, 3 mM KCl and 25 mM TRIS/HCl pH 7.5) followed by 3 x 10 min washing in TBS-T (TBS, 0.05% Tween-20) and incubation for 60 min with His·Tag antibody (1:2000 dilution, Novagen) in TBS-T. Filters were washed 3 x 5 min in TBS-T and then incubated for 30 min with secondary antibody (1:5000 dilution, goat anti-mouse-HRP, Santa Cruz). Filters were washed twice in TBS-T and twice with TBS; then, labeled proteins were detected using the ECL system (Pharmacia/GE).

7.7. Transport assays with β-Ala-Lys(AMCA)

Transport assays were performed *in vivo* with cells 3 h after induction with IPTG (see above) with the fluorescent dipeptide β-Ala-Lys-N_ε-7-amino-4-methyl-coumarin-3-acetic acid (β-Ala-Lys(AMCA)) (custom-synthesis by Biotrend, Cologne, Germany). β-Ala-Lys(AMCA) was

previously established as a reporter substrate for peptide transport (Dieck *et al.*, 1999; Otto *et al.*, 1996). Around 5 x 10^9 cells (15 OD units) were harvested by centrifugation (2 500 x g, 5 min) and resuspended in 1.5 ml modified Krebs-buffer (25 mM Hepes/Tris 7.4, 140 mM NaCl, 5.4 mM KCl, 1.8 mM $CaCl_2$, 0.8 mM $MgSO_4$ and 5 mM glucose). The assay volume of 100 µl was made up with 40 µl bacteria cells (1.3 x 10^8 cells), 10 µl of a 500 µM β-Ala-Lys(AMCA) stock solution (final concentration 50 µM), and 50 µl of Krebs-Buffer (control) or a competitor solution. Uptake was performed for 15 min at 37 °C and stopped by washing the cells twice with ice-cold Krebs-buffer by centrifugation (13 000 x g, 5 min). Uptake of β-Ala-Lys(AMCA) was quantified by fluorescence (excitation at 340 nm and emission at 460 nm, Varioscan, Thermo, Vantaa, Finnland).

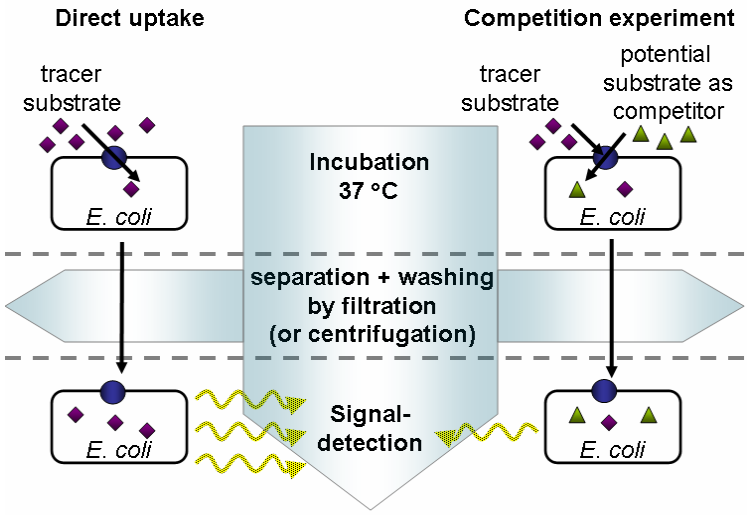

Fig. 69 Uptake experiments in *E. coli*: In direct uptakes the tracer substrate is taken up during the incubation at 37 °C following separation and washing with buffer. Then the signal of the substrate inside the cell is quantified. In competition experiments, a second substrate is present that competes for transport with the tracer.

7.8. Transport assays with radiolabeled tracer substrates

Transport assays were performed 3 h after induction with IPTG with radioactively labeled compounds (Table 11). If not otherwise indicated the activity per sample and final concentrations used were for [^{14}C]Gly-Sar 0.1 µCi in 1 mM Gly-Sar, for [^{3}H]lysine 0.1 µCi in 50 µM lysine, for [^{14}C]6-aminohexanoic acid (6-AHA) 0.2 µCi in 1 mM 6-AHA and for all other compounds 0.1 µCi without modification of the concentration.

Around 3 × 10^9 cells (10 OD units) were harvested by centrifugation and resuspended in 1 ml buffer (25 mM Hepes/Tris 7.4, 150 mM NaCl, 5 mM glucose). The assay volume of 50 µl consisted of 20 µl cells (6 × 10^7 cells), 5 µl of the radiolabeled reporter substrate, and 25 µl of buffer (control) or a 20 mM competitor solution (final concentration 10 mM). The cells were

incubated with the substrate for 30 s (5 min for DtpC) at 37 °C, followed by filtration (0.45 µm mixed cellulose esters, ME25 Whatman) and washing on the filter twice with 1 ml ice-cold buffer. Uptake was quantified by liquid scintillation counting (Betacounter Trilux Microbeta, Perkin Elmar). Significance ($p < 0.05$) was determined by t-test using SigmaPlot. For determination of apparent K_t values uptake rates at different substrate concentrations were determined by linear regression of time course experiments (10, 20, 40, 60 s). Then K_t values were determined by nonlinear regression of the rates versus concentration using SigmaPlot. For the increasing substrate concentrations, the concentration of the radiolabeled tracer remained constant, but counts were multiplied by the ratio of total substrate to radiolabeled substrate.

Table 11: Radiolabeled compounds

Substance	Specific activity [mCi/mmol]	Volume-activity [mCi/ml]	Concentration [mM]	Supplier
[^{14}C]Gly-Sar	57	1	17.54	Biotrend, Cologne
[^{3}H]D-Phe-Ala	40 000	1	0.025	Biotrend, Cologne
[^{3}H]5-aminolevulinic acid	3 000	1	0.33	NEN, USA
[^{14}C]6-aminohexanoic acid	55	0.1	1.818	ARC, USA
[^{3}H]lysine	90 000	1	0.011	GE; Germany
[^{3}H]arginine	60 000	1	0.017	GE; Germany
[^{3}H]histidine	51 000	1	0.0196	GE; Germany
Bip-[^{3}H]Pro	50 100	1	0.020	Prof. M. Brandsch

7.9. Transport assays with KO-strains

Single gene knockout strains were obtained from the Keio collection (Baba *et al.*, 2006). The parent strain is the *E. coli* K12 derivative BW25113 [*rrnB3* Δ*lacZ4787 hsdR514* Δ*(araBAD)567* Δ*(rhaBAD)568 rph-1*] (Datsenko and Wanner, 2000) and genes were exchanged by a kanamycin resistance gene applying homologues recombination (Fig. 70.). The strains used here are listed in Table 12. Strains were grown for the same time as cells for over-expression and afterwards treated in the same way for uptake experiments.

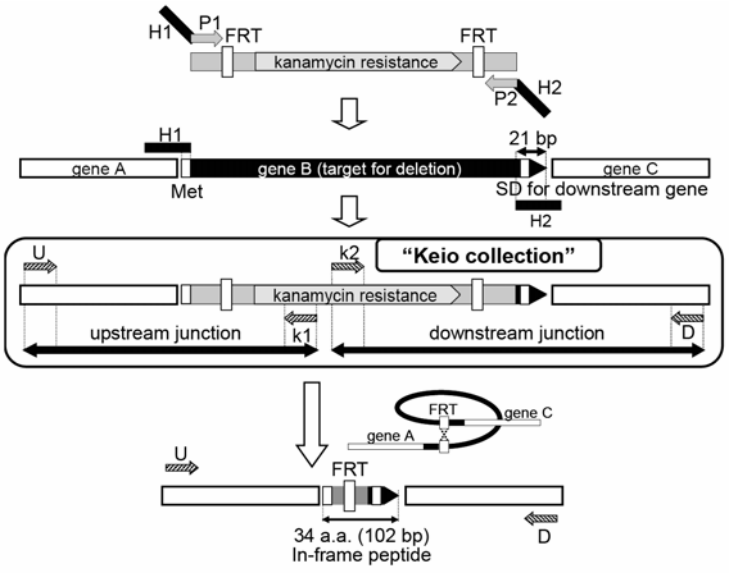

Fig. 70: Construction of the knockout strains of the Keio collection. Picture taken from Keio collection documentation similar to (Baba *et al.*, 2006). H1/H2: homologues regions for recombination. SD: potential Shine-Dalgarno sequence that is left intact. FRT: recognition sites for the FLP recombinase.

Table 12: Knockout-strains used

Strain	marker
BW25113 (Host strain for KO; *E. coli* K-12 derived)	*rrnB3 ΔlacZ4787 hsdR514 Δ(araBAD)567 Δ(rhaBAD)568 rph-1*
KO *ydgR (dtpA, tppB)*	BW25113, Δ *ydgR, kan*
KO *yhiP (dtpB)*	BW25113, Δ *yhiP, kan*
KO *yjdL (dtpC)*	BW25113, Δ *yjdL, kan*
KO *ybgH (dtpD)*	BW25113, Δ *ybgH, kan*

7.10. Purification by Ni^{2+} affinity chromatography

Cell pellets from 500 ml culture were resuspended in 25 ml lysis buffer (10 mM Hepes/Tris pH 7.4, 1 mM dithiotreitol (DTT), 0.5 mM EDTA) and broken by sonication (10 cycles of 30 s). After a short low speed centrifugation to separate unbroken cells (4 500 x g, 8 min) and a short high speed centrifugation to pellet the outer membrane (120 000 x g, 5 min) the inner membranes from the supernatant were collected by centrifugation at 120 000 x g for 1.5 h (all at 4 °C).

For experiments except crystallization, the pellets were resuspended in 1 ml buffer (20% glycerol, 10 mM Hepes/Tris pH 7.4, 0.5 mM Tris-2-carboxyethyl-phosphine (TCEP), frozen in liquid nitrogen and stored at -80 °C. Membranes were solubilized (60 min, 4 °C) in 10 mM Hepes/Tris pH 7.4, 150 mM NaCl, 1% DDM, 5% glycerol, 0.1 mM TCEP, 30 mM imidazole at a protein concentration of 1-3 mg/ml. After centrifugation (40 000 × g, 20 min) the

supernatant was loaded to a Ni^{2+}-Sepharose column (HisTrap FF, GE) with a FPLC (ÄKTA, Amersham/GE, Uppsalla, Sweden) and washed with running buffer (10 mM Hepes/Tris pH 7.4, 150 mM NaCl, 30 mM imidazole, 0.06% DDM, 5% glycerol, 0.1 mM TCEP). Protein was eluted with a gradient from 30 to 250 mM imidazole in running buffer. Elution yielded a sharp peak at about 150 mM imidazole, which was shown by SDS-PAGE and Western blotting to contain the purified transporter.

Purification for crystallization at the University of Basel was performed differently: Membrane pellets from 1-2 L culture were resuspended in buffer (10 mM TRIS/HCl pH 8, 10% glycerol, 300 mM NaCl, 250 mM betaine, 0.01 % NaN_3) and solubilized with detergent (e.g. 1% DDM) for 1-3 h at 4 °C and agitation. The non solubilized fraction was separated by ultracentrifugation (100 000 x g, 4 °C, 1 h) and solubilized protein was incubated with 1 ml Ni-NTA agarose or Ni-superflow (Qiagen, Hilden) for binding at 4 °C for 2-4 h. In gravity flow columns (BioRad), the supernatant was separated and the Ni-NTA-resign was washed with 30 ml column buffer (as above, plus detergent slightly above the CMC (e.g. 0.06% DDM) and 1 mM histidine). Residual fluid was removed by centrifugation (2 000 x g, 4 °C, 2 min) and protein was eluted by incubation with 500 µl elution buffer (column buffer plus 200 mM histidine) for 30 min at 4 °C and agitation and subsequent centrifugation (13 000 x g, 2 min, 4 °C). Protein quality and concentration was determined by UV-spectrometry.

7.11. Reconstitution into proteoliposomes

For reconstitution, 250 µl *E. coli* lipids at a concentration of 20 mg/ml in $CHCl_3$ (total extract, Avanti Polar Lipids, Alabaster, AL, USA) were dried to a thin film under a stream of N_2 and further incubated for 30 min in vacuum. The lipids were resuspended in 500 µl buffer (50 mM KPO_4 pH 6.3), sonicated until clearing (3 × 3 s, probe type sonifier) and destabilized with 0.5 % DDM. 100 µg (about 100 µl) purified protein as eluted from the Ni^{2+}-NTA column was added. After 10 min on ice, the detergent was removed by adding 200 mg Bio-Beads SM-2 (BioRad, Hercules, CA, USA) and incubation for 4 h at 4 °C. The detergent removal step was repeated 3 times with new Bio-Beads and incubation at 4 °C for a total of 24 h.

7.12. Uptake in cytochrome *c* oxidase energized proteoliposomes

To generate a proton gradient, membrane vesicles or proteoliposomes were fused with proteoliposomes containing cytochrome *c* oxidase (Driessen *et al.*, 1985; Stolz *et al.*, 1994). Cytochrome *c* oxidase (1 mg, purified from bovine heart (Yu *et al.*, 1975)) was reconstituted with 40 mg *E. coli* lipids (total extract, Avanti Polar Lipids, Alabaster, AL, USA) and 12 mg octyl-glucoside in 2 ml buffer (50 mM KPO_4 pH 6.3) and detergent was removed by dialysis.

These proteoliposomes were mixed with *E. coli* membranes (usually 2 mg lipid + 100 µg membrane protein) or with liposomes containing purified transporter (usually 27 µg protein) in a final volume of 250 µl. After addition of 1 mM $MgSO_4$ a cycle of freezing (liquid nitrogen) and thawing (room temperature) was performed, which was followed by sonication for 3 s with a probe type sonifier at low energy (Fig. 71). For the uptake assay, radiolabeled substrate, e.g. 2.5 µl [^{14}C]glycyl-sarcosine (2.5 µCi, 175 µM final concentration) was added to the proteoliposomes, which were stirred at 37 °C. At indicated times (usually in 10 minute steps), 25 µl aliquots were withdrawn, diluted with 2 ml 100 mM LiCl, and filtered (0.45 µm, mixed cellulose esters: ME25, Whatman). The filters were washed with 2 ml 100 mM LiCl followed by scintillation counting.

Proton gradient generation was started by the addition of 20 mM ascorbate, 200 µM TMPD (N,N,N',N',Tetramethyl-p-phenylenediamine) and 20 µM cytochrome *c* (from equine heart, Sigma), which energizes the cytochrome *c* oxidase to transport H^+ to the outside (Fig. 71). Only cytochrome *c* oxidase inserted in this orientation will interact with the cytochrome *c,* which is applied outside. Fresh ascorbate was added (1:50) when the assay solution had turned blue due to oxidized TMPD. CCCP (Carbonyl cyanide 3-chlorophenylhydrazone, Sigma) was used at a final concentration of 10 µM to destroy the proton gradient.

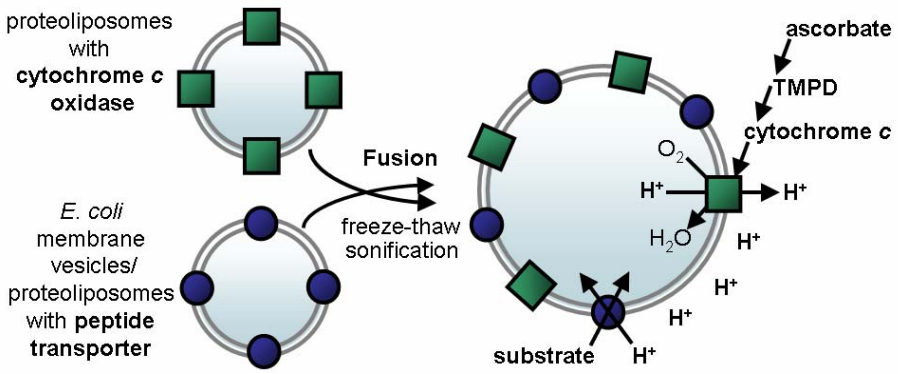

Fig. 71 Uptake experiments with cytochrome *c* oxidase proteoliposomes: After fusion of the cytochrome *c* oxidase and the peptide transporter containing proteoliposomes, a proton gradient can be generated that then drives the uptake by the peptide transporter. To export H^+, cytochrome *c* oxidase is supplied with electrons which are transferred from ascorbate via TMPD and cytochrome *c*.

7.13. Electrical measurements with the SURFE^{2}R^{one} setup

Electrical measurements were based on the solid-supported membrane (SSM) technology, which allows detection of capacitively coupled currents (Meyer-Lipp *et al.*, 2004). The currents are caused by the shift of electrical charges as the transporters go through the transport cycle and originate from the movement of charged substrates, cotransported ions or of protein moieties carrying (partial) charges. Adsorption of the proteoliposomes to the

gold surface sensors was performed as described by Zuber (Zuber *et al.*, 2005), using SURFE^{2}R^{one} gold electrodes from IonGate BioSciences GmbH (Frankfurt, Germany). With the SURFE^{2}R^{one} setup (IonGate), the solution flowing over the adsorbed liposomes could be changed rapidly and the charging of the gold chip is measured on-line. Transport was activated when a buffer without substrate (30 mM glycine, 140 mM KCl, 25 mM Hepes, 25 mM MES, 2 mM $MgCl_2$, pH 7.0) was exchanged to the same buffer containing the substrate glycyl-glycine (30 mM) instead of glycine. After a rapid fluid exchange to the Gly-Gly containing solution, the charging of the proteoliposomes on the sensor driven by the H^+/peptide symport was measured. The wash-out of dipeptide reversed the current flow representing an electrogenic back-flux of peptide and proton along the now reversed substrate gradient.

Previous comparisons of the characteristics of rheogenic (current generating) transporters employing this new cell-free electrophysiological technique with findings from patch clamp studies revealed a very good correlation in all features (Geibel *et al.*, 2006).

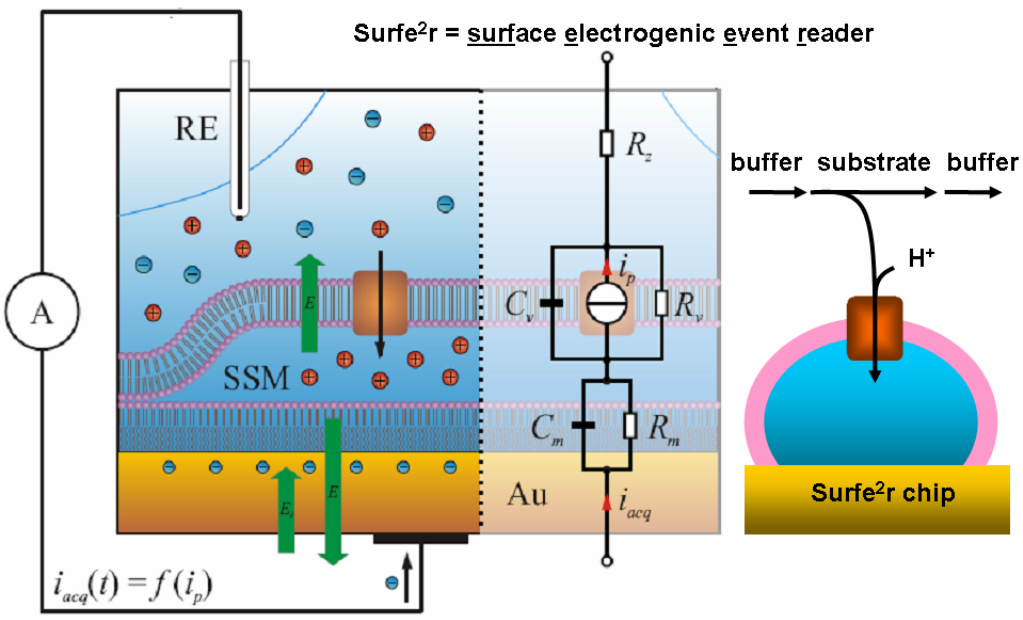

Fig. 72: Scheme of Surfe^{2}r setup: On the gold surface (Au) lies a special solid supported membrane (SSM) where proteoliposomes can be adsorbed. With the reference electrode (RE), translocation of charges by a transporter over the liposome membrane can be detected. This is based on a capacitively coupled system as indicated by the equivalent circuit (left part taken from (Kelety *et al.*, 2006)). On the right panel the procedure of an experiment is shown: when buffer flows over the sensor, nothing happens. When substrate flows, co-transport with H^+ occurs and a current peak is measured.

7.14. Expression in *Xenopus* oocytes

Xenopus laevis maintenance and oocyte harvest procedures were approved by the local authority for animal care in research (Regierung von Oberbayern, approval nr. 211-2531.3-

9/99). Female *X. laevis* oocytes were purchased from African Xenopus facility (Knysna, RSA). Surgically removed oocytes were separated by 1.75 mg/ml collagenase A (Roche Diagnostics) treatment for 1.5-2 h at room temperature in Ca^{2+}-free ORII solution (82.5 mM NaCl, 2 mM KCl, 1 mM $MgCl_2$ and 10 mM HEPES (pH 7.5) to remove follicular cells. After sorting, healthy oocytes of stage V and VI were kept at 18 °C in modified Barth solution containing 88 mM sodium chloride, 2 mM KCl, 2 mM $MgCl_2$, 1.8 mM $CaCl_2$, 10 mM HEPES (pH 7.5). The next day individual oocytes were injected with 27 nl of sterile water (control) or 27 nl of *dtpA* or *dtpD*-mRNA (13-50 ng) solution at concentrations between 0.5 and 2 µg/µl for initial functional tests. The oocytes were kept in modified Barth solution at 18 °C until further use (3-5 days after injection).

7.14.1. RNA production by *in vitro* transcription

Cloning of the plasmids for RNA *in vitro* transcription was performed in *E. coli* TOP10F' (Novagen/Merck). The transporter genes were obtained by PCR using the expression plasmids (7.3, Table 10, p. 86) as template with the primers shown in Table 13. Thereby a 5' Kozak consensus sequence (GCCACC) was added at the 5' end of the genes to enable translation in eukaryotes, and the restriction sites for cloning (EcoR IV and EcoR I). The PCR products were subcloned into the pCRII (BD, PharMingen) vector under the control of a T7 promoter. Additionally downstream a ~700-bp 3' non-translated end fragment of rabbit PEPT2 and a poly(A) tail had been introduced (Boll *et al.*, 2002), what usually stabilizes the synthesized RNA for efficient expression in *X. laevis* oocytes. As a second approach, the *kozak-ydgR* (*dtpA*) gene was subcloned with EcoR IV/EcoR I in the pGHJ vector (derived from pGHJ-XT3s1 (Kowalczuk *et al.*, 2005), pGEMHE (Liman *et al.*, 1992); kindly provided by S. Bröer), which carries non translated sequences of *X. laevis* beta-globin upstream and downstream of the cloning site to increase RNA stability in oocytes. Production of the RNA for injection was done by *in vitro* transcription using the mMessage-mMashine-T7 Kit (Ambion) according to manufacturer's instructions on plasmid DNA that was linearized by restriction after the poly-A tail.

Table 13: Primers for oocyte expression vectors. Kozak sequence in bold type.

gene name	Primers forward (Fw, + Eco RV) and reverse (Rev, + Eco RI)
kozak-*ydgR* (*dtpA*)	Fw: ATC**GCCACC**ATGTCCACTGCAAACCAAAAAC
	Rv: CCGGAATTCTTGTTAGCAGCCGGATCTCA
kozak-*ybgH* (*dtpD*)	Fw: ATC**GCCACC**ATGAATAAACACGCATCACAG
	Rv: CCGGAATTCTTGTTAGCAGCCGGATCTCA

7.14.2. Two-electrode voltage clamp

Two-electrode voltage clamp (TEVC) experiments are used to detect transport of currents over the oocyte plasma membrane (Wagner *et al.*, 2000) like in the present case the cotransport of protons with substrate. The oocyte was placed in an open chamber and continuously superfused with incubation buffer (88 mM NaCl, 1 mM KCl, 0.8 mM $MgSO_4$, 0.4 mM $CaCl_2$, 0.3 mM $Ca(NO_3)_2$, 2.4 mM $NaHCO_3$, and 10 mM Mes or Hepes, pH 5.5-8.5) in the absence or presence of the substrates Gly-Gln for DtpA or 6-AHA for DtpD. Oocytes were voltage-clamped at -60 mV, and current-voltage (I-V) relations were measured using short (100 ms) pulses separated by 200-ms pauses in the potential range -160 to +80 mV with 20 mV steps. *I-V* measurements were made immediately before and 20-30 s after substrate application, when current flow reached steady state. The currents at a given membrane potential were calculated as the difference between the currents measured in the presence and the absence of substrate.

7.14.3. Lysis of oocytes for Western blot

Lysis for Western blot analysis was done by homogenizing 10 oocytes in 100 µl 1% Triton-x-100 in buffer (20 mM Hepes/Na pH 7.4, 100 mM NaCl, 0.5 mM phenylmethanesulphonylfluoride (PMSF)) by pipetting up and down and solubilized for 10 min at 4 °C. The not solubilized fraction was separated by centrifugation (18 000 x g, 10 min, 4 °C), and 30 µl supernatant plus 15 µl Lemmli loading buffer was loaded onto the gel and treated as Western blot (7.6, p. 88).

7.14.4. Immunohistochemistry

Before cutting in sections, the oocytes were fixed and embedded in paraffin. Therefore, in a 2 ml reaction tube 5 oocytes were incubated in 1.8 ml 4% paraformaldehyde (PFA) in modified Barth solution (88 mM sodium chloride, 2 mM KCl, 2 mM $MgCl_2$,1.8 mM $CaCl_2$, 10 mM HEPES pH 7.5) for 2 h under agitation at 4 °C (pH adjusted with NaOH). Solution was changed according toTable 14 and finally oocytes were embedded in paraffin in racks for the microtome and let cooling at 4 °C over night. 7 µm sections were cut with a microtome, transferred to an object slide and let dry at 37 °C. Removal of the paraffin was performed by incubation at RT in solutions as indicated in Table 15 following antigen retrieval by cooking in 1.5 L citric acid buffer pH 6 (18 mM citric acid, 8.2 mM sodium citrate, 0.1 % Tween 20) for 20 min in a pressure cooker. After releasing the pressure immediately blocking was performed by incubation in 3% goat-serum in TBS buffer (137 mM NaCl, 3 mM KCl and

25 mM TRIS/HCl pH 7.5) for 20 min at RT. 100 µl primary antibody solution (His·Tag antibody 1:10 000 in TBS, Novagen) was placed as drop on the object slide over the oocyte section and incubated over night at RT. After 2 x 3 min washing with TBS followed 5 min incubation with 3% goat-serum. Then incubation with the secondary antibody (Alexa Fluor® 488 goat anti-mouse, 1:1000, Invitrogen) was performed for 1 h in darkness with subsequent washing (3 x 5 min TBS). After drying fluorescence mounting solution (DAKO) was added and sections were viewed using a confocal laser-scanning microscope (model TCS SP2, Leica).

Table 14: Oocyte fixation

repeats	solution	temp	time
1 x	70% ethanol	45 °C	15 min
1 x	80% ethanol	45 °C	20 min
2 x	99% ethanol	45 °C	20 min
3 x	100% ethanol (p.A.)	45 °C	20 min
2 x	xylol	45 °C	20 min
4 x	paraffin	60 °C	15 min

Table 15: Paraffin removal

repeats	solution	time
2 x	xylol	5 min
2 x	100% ethanol (p.A.)	5 min
1 x	100% ethanol (p.A.)	2 min
2 x	99% ethanol	2 min
1 x	80% ethanol	2 min
flushing at water tap		3 min

7.14.5. Radiolabeled uptake in *Xenopus* oocytes

8 oocytes expressing *dtpA* and 8 control oocytes were equilibrated for 2 min in modified Barth buffer pH 6.5 (88 mM sodium chloride, 2 mM KCl, 2 mM $MgCl_2$,1.8 mM $CaCl_2$, 10 mM MES). Uptake was performed for 30 min at RT under agitation in 100 µl buffer with 175 µM [^{14}C]Gly-Sar (1 µCi). Oocytes were washed three times with 900 µl cold buffer and lysed individually in scintillation vials by addition of 100 µl 10% SDS and agitation for 30 min at RT. After mixing with 3 ml scintillation cocktail (EcoScint, Roth) the signals were detected in a beta counter (TriluxMicrobeta, Wallac/Perkin Elmer).

7.15. Chemical crosslink experiments

For crosslinking concentrations of the protein of 5 µM or lower were chosen to avoid unspecific crosslinking. The concentration was usually 100 µg/ml what corresponds to 2 µM (all four proteins have molecular mass of ~50 000 g/mol). The crosslinker substances were prepared freshly before the experiment with bis-sulfosuccinimidyl suberate (BS^3) 50 µM in H_2O and disuccinimidyl suberate (DSS) 50 µM in DMSO. 50 µl of protein solution was mixed with 1 µl or 0.5 µl of crosslinker and after incubation at RT stopped with 50 µl Lemmli buffer

(amino groups of TRIS consume the remaining crosslinker). 12 µl of this were loaded on 12.5% PAA-SDS gels and subsequently blotted and detected by the anti-His-tag antibody. The principle of the method is illustrated in Fig. 73. Free amino groups from the protein form an amid bond with the suberate backbone, substituting the succinimidyl groups. If this happens with two amino groups from different proteins with one suberate molecule, the two proteins are covalently crosslinked and will hold together even when treated with SDS.

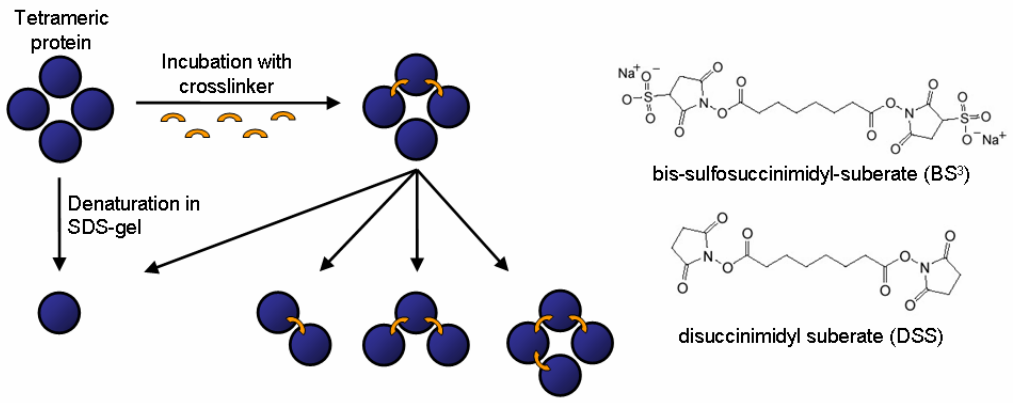

Fig. 73: Principle of chemical crosslink experiments. A multimeric protein in the denaturing SDS gel is divided into its monomers. To see multimeric forms the monomers can be covalently crosslinked to each other before denaturing; in the gel there will now be visible also multimeric stages of the protein as bands of higher molecular mass. The molecular structure of the two crosslinkers BS^3 and DSS is shown.

7.16. Gel filtration

The principle of the method is differential mobility of particles in the column according to their size. Large particles pass rapidly while smaller particles enter the pores of the column material and are delayed. Gel filtration was performed using the tricorn superpose 6 (Amersham/GE) at the ÄKTA FPLC (Amersham/GE) for determination of the hydrodynamic radius to estimate mass and oligomeric state. Buffer used for gel filtration was 10 mM HEPES 7.4 (TRIS), 150 mM NaCl, 0.06 % DDM. Calibration was done with marker proteins purchased from Sigma: Equine heart myoglobin (17 kDa), ovalbumin (44 kDa), BSA (67 kDa), rabbit muscle aldolase (158 kDa), bovine liver catalase (232 kDa). The calibration curve is shown in Fig. 74. On the x-axis is the log function of the molecular mass and on the y-axis the experimental value K_{av} (approximate partition coefficient) that is calculated from the elution volume as indicated in Fig. 74. Experimental elution volumes from proteins can be calculated to a molecular mass using the curve.

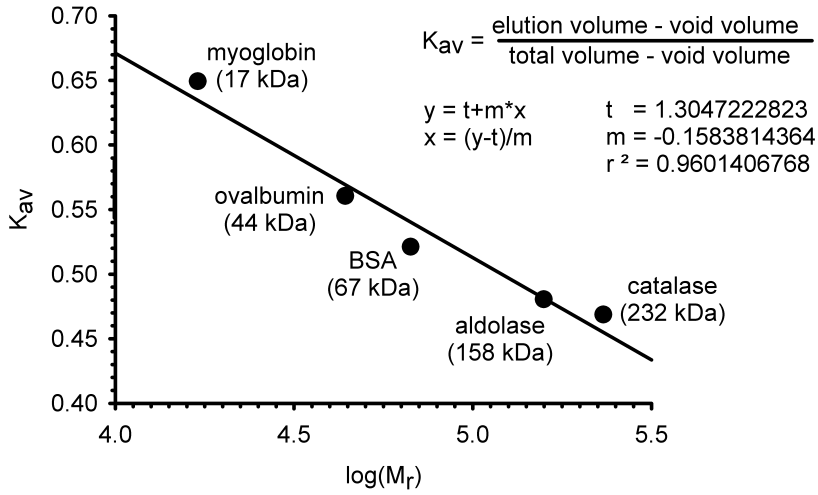

Fig. 74: Calibration curve for gel filtration. Elution volumes for the marker proteins are transformed to the K_{av} for the tricorn sepharose 6 column (void volume 8 ml, total volume 24 ml). This is plotted versus the log function of the known molecular mass.

7.17. Dynamic light scattering

This technique was used to determine the hydrodynamic radius and to estimate thereby the molecular mass, which may indicate the oligomeric state. Measurement is based on the dependence of light scattering fluctuations on the mobility and thereby the size (hydrodynamic radius) of particles in solution. It was performed with a Malven Zetasizer Nano-S with a 45 µl cuvette. Buffer conditions from nickel affinity purified protein (545 µg/ml) were changed by dialysis (10 kDa exclusion size) to 20 mM KPO_4 pH 7.5, 50 mM K_2SO_4, 0.03% DDM. Aggregates were separated by centrifugation (14 000 g, 10 min, 4 °C) before performing four measurements. The molecular mass was estimated by the instrument implying a globular shape.

7.18. Circular dichroism spectrometry

CD spectrometry was used to get information about the secondary structure of a protein. It is based on the different absorption of positive and negative circular polarized light by alpha-helices or beta-sheet structures of proteins. Buffer conditions from nickel affinity purified protein (545 µg/ml) were changed by dialysis (10 kDa exclusion size) to 20 mM KPO_4 pH 7.5, 50 mM K_2SO_4, 0.03% DDM. CD-spectra were measured with a Jasco-J-810 CD-spectrometer and Helma QS 110 quartz cuvettes with Teflon cap. 20 spectra at 20 °C between 190 nm and 240 nm (bandwidth 1 nm, scan speed 100 nm/min) were averaged and buffer background subtracted. The molar ellipticity per amino acid θ_{MRW} [deg*cm^2*dmol^{-1}] (MRW = *mean residue weight*) was calculated from the determined ellipticity θ [deg], the

molecular mass M_W of the protein, the concentration c, the cuvette path length d and the number of amino acid N_A using the formula:

$$\theta_{MRW} = \frac{\theta \times M_W}{c \times d \times N_A}$$

θ_{MRW} = molar ellipticity per amino acid
θ = ellipticity, M_W = molecular mass
c = concentration, d = cuvette path length
N_A = number of amino acid

The shape of the spectrum contains the information about secondary structure elements: Strong negative minima at 208 nm and 222 nm and a positive maximum at 192 nm indicate alpha-helices, while β-sheets are characterized by a negative minimum at 216 nm, a positive maximum between 195 and 200 nm and another negative minimum near 175 nm (Greenfield, 1996; Pelton and McLean, 2000). Typical shapes of spectra are shown in Fig. 75.

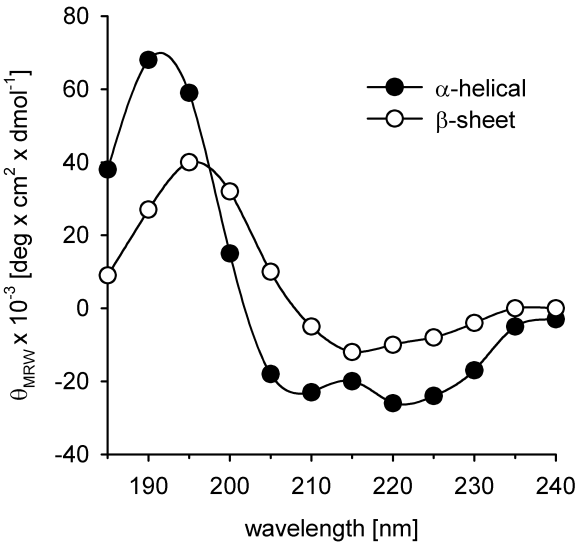

Fig. 75: Typical shape of CD spectra for α-helical or β-sheet secondary structure of proteins. Redrawn based on Greenfield (Greenfield, 1996).

7.19. MALDI-TOF

Matrix assisted laser desorption/ionization time of flight (MALDI-TOF) mass spectrometry was intended to show that the overproduced proteins are present at full length. Principle of the method is to determine exact molecule masses by a time of flight mass spectrometer. Proteins are brought into the spectrometer by the help of a solid matrix in which they are integrated. Using a laser, matrix and proteins are desorpted and ionized and accelerated in an electrical field (Fuchs *et al.*, 2005; Kaufmann, 1995).

7.19.1. Analysis of undigested protein

For analysis of undigested DtpA, nickel-affinity purified protein was dialyzed against 5 mM Hepes pH 7.4 to remove glycerin, salt and detergent. At a concentration of 5 µM DtpA, 1 µl was mixed with 1 µl of a saturated solution of matrix (sinapinic acid or 2,5-dihydroxybenzoic acid) in 30% acetonitrile, 20% acetone, 50% H_2O. On the Anchor Chip^{TM} MALDI-target 400/384 was first spotted a basislayer of 2 µl of a saturated solution of matrix (sinapinic acid or 2,5-dihydroxybenzoic acid) in 39% acetone, 60% methanol, 1% trifuoracetic acid. On top three times 0.5 µl of the protein/matrix mix were pipetted and let dry. Analysis was done with the Autoflex MALDI-TOF mass spectrometer (Bruker Daltonics) operating in linear mode.

7.19.2. Analysis of trypsin digested protein

For analysis of digested samples, either 3 µg purified DtpA (500 µg/ml) were used directly or 4 µg were loaded on SDS-PAA gel and the band at 40 kDa was excised or the spot from a 2D-SDS-gel was excised. The 2D-gel was done as follows: 150 µg DtpA (concentrated to 50 µl by a spin-column) were mixed with 285 µl buffer (7 M urea, 2 M thiourea, 4% CHPA, 2% pharmalyte pH 3-10) and 15 µl 30% DTT and loaded on the first dimension stripe (pH 4-10, GE) by cup-loading for isoelectric focusing (500 V (10 min, gradient), 4000 V (2.5 h, gradient), 8000 V (30000 Vh, step-n-hold, Ettan IPG Phor II, GE Healthcare)) as described (Gorg *et al.*, 1999; Gorg *et al.*, 2000). Equilibrated strips were transferred onto a 12.5% acrylamide gel and second dimension was run in the ETTAN Dalt II system (GE Healthcare) with 4 mA/gel for 1 h and then 12 mA/gel for ~15 h. Gels were fixed in 40% (v/v) ethanol and 10% (v/v) acetic acid at least for 6 h before they were transferred to the Coomassie staining solution (10% (w/v) $(NH_4)_2SO_4$, 2% (v/v) phosphoric acid, 25% (v/v) methanol and 0,625% (w/v) Coomassie brilliant blue G250) overnight. The destaining was performed in Milli Q water until the desired contrast was obtained. Spots (or the 1D-gel the band) were transferred into 0.2 ml Eppendorf tubes loaded with 50 µl of 50 mM ammonium bicarbonate solution. The destaining of the gel pieces was performed with alternating washing procedures in 50 µl of acetonitrile/50 mM ammonium bicarbonate solution (1/1, v/v) and pure 50 mM ammonium bicarbonate until the Coomassie was removed. Subsequently, spots were dehydrated in 50 µl 100% acetonitrile for 10 min and dried in a vacuum table centrifuge. Swelling of the spots with 6 µl of 0.02 µg/µl sequencing-grade modified trypsin was done on ice. After 1 h at 4 °C the excess enzyme was removed and the in gel digest was performed at 37 °C for 8-10 h (for the direct pure DtpA, just 5 µl trypsin solution was added). The generated peptide mixtures were extracted with 8 µl of 1% TFA solution per spot and 10 min in the sonication bath.

The generated peptide mixture samples were spotted by hand onto an Anchor Chip™ MALDI-target 400/384 by using the HCCA thin layer affinity method.(Gobom *et al.*, 2001). The samples were acidified by using aqueous 0.1% TFA as washing solution and air-dried at room temperature. Analysis was performed with an Autoflex MALDI-TOF mass spectrometer (Bruker Daltonics) operating in reflectron mode with a 20-kV accelerating voltage and a 130-ns delayed extraction. Peptide mass fingerprint spectra were acquired in the automatic mode using the AutoXecute module of flexControl software version 2.4 (Bruker Daltonics). Peptides were selected in the mass range of 800-3500 Da. The resulting mass list was evaluated using Bio Tools 3.0 with the search engine Mascot (version 1.9.00, www.matrixscience.com) and the MSDB database. Following search criteria were applied: trypsin as digestion enzyme, ±50-150 ppm peptide mass tolerance, 1 missed cleavage, carbamidomethyl modification of cysteine as global and methionine oxidation as variable modification, and charged state as MH^+.

7.20. Protein crystallization

For determination of the protein structure of the transporters, crystallization was done in cooperation with Dimitrios Fotiadis and Fabio Casagrande from the Institute for structural Biology of the University of Basel. Protein crystals (2D or 3D) can be used in diffraction experiments to obtain high quality and high resolution structural information about the protein (McPherson, 2004).

7.20.1. 2D-crystallization

In 2D crystallization membrane proteins are reconstituted as proteoliposomes with a very low lipid to protein ratio (LPR). Under suitable circumstances the proteins form crystalline patches in the membrane that can be used for electron diffraction in electron microscopy; 3D information are obtained by tilting the sample (Hite *et al.*, 2007). 2-D crystallization is especially suitable for membrane proteins because the protein is in its natural lipid environment. A scheme of the reconstitution assays in shown in Fig. 76. Purified protein (in various detergents) at a concentration of ~1 mg/ml was mixed with detergent solubilized lipid (5 mg/ml) at different ratios (LPR) in a volume of 60 µl. For the calculation of the volume of the protein needed for a specific LPR, the following formula was used:

$$V_{protein} = \frac{60\,\mu l \times c_{lipid}}{(LPR \times c_{protein}) + c_{lipid}}$$

$V_{protein}$ = volume of the protein solution
c_{lipid} = concentration of the lipid solution
$c_{protein}$ = concentration of the protein solution
LPR = lipid to protein ratio

This was pipetted in a small special vile (dialysis button) that was closed with a dialysis membrane (100 kDa cutoff) and subsequently put into a 2 L flask with dialysis buffer (basic composition: 20 mM TRIS/HCl pH 8, 10% glycerol, 150 mM NaCl, 0.01% NaN_3). The 100 kDa cutoff was chosen to maintain a rapid dialysis of the mostly low CMC (critical micelle concentration: minimal concentration where micelles start to form) detergent, which often also form big micelles. Several dialysis vials could be in the same flask that was usually incubated at RT (or sometimes 37 °C) until cloudiness in the vials appeared (~1-4 weeks). This indicated that the detergent was removed by dialysis and the protein and lipid had formed proteoliposomes (or precipitated). Samples from the dialysis buttons were analyzed by negative stain electron microscopy (7.21, p. 105). Thereby proteoliposomes were searched for crystalline protein grids that are large and homogeneous. Modified parameters are summarized in Table 16. Influences on the crystallization process come from the type of detergent and its CMC, the protein concentration and its purity (both should be high), the type of lipid and the ratio of lipid to protein (LPR) and the composition of the dialysis buffer.

Table 16: Variables modified in 2D crystallization

protein:	concentration from purification 1-5 mg/ml
detergent:	DDM (1%, 1.5%), DM (2%), Cymal-6 (1%), Cymal-7 (1%)
lipid:	dimyristoylphosphatidylcholine (DMPC), *E. coli* lipid
LPR:	0, 0.05, 0.1, 0.25, 0.4, 0.5, 0.8, 1
dialysis buffer pH:	MES pH 6, TRIS/HCl pH 8, CAPS pH 10
dialysis buffer Ionic strength:	NaCl: 10 mM, 50 mM, 150 mM, 500 mM or KCl:150 mM
dialysis buffer additives:	betaine (250 mM), β-cyclodextrin (1 mM), CaCl (0.25 mM), MgCl (5 mM)
dialysis time:	3 days to 4 weeks
dialysis temperature:	RT, 37 °C

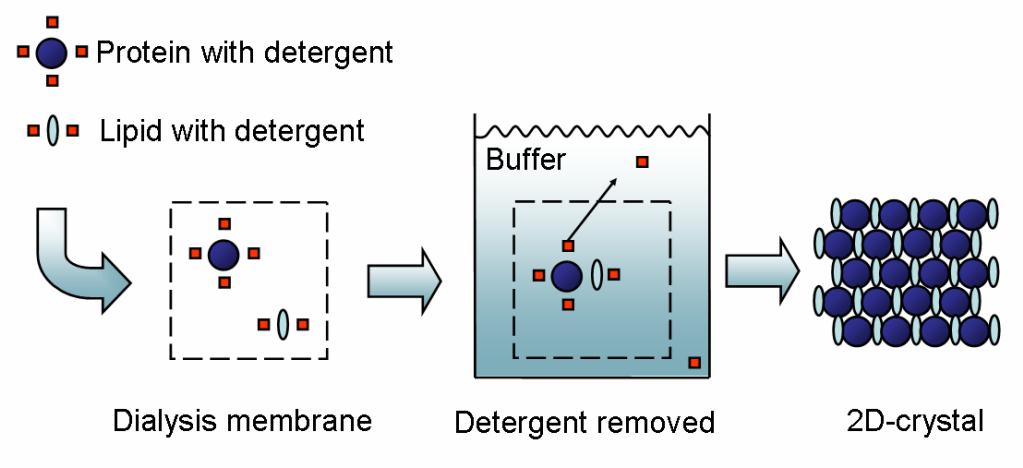

Fig. 76: 2D-crystallization of membrane proteins. Detergent solubilized protein and lipids are dialyzed to remove the detergent. When the detergent is lost, the lipids form vesicles together with the proteins. The tightly packed proteins can arrange themselves in an ordered, crystalline manner.

7.20.2. 3D-crystallization

For 3D crystallization trials purified protein was either used directly at concentrations of 4-7 mg/ml or concentrated to ~10 mg/ml with spin-columns (Amnicon, 50 kDa exclusion size). 4 µl protein from DDM or Cymal-7 purification was mixed with 4 µl buffer containing 50 mM buffer substance, NaCl and poly ethylene glycol (PEG) as specified in the results section (4.6.6.2, p. 67). The mix was placed in a well of a 24-well plate for sitting drop crystallization (Fig. 77).

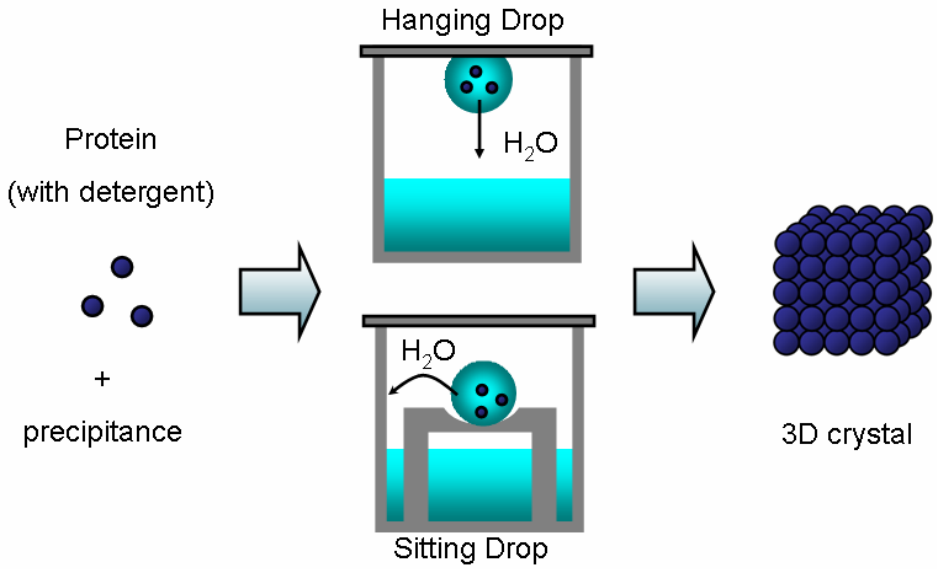

Fig. 77: 3D-crystallization of membrane proteins. Detergent solubilized protein is mixed with buffer containing various precipitants in various conditions. A drop of this is placed in a sealed compartment (sitting or hanging) where a reservoir of the same solution without protein (and therefore higher concentration) is in evaporation correspondence. As the concentration in the drop is slowly increased, protein supersaturation and crystal formation may occur.

The reservoir of the well was filled with 1 ml of the same buffer (without protein) and sealed with crystal clear sealing tape. Incubation was at constant 20 °C, crystal forming was checked after 2 weeks and then monthly. The principle of the method is shown in Fig. 77. Crystals can be analyzed by X-ray diffraction (Beauchamp and Isaacs, 1999; Chayen and Saridakis, 2008).

7.21. Transmission electron microscopy

5 µl DDM-solubilized protein as eluted from the nickel affinity chromatography column (~0.01 mg/ml) or proteoliposomes (from 2D crystallization) were adsorbed for 10 s to parlodion carbon-coated copper grids rendered hydrophilic by glow discharge at low pressure in air. Grids were washed with four drops of double-distilled water and stained with 2 drops of 0.75% uranyl formate. Images were recorded on Eastman Kodak Co. SO-163 sheet films with a Hitachi H-7000 electron microscope operated at 100 kV.

8. REFERENCES

Abdel-Sayed, S. (1987) Transport of chloramphenicol into sensitive strains of Escherichia coli and Pseudomonas aeruginosa. *J Antimicrob Chemother* **19**: 7-20.

Abouhamad, W.N., Manson, M., Gibson, M.M., and Higgins, C.F. (1991) Peptide transport and chemotaxis in Escherichia coli and Salmonella typhimurium: characterization of the dipeptide permease (Dpp) and the dipeptide-binding protein. *Mol Microbiol* **5**: 1035-1047.

Abramson, J., Smirnova, I., Kasho, V., Verner, G., Kaback, H.R., and Iwata, S. (2003) Structure and mechanism of the lactose permease of Escherichia coli. *Science* **301**: 610-615.

Altschul, S.F., Madden, T.L., Schaffer, A.A., Zhang, J., Zhang, Z., Miller, W., and Lipman, D.J. (1997) Gapped BLAST and PSI-BLAST: a new generation of protein database search programs. *Nucleic Acids Res* **25**: 3389-3402.

Amasheh, S., Wenzel, U., Boll, M., Dorn, D., Weber, W., Clauss, W., and Daniel, H. (1997) Transport of charged dipeptides by the intestinal H+/peptide symporter PepT1 expressed in Xenopus laevis oocytes. *J Membr Biol* **155**: 247-256.

Baba, T., Ara, T., Hasegawa, M., Takai, Y., Okumura, Y., Baba, M., Datsenko, K.A., Tomita, M., Wanner, B.L., and Mori, H. (2006) Construction of Escherichia coli K-12 in-frame, single-gene knockout mutants: the Keio collection. *Mol Syst Biol* **2**: 2006 0008.

Bassilana, M., Damiano, E., and Leblanc, G. (1984) Relationships between the Na+-H+ antiport activity and the components of the electrochemical proton gradient in Escherichia coli membrane vesicles. *Biochemistry* **23**: 1015-1022.

Beauchamp, J.C., and Isaacs, N.W. (1999) Methods for X-ray diffraction analysis of macromolecular structures. *Curr Opin Chem Biol* **3**: 525-529.

Biegel, A., Knutter, I., Hartrodt, B., Gebauer, S., Theis, S., Luckner, P., Kottra, G., Rastetter, M., Zebisch, K., Thondorf, I., Daniel, H., Neubert, K., and Brandsch, M. (2006) The renal type H+/peptide symporter PEPT2: structure-affinity relationships. *Amino Acids* **31**: 137-156.

Bolger, M.B., Haworth, I.S., Yeung, A.K., Ann, D., von Grafenstein, H., Hamm-Alvarez, S., Okamoto, C.T., Kim, K.J., Basu, S.K., Wu, S., and Lee, V.H. (1998) Structure, function, and molecular modeling approaches to the study of the intestinal dipeptide transporter PepT1. *J Pharm Sci* **87**: 1286-1291.

Boll, M., Foltz, M., Rubio-Aliaga, I., Kottra, G., and Daniel, H. (2002) Functional characterization of two novel mammalian electrogenic proton-dependent amino acid cotransporters. *J Biol Chem* **277**: 22966-22973.

Brandsch, M., Knutter, I., and Leibach, F.H. (2004) The intestinal H+/peptide symporter PEPT1: structure-affinity relationships. *Eur J Pharm Sci* **21**: 53-60.

Bretschneider, B., Brandsch, M., and Neubert, R. (1999) Intestinal transport of beta-lactam antibiotics: analysis of the affinity at the H+/peptide symporter (PEPT1), the uptake into Caco-2 cell monolayers and the transepithelial flux. *Pharm Res* **16**: 55-61.

Burns, J.L., and Smith, A.L. (1987) Chloramphenicol accumulation by Haemophilus influenzae. *Antimicrob Agents Chemother* **31**: 686-690.

Caldara, M., Minh, P.N., Bostoen, S., Massant, J., and Charlier, D. (2007) ArgR-dependent repression of arginine and histidine transport genes in Escherichia coli K-12. *J Mol Biol* **373**: 251-267.

Casagrande, F., Harder, D., Tittmann, P., Engel, A., Weitz, D., Gross, H., Daniel, H., and Fotiadis, D. (2009) Projection structure of DtpD (YbgH), a prokaryotic member of the PTR peptide transporter family. *in preparation*.

Chayen, N.E., and Saridakis, E. (2008) Protein crystallization: from purified protein to diffraction-quality crystal. *Nat Methods* **5**: 147-153.

Chen, X.Z., Zhu, T., Smith, D.E., and Hediger, M.A. (1999) Stoichiometry and kinetics of the high-affinity H+-coupled peptide transporter PepT2. *J Biol Chem* **274**: 2773-2779.

Cheng, Y., and Prusoff, W.H. (1973) Relationship between the inhibition constant (K1) and the concentration of inhibitor which causes 50 per cent inhibition (I50) of an enzymatic reaction. *Biochem Pharmacol* **22**: 3099-3108.

Chenna, R., Sugawara, H., Koike, T., Lopez, R., Gibson, T.J., Higgins, D.G., and Thompson, J.D. (2003) Multiple sequence alignment with the Clustal series of programs. *Nucleic Acids Res* **31**: 3497-3500.

Chiang, C.S., Stacey, G., and Tsay, Y.F. (2004) Mechanisms and functional properties of two peptide transporters, AtPTR2 and fPTR2. *J Biol Chem* **279**: 30150-30157.

Covitz, K.M., Amidon, G.L., and Sadee, W. (1998) Membrane topology of the human dipeptide transporter, hPEPT1, determined by epitope insertions. *Biochemistry* **37**: 15214-15221.

Cserzo, M., Wallin, E., Simon, I., von Heijne, G., and Elofsson, A. (1997) Prediction of transmembrane alpha-helices in prokaryotic membrane proteins: the dense alignment surface method. *Protein Eng* **10**: 673-676.

Daley, D.O., Rapp, M., Granseth, E., Melen, K., Drew, D., and von Heijne, G. (2005) Global topology analysis of the Escherichia coli inner membrane proteome. *Science* **308**: 1321-1323.

Daniel, H., Morse, E.L., and Adibi, S.A. (1992) Determinants of substrate affinity for the oligopeptide/H+ symporter in the renal brush border membrane. *J Biol Chem* **267**: 9565-9573.

Daniel, H., and Rubio-Aliaga, I. (2003) An update on renal peptide transporters. *Am J Physiol Renal Physiol* **284**: F885-892.

Daniel, H., and Kottra, G. (2004) The proton oligopeptide cotransporter family SLC15 in physiology and pharmacology. *Pflugers Arch* **447**: 610-618.

Daniel, H., Spanier, B., Kottra, G., and Weitz, D. (2006) From bacteria to man: archaic proton-dependent peptide transporters at work. *Physiology (Bethesda)* **21**: 93-102.

Datsenko, K.A., and Wanner, B.L. (2000) One-step inactivation of chromosomal genes in Escherichia coli K-12 using PCR products. *Proc Natl Acad Sci U S A* **97**: 6640-6645.

Deber, C.M., Wang, C., Liu, L.P., Prior, A.S., Agrawal, S., Muskat, B.L., and Cuticchia, A.J. (2001) TM Finder: a prediction program for transmembrane protein segments using a combination of hydrophobicity and nonpolar phase helicity scales. *Protein Sci* **10**: 212-219.

Dekker, J.P., Boekema, E.J., Witt, H.T., and Rogner, M. (1988) Refined purification and further characterization of oxygen-evolving and Tris-treated Photosystem II particles from the thermophilic Cyanobacterium synechococcus sp. *Biochimica et Biophysica Acta (BBA) - Bioenergetics* **Volume 936**: 307-318.

Detmers, F.J., Lanfermeijer, F.C., and Poolman, B. (2001) Peptides and ATP binding cassette peptide transporters. *Res Microbiol* **152**: 245-258.

Dieck, S.T., Heuer, H., Ehrchen, J., Otto, C., and Bauer, K. (1999) The peptide transporter PepT2 is expressed in rat brain and mediates the accumulation of the fluorescent dipeptide derivative beta-Ala-Lys-Nepsilon-AMCA in astrocytes. *Glia* **25**: 10-20.

Dietrich, D., Hammes, U., Thor, K., Suter-Grotemeyer, M., Fluckiger, R., Slusarenko, A.J., Ward, J.M., and Rentsch, D. (2004) AtPTR1, a plasma membrane peptide transporter expressed during seed germination and in vascular tissue of Arabidopsis. *Plant J* **40**: 488-499.

Doring, F., Dorn, D., Bachfischer, U., Amasheh, S., Herget, M., and Daniel, H. (1996) Functional analysis of a chimeric mammalian peptide transporter derived from the intestinal and renal isoforms. *J Physiol* **497 (Pt 3)**: 773-779.

Doring, F., Will, J., Amasheh, S., Clauss, W., Ahlbrecht, H., and Daniel, H. (1998) Minimal molecular determinants of substrates for recognition by the intestinal peptide transporter. *J Biol Chem* **273**: 23211-23218.

Driessen, A.J., de Vrij, W., and Konings, W.N. (1985) Incorporation of beef heart cytochrome c oxidase as a proton-motive force-generating mechanism in bacterial membrane vesicles. *Proc Natl Acad Sci U S A* **82**: 7555-7559.

Fei, Y.J., Kanai, Y., Nussberger, S., Ganapathy, V., Leibach, F.H., Romero, M.F., Singh, S.K., Boron, W.F., and Hediger, M.A. (1994) Expression cloning of a mammalian proton-coupled oligopeptide transporter. *Nature* **368**: 563-566.

Fei, Y.J., Liu, W., Prasad, P.D., Kekuda, R., Oblak, T.G., Ganapathy, V., and Leibach, F.H. (1997) Identification of the histidyl residue obligatory for the catalytic activity of the human H+/peptide cotransporters PEPT1 and PEPT2. *Biochemistry* **36**: 452-460.

Fei, Y.J., Liu, J.C., Fujita, T., Liang, R., Ganapathy, V., and Leibach, F.H. (1998) Identification of a potential substrate binding domain in the mammalian peptide transporters PEPT1 and PEPT2 using PEPT1-PEPT2 and PEPT2-PEPT1 chimeras. *Biochem Biophys Res Commun* **246**: 39-44.

Fuchs, D., Winkelmann, I., Johnson, I.T., Mariman, E., Wenzel, U., and Daniel, H. (2005) Proteomics in nutrition research: principles, technologies and applications. *Br J Nutr* **94**: 302-314.

Ganapathy, M.E., Brandsch, M., Prasad, P.D., Ganapathy, V., and Leibach, F.H. (1995) Differential recognition of beta -lactam antibiotics by intestinal and renal peptide transporters, PEPT 1 and PEPT 2. *J Biol Chem* **270**: 25672-25677.

Ganapathy, M.E., Huang, W., Wang, H., Ganapathy, V., and Leibach, F.H. (1998) Valacyclovir: a substrate for the intestinal and renal peptide transporters PEPT1 and PEPT2. *Biochem Biophys Res Commun* **246**: 470-475.

Geibel, S., Flores-Herr, N., Licher, T., and Vollert, H. (2006) Establishment of cell-free electrophysiology for ion transporters: application for pharmacological profiling. *J Biomol Screen* **11**: 262-268.

Gibson, M.M., Price, M., and Higgins, C.F. (1984) Genetic characterization and molecular cloning of the tripeptide permease (tpp) genes of Salmonella typhimurium. *J Bacteriol* **160**: 122-130.

Gobom, J., Schuerenberg, M., Mueller, M., Theiss, D., Lehrach, H., and Nordhoff, E. (2001) Alpha-cyano-4-hydroxycinnamic acid affinity sample preparation. A protocol for MALDI-MS peptide analysis in proteomics. *Anal Chem* **73**: 434-438.

Goh, E.B., Siino, D.F., and Igo, M.M. (2004) The Escherichia coli tppB (ydgR) gene represents a new class of OmpR-regulated genes. *J Bacteriol* **186**: 4019-4024.

Gorg, A., Obermaier, C., Boguth, G., and Weiss, W. (1999) Recent developments in two-dimensional gel electrophoresis with immobilized pH gradients: wide pH gradients up to pH 12, longer separation distances and simplified procedures. *Electrophoresis* **20**: 712-717.

Gorg, A., Obermaier, C., Boguth, G., Harder, A., Scheibe, B., Wildgruber, R., and Weiss, W. (2000) The current state of two-dimensional electrophoresis with immobilized pH gradients. *Electrophoresis* **21**: 1037-1053.

Granseth, E., Seppala, S., Rapp, M., Daley, D.O., and Von Heijne, G. (2007) Membrane protein structural biology--how far can the bugs take us? *Mol Membr Biol* **24**: 329-332.

Greenfield, N.J. (1996) Methods to estimate the conformation of proteins and polypeptides from circular dichroism data. *Anal Biochem* **235**: 1-10.

Hagting, A., Knol, J., Hasemeier, B., Streutker, M.R., Fang, G., Poolman, B., and Konings, W.N. (1997a) Amplified expression, purification and functional reconstitution of the dipeptide and tripeptide transport protein of Lactococcus lactis. *Eur J Biochem* **247**: 581-587.

Hagting, A., vd Velde, J., Poolman, B., and Konings, W.N. (1997b) Membrane topology of the di- and tripeptide transport protein of Lactococcus lactis. *Biochemistry* **36**: 6777-6785.

Heuberger, E.H., Veenhoff, L.M., Duurkens, R.H., Friesen, R.H., and Poolman, B. (2002) Oligomeric state of membrane transport proteins analyzed with blue native electrophoresis and analytical ultracentrifugation. *J Mol Biol* **317**: 591-600.

Higgins, C.F., and Gibson, M.M. (1986) Peptide transport in bacteria. *Methods Enzymol* **125**: 365-377.

Higgins, C.F. (2001) ABC transporters: physiology, structure and mechanism--an overview. *Res Microbiol* **152**: 205-210.

Hiles, I.D., Gallagher, M.P., Jamieson, D.J., and Higgins, C.F. (1987) Molecular characterization of the oligopeptide permease of Salmonella typhimurium. *J Mol Biol* **195**: 125-142.

Hirokawa, T., Boon-Chieng, S., and Mitaku, S. (1998) SOSUI: classification and secondary structure prediction system for membrane proteins. *Bioinformatics* **14**: 378-379.

Hite, R.K., Raunser, S., and Walz, T. (2007) Revival of electron crystallography. *Curr Opin Struct Biol* **17**: 389-395.

Hofmann, K., and Stoffel, W. (1993) TMbase - A database of membrane spanning proteins segments. *Biol. Chem. Hoppe-Seyler* **374**: 166.

Huang, Y., Lemieux, M.J., Song, J., Auer, M., and Wang, D.N. (2003) Structure and mechanism of the glycerol-3-phosphate transporter from Escherichia coli. *Science* **301**: 616-620.

Jamieson, D.J., and Higgins, C.F. (1984) Anaerobic and leucine-dependent expression of a peptide transport gene in Salmonella typhimurium. *J Bacteriol* **160**: 131-136.

Jamieson, D.J., and Higgins, C.F. (1986) Two genetically distinct pathways for transcriptional regulation of anaerobic gene expression in Salmonella typhimurium. *J Bacteriol* **168**: 389-397.

Jeong, J., Suh, S., Guan, C., Tsay, Y.F., Moran, N., Oh, C.J., An, C.S., Demchenko, K.N., Pawlowski, K., and Lee, Y. (2004) A nodule-specific dicarboxylate transporter from alder is a member of the peptide transporter family. *Plant Physiol* **134**: 969-978.

Jones, D.T., Taylor, W.R., and Thornton, J.M. (1994) A model recognition approach to the prediction of all-helical membrane protein structure and topology. *Biochemistry* **33**: 3038-3049.

Kaufmann, R. (1995) Matrix-assisted laser desorption ionization (MALDI) mass spectrometry: a novel analytical tool in molecular biology and biotechnology. *J Biotechnol* **41**: 155-175.

Kelety, B., Diekert, K., Tobien, J., Watzke, N., Dorner, W., Obrdlik, P., and Fendler, K. (2006) Transporter assays using solid supported membranes: a novel screening platform for drug discovery. *Assay Drug Dev Technol* **4**: 575-582.

Knutter, I., Hartrodt, B., Toth, G., Keresztes, A., Kottra, G., Mrestani-Klaus, C., Born, I., Daniel, H., Neubert, K., and Brandsch, M. (2007) Synthesis and characterization of a new and radiolabeled high-affinity substrate for H(+)/peptide cotransporters. *Febs J*.

Kottra, G., Stamfort, A., and Daniel, H. (2002) PEPT1 as a paradigm for membrane carriers that mediate electrogenic bidirectional transport of anionic, cationic, and neutral substrates. *J Biol Chem* **277**: 32683-32691.

Kowalczuk, S., Broer, A., Munzinger, M., Tietze, N., Klingel, K., and Broer, S. (2005) Molecular cloning of the mouse IMINO system: an Na+- and Cl--dependent proline transporter. *Biochem J* **386**: 417-422.

Krogh, A., Larsson, B., von Heijne, G., and Sonnhammer, E.L. (2001) Predicting transmembrane protein topology with a hidden Markov model: application to complete genomes. *J Mol Biol* **305**: 567-580.

Larkin, M.A., Blackshields, G., Brown, N.P., Chenna, R., McGettigan, P.A., McWilliam, H., Valentin, F., Wallace, I.M., Wilm, A., Lopez, R., Thompson, J.D., Gibson, T.J., and Higgins, D.G. (2007) Clustal W and Clustal X version 2.0. *Bioinformatics* **23**: 2947-2948.

Lecomte, C., Guillot, B., Muzet, N., Pichon-Pesme, V., and Jelsch, C. (2004) Ultra-high-resolution X-ray structure of proteins. *Cell Mol Life Sci* **61**: 774-782.

Liman, E.R., Tytgat, J., and Hess, P. (1992) Subunit stoichiometry of a mammalian K+ channel determined by construction of multimeric cDNAs. *Neuron* **9**: 861-871.

Liu, K.H., and Tsay, Y.F. (2003) Switching between the two action modes of the dual-affinity nitrate transporter CHL1 by phosphorylation. *Embo J* **22**: 1005-1013.

Maruyama, H.B., Arisawa, M., and Sawada, T. (1979) Alafosfalin, a new inhibitor of cell wall biosynthesis: in vitro activity against urinary isolates in Japan and potentiation with beta-lactams. *Antimicrob Agents Chemother* **16**: 444-451.

McGuffin, L.J., Bryson, K., and Jones, D.T. (2000) The PSIPRED protein structure prediction server. *Bioinformatics* **16**: 404-405.

McPherson, A. (2004) Introduction to protein crystallization. *Methods* **34**: 254-265.

Meng, S.Y., and Bennett, G.N. (1992) Nucleotide sequence of the Escherichia coli cad operon: a system for neutralization of low extracellular pH. *J Bacteriol* **174**: 2659-2669.

Meredith, D., and Price, R.A. (2006) Molecular modeling of PepT1--towards a structure. *J Membr Biol* **213**: 79-88.

Meyer-Lipp, K., Ganea, C., Pourcher, T., Leblanc, G., and Fendler, K. (2004) Sugar binding induced charge translocation in the melibiose permease from Escherichia coli. *Biochemistry* **43**: 12606-12613.

Moller, S., Croning, M.D., and Apweiler, R. (2001) Evaluation of methods for the prediction of membrane spanning regions. *Bioinformatics* **17**: 646-653.

Moreira, M.A., Oliveira, J.A., Teixeira, L.M., and Moraes, C.A. (2005) Detection of a chloramphenicol efflux system in Escherichia coli isolated from poultry carcass. *Vet Microbiol* **109**: 75-81.

Nierhaus, D., and Nierhaus, K.H. (1973) Identification of the chloramphenicol-binding protein in Escherichia coli ribosomes by partial reconstitution. *Proc Natl Acad Sci U S A* **70**: 2224-2228.

Otto, C., tom Dieck, S., and Bauer, K. (1996) Dipeptide uptake by adenohypophysial folliculostellate cells. *Am J Physiol* **271**: C210-217.

Pasquier, C., Promponas, V.J., Palaios, G.A., Hamodrakas, J.S., and Hamodrakas, S.J. (1999) A novel method for predicting transmembrane segments in proteins based on a statistical analysis of the SwissProt database: the PRED-TMR algorithm. *Protein Eng* **12**: 381-385.

Paulsen, I.T., and Skurray, R.A. (1994) The POT family of transport proteins. *Trends Biochem Sci* **19**: 404.

Payne, J.W., and Smith, M.W. (1994) Peptide transport by micro-organisms. *Adv Microb Physiol* **36**: 1-80.

Payne, J.W., Grail, B.M., Gupta, S., Ladbury, J.E., Marshall, N.J., O'Brien, R., and Payne, G.M. (2000a) Structural basis for recognition of dipeptides by peptide transporters. *Arch Biochem Biophys* **384**: 9-23.

Payne, J.W., Grail, B.M., and Marshall, N.J. (2000b) Molecular recognition templates of peptides: driving force for molecular evolution of peptide transporters. *Biochem Biophys Res Commun* **267**: 283-289.

Payne, J.W., and Marshall, N.J. (2001) Peptide Transport. *Microbial Transport Systems (Winkelmann, G., Ed.) Wiley-VCH, Weinheim, Germany*: 139-164.

Pelton, J.T., and McLean, L.R. (2000) Spectroscopic methods for analysis of protein secondary structure. *Anal Biochem* **277**: 167-176.

Perriere, G., and Gouy, M. (1996) WWW-query: an on-line retrieval system for biological sequence banks. *Biochimie* **78**: 364-369.

Persson, B., and Argos, P. (1997) Prediction of membrane protein topology utilizing multiple sequence alignments. *J Protein Chem* **16**: 453-457.

Rosen, B.P. (1971) Basic amino acid transport in Escherichia coli. *J Biol Chem* **246**: 3653-3662.

Rosen, B.P. (1973) Basic amino acid transport in Escherichia coli. II. Purification and properties of an arginine-specific binding protein. *J Biol Chem* **248**: 1211-1218.

Rudd, K.E. (2000) EcoGene: a genome sequence database for Escherichia coli K-12. *Nucleic Acids Res* **28**: 60-64.

Sakata, K., Yamashita, T., Maeda, M., Moriyama, Y., Shimada, S., and Tohyama, M. (2001) Cloning of a lymphatic peptide/histidine transporter. *Biochem J* **356**: 53-60.

Smith, M.W., Tyreman, D.R., Payne, G.M., Marshall, N.J., and Payne, J.W. (1999) Substrate specificity of the periplasmic dipeptide-binding protein from Escherichia coli: experimental basis for the design of peptide prodrugs. *Microbiology* **145 (Pt 10)**: 2891-2901.

Soksawatmaekhin, W., Kuraishi, A., Sakata, K., Kashiwagi, K., and Igarashi, K. (2004) Excretion and uptake of cadaverine by CadB and its physiological functions in Escherichia coli. *Mol Microbiol* **51**: 1401-1412.

Steffes, C., Ellis, J., Wu, J., and Rosen, B.P. (1992) The lysP gene encodes the lysine-specific permease. *J Bacteriol* **174**: 3242-3249.

Steiner, H.Y., Naider, F., and Becker, J.M. (1995) The PTR family: a new group of peptide transporters. *Mol Microbiol* **16**: 825-834.

Stolz, J., Stadler, R., Opekarova, M., and Sauer, N. (1994) Functional reconstitution of the solubilized Arabidopsis thaliana STP1 monosaccharide-H+ symporter in lipid vesicles and purification of the histidine tagged protein from transgenic Saccharomyces cerevisiae. *Plant J* **6**: 225-233.

Strop, P., and Brunger, A.T. (2005) Refractive index-based determination of detergent concentration and its application to the study of membrane proteins. *Protein Sci* **14**: 2207-2211.

Terada, T., Saito, H., Mukai, M., and Inui, K.I. (1996) Identification of the histidine residues involved in substrate recognition by a rat H+/peptide cotransporter, PEPT1. *FEBS Lett* **394**: 196-200.

Terada, T., Sawada, K., Irie, M., Saito, H., Hashimoto, Y., and Inui, K. (2000) Structural requirements for determining the substrate affinity of peptide transporters PEPT1 and PEPT2. *Pflugers Arch* **440**: 679-684.

Terada, T., and Inui, K. (2004) Peptide transporters: structure, function, regulation and application for drug delivery. *Curr Drug Metab* **5**: 85-94.

Theis, S., Doring, F., and Daniel, H. (2001) Expression of the myc/His-tagged human peptide transporter hPEPT1 in yeast for protein purification and functional analysis. *Protein Expr Purif* **22**: 436-442.

Theis, S., Hartrodt, B., Kottra, G., Neubert, K., and Daniel, H. (2002) Defining minimal structural features in substrates of the H(+)/peptide cotransporter PEPT2 using novel amino acid and dipeptide derivatives. *Mol Pharmacol* **61**: 214-221.

Tsai, C.J., and Ziegler, C. (2005) Structure determination of secondary transport proteins by electron crystallography: two-dimensional crystallization of the betaine uptake system BetP. *J Mol Microbiol Biotechnol* **10**: 197-207.

Tsay, Y.F., Schroeder, J.I., Feldmann, K.A., and Crawford, N.M. (1993) The herbicide sensitivity gene CHL1 of Arabidopsis encodes a nitrate-inducible nitrate transporter. *Cell* **72**: 705-713.

Tsay, Y.F., Chiu, C.C., Tsai, C.B., Ho, C.H., and Hsu, P.K. (2007) Nitrate transporters and peptide transporters. *FEBS Lett* **581**: 2290-2300.

Tusnady, G.E., and Simon, I. (2001) The HMMTOP transmembrane topology prediction server. *Bioinformatics* **17**: 849-850.

VanBogelen, R.A., Vaughn, V., and Neidhardt, F.C. (1983) Gene for heat-inducible lysyl-tRNA synthetase (lysU) maps near cadA in Escherichia coli. *J Bacteriol* **153**: 1066-1068.

Vazquez, D. (1964) Uptake and Binding of Chloramphenicol by Sensitive and Resistant Organisms. *Nature* **203**: 257-258.

Wagner, C.A., Friedrich, B., Setiawan, I., Lang, F., and Broer, S. (2000) The use of Xenopus laevis oocytes for the functional characterization of heterologously expressed membrane proteins. *Cell Physiol Biochem* **10**: 1-12.

Wang, D.N., Safferling, M., Lemieux, M.J., Griffith, H., Chen, Y., and Li, X.D. (2003) Practical aspects of overexpressing bacterial secondary membrane transporters for structural studies. *Biochim Biophys Acta* **1610**: 23-36.

Weitz, D., Harder, D., Casagrande, F., Fotiadis, D., Obrdlik, P., Kelety, B., and Daniel, H. (2007) Functional and structural characterization of a prokaryotic peptide transporter with features similar to mammalian PEPT1. *J Biol Chem* **282**: 2832-2839.

Yamashita, T., Shimada, S., Guo, W., Sato, K., Kohmura, E., Hayakawa, T., Takagi, T., and Tohyama, M. (1997) Cloning and functional expression of a brain peptide/histidine transporter. *J Biol Chem* **272**: 10205-10211.

Yeung, A.K., Basu, S.K., Wu, S.K., Chu, C., Okamoto, C.T., Hamm-Alvarez, S.F., von Grafenstein, H., Shen, W.C., Kim, K.J., Bolger, M.B., Haworth, I.S., Ann, D.K., and Lee, V.H. (1998) Molecular identification of a role for tyrosine 167 in the function of the human intestinal proton- coupled dipeptide transporter (hPepT1). *Biochem Biophys Res Commun* **250**: 103-107.

Yu, C., Yu, L., and King, T.E. (1975) Studies on cytochrome oxidase. Interactions of the cytochrome oxidase protein with phospholipids and cytochrome c. *J Biol Chem* **250**: 1383-1392.

Zhou, J.J., Theodoulou, F.L., Muldin, I., Ingemarsson, B., and Miller, A.J. (1998) Cloning and functional characterization of a Brassica napus transporter that is able to transport nitrate and histidine. *J Biol Chem* **273**: 12017-12023.

Zhu, T., Chen, X.Z., Steel, A., Hediger, M.A., and Smith, D.E. (2000) Differential recognition of ACE inhibitors in Xenopus laevis oocytes expressing rat PEPT1 and PEPT2. *Pharm Res* **17**: 526-532.

Zhuang, J., Prive, G.G., Werner, G.E., Ringler, P., Kaback, H.R., and Engel, A. (1999) Two-dimensional crystallization of Escherichia coli lactose permease. *J Struct Biol* **125**: 63-75.

Zuber, D., Krause, R., Venturi, M., Padan, E., Bamberg, E., and Fendler, K. (2005) Kinetics of charge translocation in the passive downhill uptake mode of the Na+/H+ antiporter NhaA of Escherichia coli. *Biochim Biophys Acta* **1709**: 240-250.

9. APPENDIX

9.1. Abbreviations

5-ALA	5-aminolevulinic acid
6-AHA	6-aminohexanoic acid
ACE inhibitor	angiotensin-converting enzyme inhibitor
Ala-Lys(AMCA)	β-Ala-Lys-N_ε-7-amino-4-methyl-coumarin-3-acetic acid

Amino acids:

A	Ala	Alanine	M	Met	Methionine
C	Cys	Cysteine	N	Asn	Asparagine
D	Asp	Aspartic acid	P	Pro	Proline
E	Glu	Glutamic acid	Q	Gln	Glutamine
F	Phe	Phenylalanine	R	Arg	Arginine
G	Gly	Glycine	S	Ser	Serine
H	His	Histidine	T	Thr	Threonine
I	Ile	Isoleucine	V	Val	Valine
K	Lys	Lysine	W	Trp	Tryptophan
L	Leu	Leucine	Y	Tyr	Tyrosine

CCCP	carbonyl cyanide m-chlorophenoxylhydrazone
CMC	critical micelle concentration (minimal concentration where micelles start to form)
C-terminal	carboxy-terminal
DDM	dodecyl maltoside
DM	decyl maltoside
DMPC	dimyristoylphosphatidylcholine
DTT	dithiothreitol
Gly-Sar	glycylsarcosine
IC_{50}	Inhibitor concentration at 50% effect
IPTG	Isopropyl-β-D-thiogalactopyranosid
K_i	Inhibition constant (equilibrium dissociation constant derived from inhibition)
K_t	transport constant (equilibrium dissociation constant derived from transport)
KO	knockout (mutant where a certain gene is disabled)
LPR	lipid to protein ratio
MALDI-TOF	matrix assisted laser desorption/ionization time of flight
MES	4-Morpholineethanesulfonic acid
N-terminal	amino-terminal
NTA	nitrilotriacetic acid
OG	octyl glucoside
PAA	poly acrylamide
PAGE	poly acrylamide gel electrophoresis
PEG	poly ethylene glycol
PFA	paraformaldehyde
PMSF	phenylmethanesulphonylfluoride
POT family	proton dependent oligopeptide transporter family
PTR family	peptide transporter family
SD	standard deviation
SDS	sodium dodecyl sulfate
TCEP	tris(2-carboxyethyl)phosphine
TFA	trifluor acetic acid
TEVC	two-electrode voltage clamp
TM	transmembrane domain
TRIS	Tris(hydroxymethyl) aminomethane hydrochloride

9.2. Proteinparameters

DtpA (YdgR)

Number of amino acids: 508, Molecular weight: 55056.2, Theoretical pI: 8.73

MSTANQKPTE SVSLNAFKQP KAFYLIFSIE LWERFGYYGL QGIMAVYLVK QLGMSEADSI
TLFSSFSALV YGLVAIGGWL GDKVLGTKRV IMLGAIVLAI GYALVAWSGH DAGIVYMGMA
AIAVGNGLFK ANPSSLLSTC YEKNDPRLDG AFTMYYMSVN IGSFFSMIAT PWLAAKYGWS
VAFALSVVGL LITIVNFAFC QRWVKQYGSK PDFEPINYRN LLLTIIGVVA LIAIATWLLH
NQEVARMALG VVAFGIVVIF GKEAFAMKGA ARRKMIVAFI LMLEAIIFFV LYSQMPTSLN
FFAIRNVEHS ILGLAVEPEQ YQALNPFWII IGSPILAAIY NKMGDTLPMP TKFAIGMVMC
SGAFLILPLG AKFASDAGIV SVSWLVASYG LQSIGELMIS GLGLAMVAQL VPQRLMGFIM
GSWFLTTAGA NLIGGYVAGM MAVPDNVTDP LMSLEVYGRV FLQIGVATAV IAVLMLLTAP
KLHRMTQDDA ADKAAKAAVA **LEHHHHHH**

DtpB (YhiP)

Number of amino acids: 497, Molecular weight: 54640.3, Theoretical pI: 8.47

MNTTTPMGML QQPRPFFMIF FVELWERFGY YGVQGVLAVF FVKQLGFSQE QAFVTFGAFA
ALVYGLISIG GYVGDHLLGT KRTIVLGALV LAIGYFMTGM SLLKPDLIFI ALGTIAVGNG
LFKANPASLL SKCYPPKDPR LDGAFTLFYM SINIGSLIAL SLAPVIADRF GYSVTYNLCG
AGLIIALLVY IACRGMVKDI GSEPDFRPMS FSKLLYVLLG SVVMIFVCAW LMHNVEVANL
VLIVLSIVVT IIFFRQAFKL DKTGRNKMFV AFVLMLEAVV FYILYAQMPT SLNFFAINNV
HHEILGFSIN PVSFQALNPF WVVLASPILA GIYTHLGNKG KDLSMPMKFT LGMFMCSLGF
LTAAAAGMWF ADAQGLTSPW FIVLVYLFQS LGELFISALG LAMIAALVPQ HLMGFILGMW
FLTQAAAFLL GGYVATFTAV PDNITDPLET LPVYTNVFGK IGLVTLGVAV VMLLMVPWLK
RMIATPESH**L EHHHHHH**

DtpC (YjdL)

Number of amino acids: 493, Molecular weight: 54119.7, Theoretical pI: 7.70

MKTPSQPRAI YYIVAIQIWE YFSFYGMRAL LILYLTHQLG FDDNHAISLF SAYASLVYVT
PILGGWLADR LLGNRTAVIA GALLMTLGHV VLGIDTNSTF SLYLALAIII CGYGLFKSNI
SCLLGELYDE NDHRRDGGFS LLYAAGNIGS IAAPIACGLA AQWYGWHVGF ALAGGGMFIG
LLIFLSGHRH FQSTRSMDKK ALTSVKFALP VWSWLVVMLC LAPVFFTLLL ENDWSGYLLA
IVCLIAAQII ARMMIKFPEH RRALWQIVLL MFVGTLFWVL AQQGGSTISL FIDRFVNRQA
FNIEVPTALF QSVNAIAVML AGVVLAWLAS PESRGNSTLR VWLKFAFGLL LMACGFMLLA
FDARHAAADG QASMGVMISG LALMGFAELF IDPVAIAQIT RLKMSGVLTG IYMLATGAVA
NWLAGVVAQQ TTESQISGMA IAAYQRFFSQ MGEWTLACVA IIVVLAFATR FLFSTPTNMI
QESND**LEHHH HHH**

DtpD (YbgH)

Number of amino acids: 501, Molecular weight: 55224.0, Theoretical pI: 8.76

MNKHASQPRA IYYVVALQIW EYFSFYGMRA LLILYLTNQL KYNDTHAYEL FSAYCSLVYV
TPILGGFLAD KVLGNRMAVM LGALLMAIGH VVLGASEIHP SFLYLSLAII VCGYGLFKSN
VSCLLGELYE PTDPRRDGGF SLMYAAGNVG SIIAPIACGY AQEEYSWAMG FGLAAVGMIA
GLVIFLCGNR HFTHTRGVNK KVLRATNFLL PNWGWLLVLL VATPALITIL FWKEWSVYAL
IVATIIGLGV LAKIYRKAEN QKQRKELGLI VTLTFFSMLF WAFAQQGGSS ISLYIDRFVN
RDMFGYTVPT AMFQSINAFA VMLCGVFLAW VVKESVAGNR TVRIWGKFAL GLGLMSAGFC
ILTLSARWSA MYGHSSLPLM VLGLAVMGFA ELFIDPVAMS QITRIEIPGV TGVLTGIYML
LSGAIANYLA GVIADQTSQA SFDASGAINY SINAYIEVFD QITWGALACV GLVLMIWLYQ
ALKFRNRALA LES**LEHHHHH H**

Calculation by ProtParam: http://www.expasy.org/tools/protparam.html

9.3. Acknowledgments

For the success of this work, the support of many other people was beneficial or essential.

Therefore, I like to thank Dr. Dietmar Weitz who was a very kind and motivating guide to scientific work, unfortunately only until half-time. Thanks also to Prof. Dr. Hannelore Daniel for her scientific support and inspiration. Her ceaseless work to maintain excellent equipment and cooperations increased productivity and success. For their efforts in the evaluation of this work I thank Prof. Dr. Scherer and Prof. Dr. Klingenspor.

As financial backbone the Eugindat project (European genomics initiative on disorders of plasma membrane amino acid transporters) form the 6th framework program of European Union has to be acknowledged, which was coordinated by Prof. Dr. Manuel Palacin. Special thanks here to our direct cooperation partners from the Biozentrum Basel, Fabio Casagrande and Dr. Dimitrios Fotiadis, who introduced me to protein crystallization and were pleasant and valuable fellows. It were interesting and nice days in Basel and also the last meeting in Rome and the tunnel of death will stay legend.

Other important allies from outside were Kersin Dirlam from the Degussa, who was kindly supporting the use of their fermenter, the people form Iongate, Dr. Petr Obrdlik, Dr. Inga Barth and Dr. Stefan Schork, who were of friendly assistance with the Surfe2r experiments, and Dr. Markus Gütlich from the Lehrstuhl für Biopolymere, who was very kind and enthusiastic in sharing his knowledge and expertise with liposomes.

Many thanks also to a lot of people of our own Lab: Daniela Kolmeder was a big help in lab-work and contributed also by thinking about the project and asking critical questions. Over all the time she was a very pleasant company in the “big lab”. Dr. Jürgen Stolz became an important advisor, special thanks here for the breakthrough in proteoliposome uptakes. Thanks to Natalie Steck for her good work on DtpB in her bachelor project. For support with oocytes I thank Dr. Gabor Kottra, Helene Prunkl and Rainer Reichelmaier, who were also friendly company for all the years. Isabel Winkelmann, Barbara Gelhaus, and Caroline Heim I want to thank for MALDI assistance and Ingolf Krause and Gabi Schmidt for their efforts with LC-MS/MS. Thanks also to Isabel Rubio, who showed me oocyte histofluorescence and Alexander Nickel for assistance with the confocal microscope.

For the nice company in the office, discussions about science and non-science and emotional stabilization, I am grateful to Katrin Lohner, Katja Bühlmeyer, Isabel Winkelmann, Alex Nickel, Dagmar Fuchs, Charles Desmarchelier, Anne Näßl, Caro Heim, Florencia Andreoli and Adina Bangert. Special thanks to Anne for Bavarian language coaching and to Alex, my Eugindat-brother, with whom I have walked for so long the same road and shared success and disappointment, four o'clock banana and philosophic table tennis.
Thanks also to all the other colleagues who made the time in the institute interesting and enjoyable.

Finally I want to thank my family, especially my parents, who always support and encourage me.

9.4. Curriculum Vitae

Personal

Name:	Harder
First name:	Daniel
Address:	Isarstrasse 6, D-85356 Freising (Germany)
email:	harder@wzw.tum.de
Birth:	2. June 1977 in Erlangen (Germany)

Education and training

3/2004 - 5/2009	Promotion at the Technische Universität München (Germany), molecular nutrition unit, with Prof. Hannelore Daniel about *biochemistry of membrane proteins*: Characterization of the PTR peptide transporter family of *E. coli.* Degree: PhD (Dr. rer. nat.)
6/2006 - 9/2006	Research experience at the Biozentrum Basel (Switzerland) in the group of Prof. Andreas Engel on crystallization of membrane transporters
9/1998 - 7/2003	Biology studies at the Friedrich-Alexander-Universität Erlangen-Nürnberg (Germany). Specialization: *Microbiology* (focus), *Genetics, Zoology, Informatics.* Diploma thesis: Surface-expression of antigens in Mycobacteria Degree: Diploma Biology (very good)
9/1988 - 6/1997	General qualification for university entrance at the Ehrenbürg-Gymnasium Forchheim (Germany): Specialized courses: *Biology*, *Math*. Degree: Abitur (good)
9/1983 - 7/1988	Basic School Ehrenbürg, Mittelehrenbach (Germany)

9.5. List of publications

Peer reviewed original papers

Weitz, D.*, **Harder, D.***, Casagrande, F., Fotiadis, D., Obrdlik, P., Kelety, B., and Daniel, H. (2007) Functional and structural characterization of a prokaryotic peptide transporter with features similar to mammalian PEPT1. *J Biol Chem* **282**: 2832-2839.
* **Authors contributed equally**

Siroy A., Mailaender C., **Harder D.**, Koerber S., Wolschendorf F., Danilchanka O., Wang Y., Heinz C., Niederweis M. (2008) Rv1698 of Mycobacterium tuberculosis represents a new class of channel-forming outer membrane proteins. *J Biol Chem* **283**:17827-17837

Harder, D., Stolz, J., Casagrande, F., Obrdlik, P., Weitz, D., Fotiadis, D., and Daniel, H. (2008) DtpB (YhiP) and DtpA (TppB, YdgR) are prototypical proton-dependent peptide transporters of *E. coli. FEBS J* **275:** 3290-3298

Harder, D., Stolz, J., and Daniel, H. (2009) YjdL is a bifunctional membrane transporter from *E. coli* that mediates the uptake of cationic amino acids and of cationic di-and tripeptides.
In revision

Casagrande, F*., **Harder, D.***, Tittmann, P., Engel, A., Weitz, D., Gross, H., Daniel, H. and Fotiadis, D. (2009) Projection structure of DtpD (YbgH), a prokaryotic member of the PTR peptide transporter family. **In preparation**
* **Authors contributed equally**